WSRC-TR-2002-00318, Rev. 1

THERMODYNAMIC MODELING OF THE SRS EVAPORATORS: PART III. TEMPERATURE, EVAPORATION, AND COMPOSITION EFFECTS ON PROCESS CONTROL STRATEGY (U)

C. M. Jantzen, T.B. Edwards, and J.M. Pareizs

March 31, 2003

TTP #: SR-1-9-WT-31, Subtask D

Approved by:

W.L. Tamosaitis, Research Manager
Waste Processing Technology

WSRC-TR-2002-00318, Rev. 1

Distribution Category: Unlimited
Keywords: Evaporators, activity diagrams, zeolite, 2H Evaporator
Retention: Permanent

THERMODYNAMIC MODELING OF THE SRS EVAPORATORS: PART III. TEMPERATURE, EVAPORATION, AND COMPOSITION EFFECTS ON PROCESS CONTROL STRATEGY (U)

C. M. Jantzen, T.B. Edwards, and J.M. Pareizs

Publication Date: March 31, 2003

TTP #: SR-1-9-WT-31, Subtask D

Approved by:

W.L. Tamosaitis, Research Manager
Waste Processing Technology

Approvals

C. M. Jantzen, Author, Immobilization Technology	Date
W.R. Wilmarth, Technical Reviewer, Waste Processing Tech.	Date
D.T. Hobbs, Technical Reviewer, Waste Processing Technology	Date
Richard E. Edwards, Manager, HLW Process Engineering	Date
E.J. Freed, Manager, CST Engineering	Date
W.L. Tamosaitis, Manager, Waste Processing Technology	Date

Westinghouse Savannah River Company
Savannah River Site
Aiken, SC 29808

Savannah River Technology Center
SRTC
We Put Science to Work

PREPARED FOR THE U.S. DEPARTMENT OF ENERGY UNDER CONTRACT NO. DE-AC09-96SR18500

EXECUTIVE SUMMARY

Accumulations of two solid phases (a nitrated aluminosilicate) and sodium diuranate, in the form of scale, caused the SRS 2H Evaporator pot to become completely inoperable in October 1999. The accumulation of the sodium diuranate phase, which selectively precipitated with the aluminosilicate phase, caused criticality concerns in the 2H Evaporator. In order to understand the role of steady state saturation on the scale formation, solutions processed from the SRS 2H, 2F, and 3H Evaporators were evaluated with a commercially available thermodynamic equilibrium code known as Geochemist's Workbench (GWB).

Reactive oxides, soluble silicates, and soluble aluminates in caustic solution can form a sodium aluminosilicate gel (NAS_{gel}) at ambient temperature when the solution stoichiometry of the aluminate and silicate species is ~1:1. The NAS_{gel} converts to Zeolite-A under hydrothermal conditions similar to those existing in the SRS evaporators. The nitrated-cancrinite/sodalite formed in the SRS 2H Evaporator was found to have formed NAS_{gel} and Zeolite-A. Zeolite-A and hydroxysodalite formation from NAS_{gel} has also been observed in evaporators used in the wood pulp industry while formation of NAS_{gel} and transformation into Zeolite-A→sodalite→cancrinite has been observed in the Bayer aluminum process. Thermodynamic data developed for the pulp and aluminum processes were used to augment the database of Geochemist's Workbench.

The potential to form the NAS_{gel} phase in the evaporator was modeled because this phase is the primary phase from which all the other aged crystalline product species are derived. In addition, the formation of the NAS_{gel} phase is kinetically the most rapid step in the formation sequence [species in solution]→ NAS_{gel} →Zeolite-A→sodalite→cancrinite. Modeling the denser crystalline phases, which are more thermodynamically stable but less soluble than the NAS_{gel}, would unnecessarily constrict the solution chemistry range of the SRS evaporators.

A saturation index, $\log (Q/K)_{NAS}$, was calculated for the NAS_{gel} using Geochemist's Workbench. The saturation index was calculated assuming a 40 wt % nominal evaporation for each of the SRS evaporators (2H, 2F, and 3H). Nominal operating temperatures of 120-140°C were also assumed based on evaporator operational history from 1995-2001. The $\log (Q/K)_{NAS}$ calculated for a 40 wt % evaporation at 120-140°C was regressed against the molar concentrations of Al, Si, and OH measured routinely in the evaporator tanks at ambient temperature, $\log Q\ (NAS)_{25°C}$. A process control strategy was developed to relate the ambient $\log Q\ (NAS)_{25°C}$ in the feed tank to the saturation of that feed in the evaporator pot ($\log (Q/K)_{NAS}$) at elevated temperature after a nominal 40 wt % evaporation.

In this study the process control strategy is expanded to different evaporation concentrations between 10% and 60% and temperatures up to 180°C. The $\log (Q/K)_{NAS}$ is fairly independent of evaporator operating temperature in the range of 120-180°C based on the solubility data of the NAS_{gel} as measured in the Bayer aluminum process. In addition, an orthogonal latin hypercube (OLH) design was used to generate compositions over this expanded evaportion and temperature space. The Geochemist's Workbench

results for these OLH points demonstrate that the nominal process control model is not applicable to compositions outside the range of the original evaporator solutions modeled in its present form based on the solubility data of the NAS_{gel} from the bayer aluminum process.

Operational histories of the SRS 2H, 2F, and 3H evaporators from 2001-2002 were also reviewed. Production samples from the SRS 3H Evaporator system (January 2002) confirmed the operational process control limit previously determined based on production samples from the SRS 2F Evaporator system.

TABLE OF CONTENTS

LIST OF FIGURES

LIST OF TABLES

LIST OF ACRONYMS

ACT-2:	ACTivity Diagram Subroutine in GWB
DOE:	United States Department of Energy
GDL:	Gravity Drain Line
GWB:	The Geochemist's Workbench Software
HLW:	High Level Waste
LHS:	Left Hand Side
LLNL:	Lawrence Livermore National Laboratory
NAS:	Sodium Aluminosilicate gel
OLS:	Ordinary Least Squares
OLH:	Orthogonal Latin Hypercube
ORNL:	Oak Ridge National Laboratory
PNNL:	Pacific Northwest National Laboratory
REACT:	Reaction Path Subroutine in GWB
RHS:	Right Hand Side
RW-0333P:	DOE Level of Quality Assurance
SRS:	Savannah River Site
SRTC:	Savannah River Technology Center
VDS:	Variable Depth Samples
WSRC:	Westinghouse Savannah River Company

THERMODYNAMIC MODELING OF THE SRS EVAPORATORS: PART III. TEMPERATURE, EVAPORATION, AND COMPOSITION EFFECTS ON PROCESS CONTROL STRATEGY (U)

C. M. Jantzen, T.B. Edwards, and J.M. Pareizs
Savannah River Technology Center
Westinghouse Savannah River Company
Aiken, South Carolina 29808

1.0 INTRODUCTION

Accumulations of two solid phases (a nitrated aluminosilicate[f] and sodium diuranate[*]) formed scale deposits in the Savannah River Site (SRS) 2H Evaporator system.[1, 2] The aluminosilicate scale deposits caused the evaporator pot to become inoperable in October 1999. Accumulations of the diuranate phase have caused criticality concerns in the SRS 2H Evaporator. In Part I of this study, [3] thermodynamically derived activity diagrams, also known as stability diagrams, were used on historic 2H feed tank (Tank 43) and drop tank (Tank 38) chemistries in order to understand the effects of tank chemistry on solids formation in the 2H Evaporator. Evaluation of the 2F feed tank (Tank 26) and drop tank (Tank 46) chemistries evaluated in Part I of this study showed that the SRS 2F Evaporator system had not and was not near saturation with respect to aluminosilicate scale. In order to ensure that similar deposits had not and were not depositing in the SRS 3H Evaporator, a similar evaluation was performed specific to the feeds processed from Tank 32 (feed tank) and Tank 30 (drop tank) in Part II of this study.[4]

Activity diagram representation was used to calculate if an evaporator feed tank composition fell in the formation field of the undesirable aluminosilicate species, e.g. was a given evaporator solution saturated or supersaturated with respect to the undesirable aluminosilicate species that caused scaling. Modeling the deposition of the aluminosilicates and sodium diuranate in the SRS evaporators entailed calculations in the complex Na-N-Si-Al-U-H_2O system at elevated temperatures and at high ionic strengths (I~8.5). Modeling accuracy was evaluated against the following parameters:

- quality of the chemical data available from the feed and drop tanks
- how representative the analytic dip samples from the feed and drop tank are of the feed entering the evaporator
- quality of the solubility data used from the literature
- quality of the approximations that must be made to determine the activity coefficients for high ionic strength solutions.

---

[f] a mixture of nitrated cancrinite, $Na_8Al_6Si_6O_{24}(NO_3)_2 \bullet 4H_2O$, and nitrated sodalite, $Na_8Al_6Si_6O_{24}(NO_3)_2$

[*] $Na_2U_2O_7$

The quality of the solubility data used from the Bayer aluminum process and the paper and pulp industry and the quality of the approximations that are used to model high ionic strength solutions are discussed in Part I of this study.[3] Validation of the calculation approach in simple one component systems and in the complex Na-N-Si-Al-U-H_2O system is also discussed in Part I of this study.[3] The quality of the chemical data available for the SRS 2H and 2F Evaporators is also discussed in Part I of this study[3] while the quality of the chemical data for the SRS 3H Evaporator is discussed in Part II of this study.[4]

A process control strategy was developed in Part I of this study[3] to relate the ambient temperature chemistry in an evaporator feed tank to the saturation of that feed in the evaporator pot at elevated temperature during a nominal 40 wt % evaporation. In this study (Part III) the usage of this process control strategy is expanded to 10%, 20%, 30%, 50%, and 60% evaporation and temperatures spanning 120-180°C. In addition, the model applicability and Geochemist's Workbench are validated with a statistically designed tank composition data set which included composition ranges far outside those modeled in Part I[3] and II[4] and to evaporations up to 80%, and to temperatures up to 180°C. This statistically designed validation is demonstrated via an orthogonal latin hypercube (OLH) analysis. Recent operation of the SRS 2H, 2F, and 3H evaporators is reviewed in terms of this process control strategy but the model developed in Part I[3] of this study is not revised in this study.

Part IV of this study will incorporate new solubility data for the aluminosilicate phases obtained in simulated SRS evaporator solutions by researchers at the University of Southern Australia.[5] This solubility data is considered more applicable to the SRS Evaporator modeling since the dissolution solution contained the constituents found in SRS solutions such as NO_3 and NO_2 instead of just NaOH solubility which was the basis of the data used from the Bayer aluminum process. The process control model from Part I[3] will be revised in Part IV. In Part IV the recent SRS Evaporator data given in this study (Part III) will be included in the modeling data and all the data modeled will be based on the new solubility data for NAS_{gel} in SRS evaporator like high caustic solutions. The temperature and evaporation dependence of the process model will be revaluated in Part IV. Validation of the revised process control model in the complex Na-N-Si-Al-U-H_2O system will be revalidated in Part IV as was done in Part I. Additional validation with designed experiments performed by researchers at the Pacific Northwest National Laboratory (PNNL) and the Oak Ridge National Laboratory (ORNL) are discussed in Part V of this study.[6]

2.0 BACKGROUND

2.1 Operation of SRS Evaporators

For ~40 years, the SRS tank farm evaporators have run with only occasional operational problems, e.g., salt ($NaNO_3$) buildup has caused difficulty in draining evaporators but these deposits are water soluble and easily removed by flushing with hot water. The SRS 2F and 3H Evaporators continue to operate with only occasional salt buildup. However, operation of the SRS 2H evaporator had become problematic due to the formation of aluminosilicate scale between 1997 and 1999.

A new 2H Evaporator pot was installed and began receiving waste in January 1996. From mid 1996 until August 1997 the SRS 2H Evaporator was increasingly hard to control. When the evaporator was shut down in August 1997 for cleaning, deposits of the sodium aluminosilicate and sodium uranate phases were found in the gravity drain line (GDL).[7] The GDL was pressure washed in the direction of the drop tank. The line remained clean and the evaporator showed minimal deposits on the walls or in the lines from August 1997 to June 1998. In June 1998 the GDL needed to be pressure washed a second time and deposits were observed in the evaporator cone, on the vessel walls and on the warming tubes. The GDL was pressure washed in the direction of the evaporator and in the direction of the drop tank to ensure that it was clean. Operation continued, with difficulty, from June 1998 until October 1999, when the evaporator was shut down. At this time, significant accumulations of the aluminosilicate scale and sodium diuranate deposits were found on many of the exposed surfaces of the evaporator pot. The scale in the 2H Evaporator was cleaned using a depleted uranyl nitrate solution in August 2001[8] and began operating again in October 2001.

Several important changes have been made in the handling of wastes entering the SRS evaporators in the last decade.* Prior to the mid 1990's, high activity waste was stored for >1 year before being processed in the evaporators so that the short lived radionuclides could decay before waste was concentrated. This also allowed any solids or colloidal species in the wastes to settle to the bottom of the tank before being processed. When the SRS reactors shut down and wastes were less radioactive, the one year hold strategy was no longer required.

In addition, the evaporators discharged to alternate drop tanks. When one drop tank was filled it was left to settle, and cool, and a second drop tank was used. Typically recycles to the feed tank were made from the passive drop tank and not from the active drop tank. This allowed any particulates or colloids in a given drop tank to settle before being recycled to the feed tank again for further concentration. The active/passive drop tank practice had to be discontinued in the early 1990's since there was no longer enough salt drop space in the concentrate receipt tanks.

* Synopsis by Kent Gilbreath, Mark Mahoney, and Thomas Caldwell (May, 2001)

In 1997, the 1st inter-area waste transfers were made between the SRS H-area and the SRS F-area waste tanks for the purpose of volume reducing the waste. This allowed co-mingling of wastes of different chemistries.

More recently, a decision was made to evaporate canyon and back-log waste in the 2F evaporator for initial salt separation. This occurs when the hydroxide molarity exceeds 6-8M. Then the desalted liquor is routed to the 3H evaporator for final dehydration, which can drive the hydroxide molarity above 12M.‡

These changes in operational strategy and co-mingling of waste have caused concerns that the aluminosilicate scaling problems experienced with the operation of the SRS 2H Evaporator could now become system wide. Thus a process control strategy was developed[3] using Geochemist's Workbench (GWB) to prevent aluminosilicate scale formation in the SRS evaporators. Control of the aluminosilicate scale formation controls any criticality concerns caused by the adherent sodium diuranate which is partially enriched U^{235}.

2.2 Geochemist's Workbench (GWB)

The Geochemist's Workbench (GWB) database was modified to include various solids including stable and metastable aluminosilicate minerals such as Zeolite-A, hydroxy-sodalite, NAS_{gel}, and "mixed zeolite."[3] Modifications to the solid aluminate species had been made as well.[3] The solubility data incorporated into the database for the aluminosilicate and aluminate species had been measured at high Na molarity which then allowed the GWB code to be used for modeling high Na molarity solutions such as those in the SRS evaporators. In addition the GWB software has the following attributes:

- ability to estimate activity coefficients for high ionic strength solutions such as those in the evaporator
  - ability to improve the basis upon which the activity coefficients are estimated
- usage of Lawrence Livermore National Laboratory (LLNL) extensive database for minerals and aqueous species used to model the performance of waste forms in the High Level Waste (HLW) Repository
  - includes sodium diuranate and aqueous uranate species
- ability to calculate the relative stability of multiple solid phases simultaneously
- ability to graphically represent the relative stability of multiple phases in terms of three parameters simultaneously on activity or stability diagrams, e.g. Si, Al, and pH of a solution
- ability to perform polythermal reaction paths, e.g. reaction path can vary temperature linearly from an initial to a final value so that elevated evaporator temperatures could be modeled

‡ HLW System Plan, Rev. 12

- ability to simulate evaporation by removing a percentage of the water from the calculation, e.g. base the calculation on 0.6 kg of water rather than on the default of 1 kg of water for a simulated 40 wt % evaporation
- ability to calculate a supersaturation index for a given solid phase expressed as a ratio of the reaction quotient (Q) over the solubility product (K), e.g. log (Q/K)
- ability to calculate the amount of the solid phase (in $g_{(solid)}/kg_{(soln)}$) that will form at the given supersaturation if precipitation to equilibrium proceeds.

Two subroutines in GWB were used to model the precipitation of solids in the complex Na-N-Si-Al-U-H_2O system pertinent to the SRS 2H Evaporator; e.g. REACT and ACT2. The REACT subroutine models equilibrium states and processes of solids in equilibrium with aqueous fluids. The program calculates the following:

- equilibrium distribution of aqueous species in a fluid
- the fluid's saturation state with respect to mineral phases
- the fugacities of the gases dissolved in the fluid

During the process control modeling of scale formation in SRS evaporators only the REACT subroutine was used. All mineral formation (precipitation) was suppressed so that a saturation index (log Q/K) could be calculated. Positive values of log (Q/K) are supersaturated while negative values are undersaturated with respect to the solid phase that could precipitate.

2.3 Latin Hypercube Statistical Analysis

The statistical perspective of design problems involving computer experimentation, such as GWB, has been explored.[9,10,11,12] These references identify and discuss the unique aspects of this design and analysis problem. A method for generating orthogonal Latin hypercubes (OLHs)* and their advantages for such problems are presented in Reference 12. An advantage of a Latin Hypercube approach is that it facilitates each of the input variables having all portions of its range represented.[12] Thus, the approach provides a "space-filling" (for the factor space of interest, i.e., the concentrations, temperature, and percent evaporation) set of design points. Also, the estimates of linear effects of all factors are uncorrelated with each other, and the orthogonal Latin hypercube designs "guarantee that the estimates of quadratic effects and bilinear interaction effects are uncorrelated with estimates of linear effects. However, the estimates of quadratic and bilinear interaction effects are correlated with each other."[12]

From Reference 12, an OLH consisting of n rows can be constructed when n is a power of 2 or a power of 2 plus 1 (i.e., 2^m or 2^m+1). A method is provided in Reference 12 for constructing and optimizing such an OLH with 2m-2 columns. The value of 2m-2 must be equal to or greater than the number of factors of interest. A value of 9 was used for m (with 2m-2 = 16, which is greater than the 14 factors used for this study.*f* A value of m=9 leads to a value for n of 512 or 513. For this design, a value of 513 was selected for n since m=9. Thus, the interval of possible values for each input was divided into 513 equal sub-intervals.

Following the guidance provided in Reference 12, a minimax criterion was applied to random permutations of the design to provide a test matrix where the minimum Euclidean distance between any pair of design vectors is a maximum. Such an approach was used to generate the test matrix (or experimental design) to support this study. Figure 1 provides an illustration of the space filling and pairwise orthogonality of the resulting test matrix used in this study with concentrations expressed as the molar concentrations. Brown[13] provides the details of the design approach.

---

* This class of orthogonal Latin hypercubes preserves orthogonality among columns, i.e., any two columns **u** and **v** of the OLH satisfy $\mathbf{u}^T\mathbf{v}=0$ where $\mathbf{u}^T$ is the transpose of **u**.

f The 14 parameters included 12 composition parameters, temperature, and percent evaporation

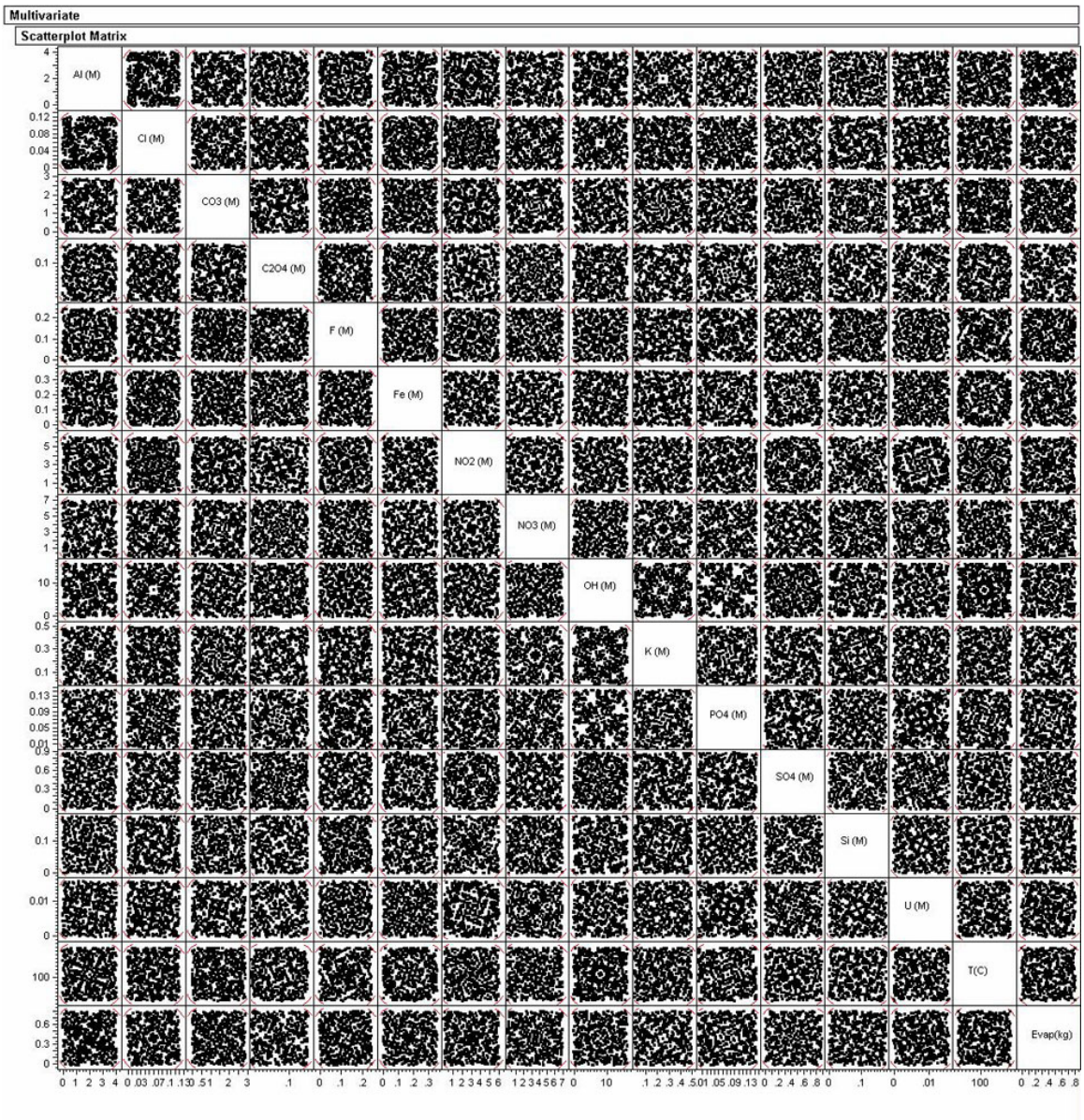

Figure 1 Scatterplot matrix for the Optimized OLH Design.

2.4 The Role of Kinetics in Thermodynamic Modeling

The Zeolite-A structure can form by any of the following mechanisms and then age to structurally related minerals such as sodalites and cancrinites:

- from a gel process where the reactants are reactive oxides, soluble silicates, and soluble aluminates in a caustic solution (Figure 2)
- from conversion of clay minerals (specifically kaolin and meta-kaolin) in the presence of soluble silicates and caustic
- by reaction of silica sols, natural SiO_2, amorphous minerals, and volcanic glass in the presence of caustic (Figure 3).[3]

The gel reactions from solution and/or the silica sol reactions are the most significant of these mechanisms for SRS evaporator modeling although small traces of clay minerals could be introduced via the process water used in the evaporators. The gel reaction from solution assumed in this study takes the form:

$$NaOH(aq) + NaAl(OH)_4(aq) + Na_2SiO_3(aq) \xrightarrow{25°C}$$
$$[Na_a(AlO_2)_b(SiO_2)_c \bullet NaOH \bullet H_2O]_{gel} \xrightarrow[\text{hydrothermal}]{25\text{–}175°C} Na_x[(AlO_2)_x(SiO_2)_y] \bullet mH_2O \qquad [1]$$

Formation from silica sols would substitute an ≡Si–OH (silanol) term into Equation 1 instead of $Na_2SiO_3(aq)$.

Zeolites are synthesized industrially from solution using the gel process shown in Equation 1. Upon mixing sodium silicate and sodium aluminate at high pH an amorphous sodium aluminosilicate gel phase forms which will be abbreviated as NAS_{gel}. Transformation of the gel to the zeolite can take hours or days depending upon the synthesis conditions. Industrial synthesis of Zeolite-A involves solutions use of 4.0M NaOH concentrations to keep the crystallization times short and allow effective recycling of the excess NaOH.[14]

Gels are amorphous as they are colloids in which the disperse phase has combined with the continuous phase to produce a semisolid material such as a jelly.[15] As a gel dewaters or ages it will form a denser gel and/or a crystalline solid phase. This is independent of the route of formation of the gel. Whether the NAS_{gel} forms from solution via a hydrogel process or whether it forms from a sol (solid particles in liquid)[16] via a sol-gel process, the aging sequence of the NAS_{gel} to denser sodalite and still denser cancrinite type species will typically follow an aging path such as that shown in Figure 2 according to Barnes, Mensah and Gerson[17] and Gerson and Zheng.[18] Note that the densification of the phases agrees with the following literature:

- Bayer[19] and Ejaz[20] found that the NAS gels would transform to Zeolite-A. Ejaz experimentally determined the composition of the precursor gel at NaOH concentrations of 3-4.5M to be $0.93Na_2O:1Al_2O_3:2.32SiO_2:5.15H_2O$.

- Barrer[19] found that the NAS gels would transform to Zeolite-A at pH values >10 in 2-3 hours at 110°C (the approximate temperature of the SRS evaporators)

- Buhl and Lons[21] showed that nitrated sodalite and nitrated cancrinite could best be made by starting with a Zeolite-A precursor in concentrated NaOH at various temperatures

- Wilmarth[22] showed that the Zeolite-A forms as a precursor but the nitrated cancrinite forms on the order of 3-5 hours at 110°C in simulated 2H Evaporator solutions

- Gasteiger et al.[23] found that hydroxysodalite $Na_8[Al_6Si_6O_{24}](OH)_2\bullet(1.5H_2O)$ and sodalite ($Na_8[Al_6Si_6O_{24}](Cl)_2$) formation was >99% complete in 24 hours at 95°C and that the sodalites formed via a Zeolite-A precursor

- Subotic, et. al.[24] demonstrated that aluminosilicate gels that have a Si/Al = 1 form Zeolite-A at lower NaOH concentrations in solution at 85°C which then transforms into hydroxysodalite; at higher NaOH concentrations the gel can transform into hydroxysodalite without the Zeolite-A precursor formation

- Bosnar and Subotic[25] demonstrated that Zeolite-A forms from an amorphous aluminosilicate precursor ($1.03Na_2O\bullet Al_2O_3\bullet 2.38SiO_2\bullet 1.66H_2O$) and the Zeolite-A growth is governed by the Davies-Jones model of growth and dissolution (growth of Zeolite-A from solution coupled with dissolution of the amorphous phase); growth rate decreases with increasing alkalinity

Although nitrated sodalite and nitrated cancrinite were found in the SRS 2H Evaporator after long periods of time they aged in the evaporator from one of the precursor phases. In Part I[3] of this study the activity diagram modeling indicated that the precursor phase most pertinent to deposition in SRS evaporators was the NAS_{gel} due to the short residence times in the evaporators. This was confirmed by kinetic testing performed at ORNL.[26]

Therefore, the thermodynamic steady state equilibrium of the NAS_{gel} forms the basis for the process control model and not the crystalline equilibrium sodalite or cancrinite phases. In Part V of this study[6] it will be shown that if a solution is saturated with respect to the NAS_{gel} phase that this phase precipitates rapidly (<30 minutes at 80°C). It is the function of the process control model to prevent the evaporator solutions from ever becoming saturated with respect to the NAS_{gel}, thus preventing the precipitation of the gel.

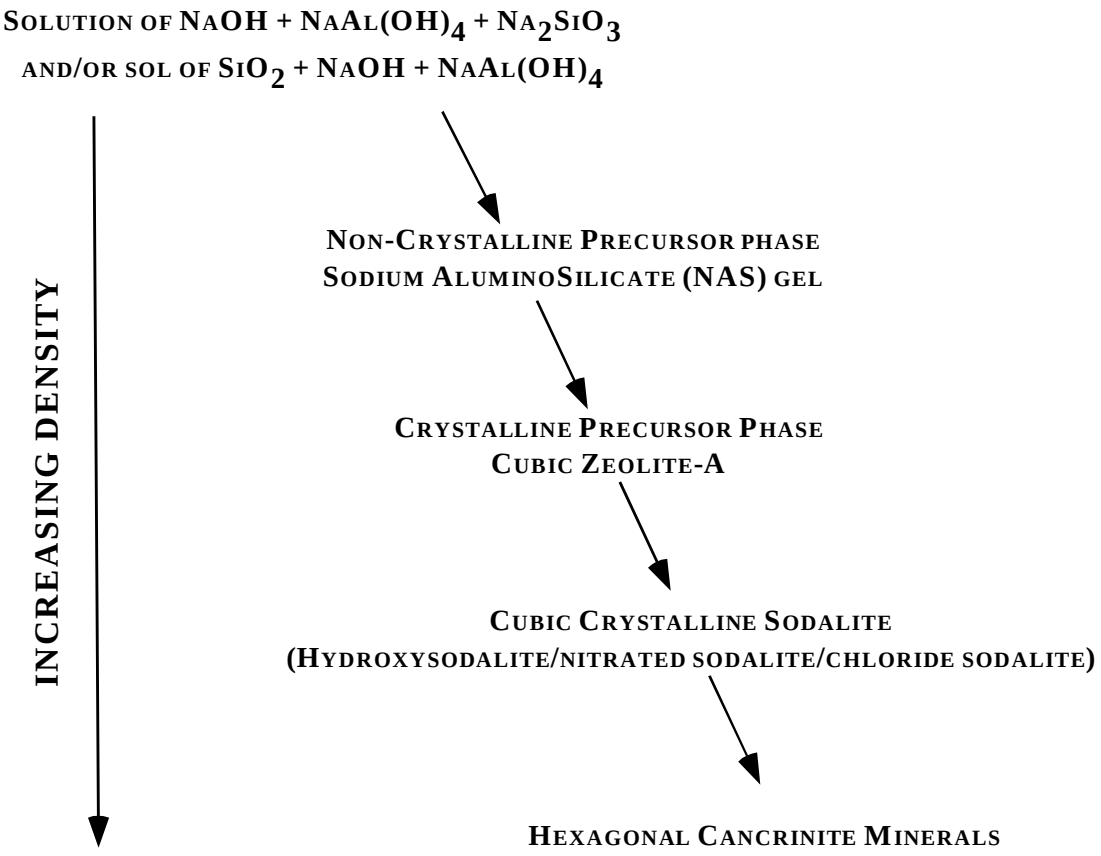

Figure 2. Typical formation and aging (densification) sequence of NAS_{gel}→Zeolite-A→ sodalite → cancrinite phases depending on the relative concentration of OH^-, Cl^-, NO_3^-, and/or $CO_3^{=}$ in the solution in contact with the NAS_{gel} (after Gerson, et.al.)[17,18]

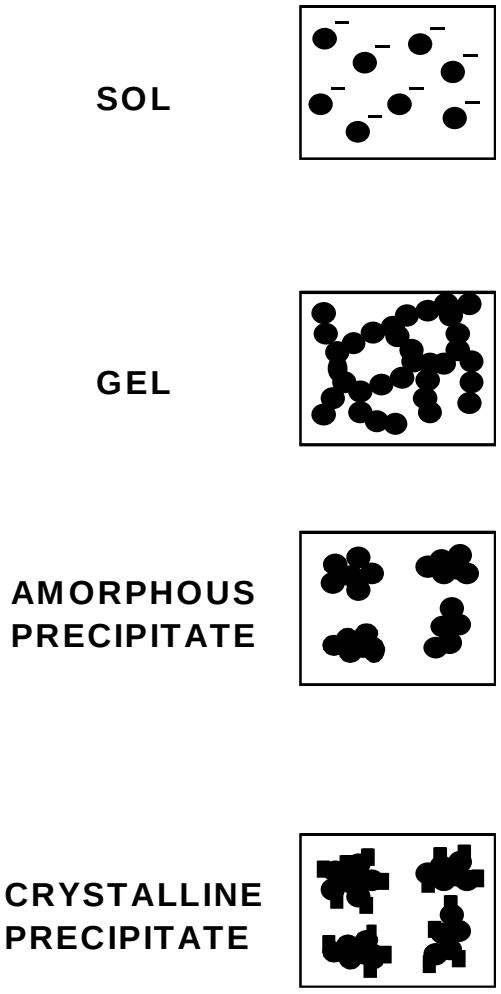

Figure 3. Pictorial diagram showing the differences between a sol, gel, and precipitate (after references 27 and 28).

3.0 PROCESS MODELING FOR NOMINAL EVAPORATOR OPERATION[3]

The SRS evaporator model presented in Part I [3] is for nominal evaporator operating conditions defined as the following:

- 40 wt % evaporation
- 120°C to 140°C

In addition, the stoichiometry of the reaction that forms the NAS_{gel} from solution or from silica sols governs the process control model. The amorphous aluminosilicate gel precursor of Ejaz[20] is the stoichiometry used in the SRS evaporator process model $0.93Na_2O{:}1Al_2O_3{:}2.32SiO_2{:}5.15H_2O$). It is very similar to that reported by Bosnar and Subotic[25] ($1.03Na_2O{:}Al_2O_3{:}2.38SiO_2{:}1.66H_2O$) but not identical (see Section 2.4).

Geochemist's Workbench assumes that the NAS_{gel} is formed from solution species since the database does not have any solubility data for a silica sol. The equations that represent the saturation of the solution with respect to the NAS_{gel} are defined by the steady state equilibrium boundary on the activity diagrams which separates the field of AlOOH (diaspore) from the field of NAS_{gel} at 120°C as given in Equation 2.

$$6\text{Diaspore} + 19H_2O + 6\frac{Al(OH)_4^-}{H^+} + 14SiO_2(aq) + 12Na^+ \Leftrightarrow NAS_{gel} \qquad [2]$$

Equation 2 can be rewritten as

$$6AlOOH + 19H_2O + 6Al(OH)_4^- + 14SiO_2(aq) + 12Na^+ \Leftrightarrow Na_{12}Al_{12}Si_{14}O_{52} \bullet 31H_2O + 6H^+ \qquad [3]$$

where the NAS_{gel} formula $Na_{12}Al_{12}Si_{14}O_{52} \bullet 31H_2O$ is equivalent to $6(Na_2O \bullet Al_2O_3 \bullet 2.32SiO_2 \bullet 5.15H_2O)$, the chemical composition of the NAS_{gel} from Ejaz[20] as given above.

Use of Equation [3] for the development of the process control algorithm would have resulted in relying on a measurement of the pH which is inherently inaccurate at pH values of >13,[7, 29] the pH values reported for the SRS evaporator feeds. Since free hydroxide is routinely measured for the SRS evaporators and it is a more accurate measurement than the pH this term was substituted in Equation [3]. Likewise, the $SiO_2(aq)$ in GWB represents silicic acid which can be represented in hydroxide form as $Si(OH)_4$ while the Na^+ should be expressed as NaOH consistent with Equation 1 and the work of Mattigod and McGrail.[30]

$$6\mathrm{AlOOH} + 6\mathrm{Al(OH)}_4^- + 14\mathrm{Si(OH)}_4(\mathrm{aq}) + 12\mathrm{NaOH} \Leftrightarrow \mathrm{Na}_{12}\mathrm{Al}_{12}\mathrm{Si}_{14}\mathrm{O}_{52} \bullet 31\mathrm{H}_2\mathrm{O} + 15\mathrm{H}_2\mathrm{O} + 6\mathrm{OH}^- \quad [4]$$

Rewriting Equation 4 in terms of the species routinely measured in the SRS Evaporator feed tanks, e.g. Al(M), Si(M), OH(M), was shown[3] to represent the formation of the aluminosilicate NAS_{gel} framework (cage) structure without Na. In addition, it was shown[3] that there was a high statistical co-linearity between Na and OH in SRS evaporator solutions. Thus Equation 4 could be rewritten without the NaOH term:

$$6AlOOH + 6Al(OH)_4^- + 14Si(OH)_4(aq) \Leftrightarrow Al_{12}Si_{14}O_{46} \bullet 31H_2O + 9H_2O + 6OH^- \quad [5]$$

The K_{sp} for this reaction is

$$K_{sp}(NAS_{gel}) = \frac{[NAS_{gel}][OH^-]^6[H_2O]^9}{[AlOOH]^6[Al(OH)_4^-]^6[Si(OH)_4]^{14}} \quad [6]$$

Equation [6] can be further simplified since the NAS_{gel} and the water in the numerator are in their standard states and equal to 1 as shown in Equation [7]

$$K_{sp}(NAS_{gel}) = \frac{[OH^-]^6}{[AlOOH]^6[Al(OH)_4^-]^6[Si(OH)_4]^{14}} \quad [7]$$

or in logarithmic form

$$\log K_{sp}(NAS_{gel}) = 6\log[OH^-] - 6\log[AlOOH] - 6\log[Al(OH)_4^-] - 14\log[Si(OH)_4] \quad [8]$$

Rewriting Equation 8 in terms of the species measured in the SRS Evaporator feed tanks, e.g. Al(M), Si(M), OH(M), multiplying both sides by –1, and assuming that the Al from AlOOH exists in an aqueous form because diaspore is not kinetically favored to form in the short evaporator residence times gives the following equation:

$$-\log \mathrm{Q}(\mathrm{NAS}_{\mathrm{gel}})_{25^\circ\mathrm{C}} = 12\log[\mathrm{Al(M)}] + 14\log[\mathrm{Si(M)}] - 6\log[\mathrm{OH(M)}] \quad [9]$$

Equation [9] represents the formation of the aluminosilicate “cage” structure of the NAS_{gel}. Basing the SRS evaporator process control model on Equation [9] allowed an ordinary least squares (OLS) correlation of the measured ambient tank concentrations to saturation of those solutions in the evaporator pot after a 40 wt % nominal evaporation (Figure 4). The simplified model is based only on three chemical parameters that are routinely measured in the tank farm, e.g. log[Al(M)], log[Si(M)]), and log[OH(M)]. The OLS correlation between evaporator pot saturation and ambient tank chemisty is given in Equation [10] and defined as the nominal SRS evaporator model as derived in Part I.[3]

$$\log(Q/K)_{NAS\,120-140°C/40\%evap} = 36.4450 + 0.9696(12\log[Al(M)] + 14\log[Si(M)] - 6\log[OH(M)] \quad [10]$$

where the tank chemistry is expressed on the RHS of Equation 10, hereafter referred to as log Q $(NAS)_{25°C}$, and the supersaturation index of the feed in the evaporator pot on the LHS is hereafter referred to as log $(Q/K)_{NAS}$. The R^2 of the OLS correlation given by Equation [10] is 0.90 based on data pooled from both F-area laboratory and SRTC. The SRTC analytic measurements are shown in pink and the F-Area laboratory data in gray.

The nominal process model from Part I[3] of this study in Figure 4 can be compared to the solubility product criteria, [Al]*[Si] in $M^2 \sim 10^{-4}$, recently used by Wilmarth[36,37] to determine the acceptability of feed tank solutions for processing in the SRS 3H-Evaporator. The Wilmarth solubility product is shown in Figure 4 compared to recent operational data for Tank 46F. Recent Tank 46F samples have been measured by SRTC and so the apparent operational limit shown in Figure 4 is based on qualified Si data (sample FTF-046 from the 2F drop tank; log $Q(NAS)_{25°C}$ of –43.3. Additional data supporting this limit will be discussed in Section 6.2. Sample FTF-046 corresponds to a log $(Q/K)_{NAS}$ limit of –5.5 based on Equation 10. It should be noted that due to random error in the model and the data the upper 95% error band in the nominal correlation could be as high as saturation, e.g. a log $(Q/K)_{NAS}$ of close to zero, -0.576, (see Table I).

As qualified Si data is accumulated this apparent operational limit may be moved. There are several historic samples from 1992 on Figure 4 that have log Q $(NAS)_{25°C}$ values more positive than –43.3. The pink symbols Y (Tank 30), square (Tank 43) and Z (Tank 26) indicate the analyses were performed at SRTC. However, these samples had not been filtered, e.g. contributions from colloidal sources of Si had not been accounted for. The log $(Q/K)_{NAS}$ values for these samples for the nominal temperature and evaporation is given in Table II and demonstrates that operational limits, within the error of the modeling, may be more positive than log $(Q/K)_{NAS}$ = -5.5. This is not unreasonable as silicate solutions can be >200% supersaturated at temperature and not precipitate until the solutions are cooled.[31] However, the apparent operational limit is currently set conservatively log Q $(NAS)_{25°C}$ of –43.3 corresponding to log $(Q/K)_{NAS}$ of –5.50 based on reliable Si analyses as discussed in Section 4.3.

Table I. Calculated log $(Q/K)_{NAS}$ for Operational Errors Defined By Tank 46 Process Samples

Temperature	**Equation Used**	**Log $(Q/K)_{NAS}$ for Sample FTF-046**
120/140°C pooled data	Upper 95% Error	-0.576
120/140°C pooled data	Equation 10	-5.501
120/140°C pooled data	Lower 95% Error	-10.426

Table II. Calculated Log $(Q/K)_{NAS}$ for Historic (1992) Samples from Tanks 30, 43, and 26

Temperature	**Equation Used**	**Log $(Q/K)_{NAS}$ Sample 199672 (Tank 30)**	**Log $(Q/K)_{NAS}$ Sample 199432 (Tank 43)**	**Log $(Q/K)_{NAS}$ Sample 193275 (Tank 26)**
120/140°C pooled data	Upper 95% Error	-1.458	+3.693	+3.044
120/140°C pooled data	Equation 10	-6.380	-1.256	-1.901
120/140°C pooled data	Lower 95% Error	-11.302	-6.205	-6.845

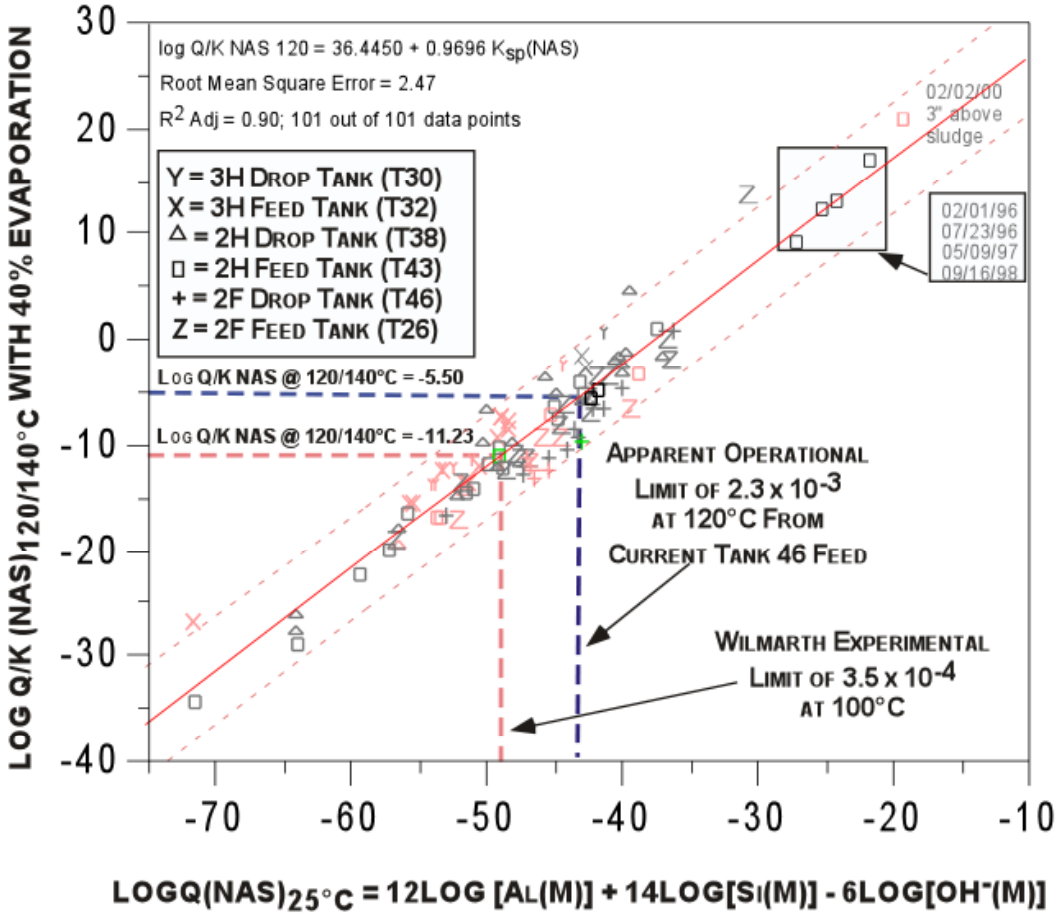

Figure 4. Nominal process control model for the SRS evaporators. This model is based on the equilibrium between diaspore and NAS_{gel} represented on the activity diagrams in Part I[3] and Equations [5] to [10]. It provides an OLS correlation between ambient feed tank chemistry and saturation of these solutions in the evaporator after a 40 wt % nominal evaporation in the 120-140°C temperature range. The intercept includes the evaporation term, the numeric conversions from molar to molal concentrations, corrections for the activity coefficients, and temperature corrections for the solubility of the solid species, diaspore and NAS_{gel} The stoichiometry of the x-axis is defined by the stoichiometry of the NAS_{gel} and cannot be applied to phases with other stoichiometries.

4.0 RECENT ANALYTIC DATA AVAILABLE FOR EVAPORATOR MODELING

4.1 Availability of Analytic Data

A compilation of molar chemical analyses for Tanks 30, 32, 26, 46, 43, and 38 appears in Table III and Table IV for the time period February 2001 to June 2002. This recent tank data is discussed in this study (but not used in modeling) while previous tank data is modeled in Part I[3] and Part II.[4] As with the previous studies there were sparse and incomplete data in the tank farm historic records. Data for several cations were missing from the tank farm historic records for minor cation species such as Fe and K, etc. In these cases ½ the instrument detection limit was substituted assuming that a small concentration below the detection limit was probably present. This accounts for errors of 100-200% for a concentration at or near the instrument detection limit. Na analyses, when available, were added into Table III and Table IV using data from two reports by Wilmarth.[32, 33] Conversely, Wilmarth did not analyze for the cation K^+ nor several anions, e.g. Cl, CO_3^{2-}, F^-, PO_4^{3-}, SO_4^{2-}. When minor anion species such as these were missing, ½ the instrument detection limit was substituted in the same manner as for missing minor cation constituents.

All available data modeled was measured in the laboratory at 25°C regardless of the tank temperature at the time it was sampled. Tank temperatures can vary from 40°C to 75°C but this cannot be accounted for during measurement. All measurements from 1992-2002 have been modeled by consistently using analyses measured at 25°C.

4.2 Consistency of Analytic Data

In order to use the chemical analyses compiled in Table III and Table IV for modeling, the data had to be made internally consistent, e.g., anion and cation charges were balanced. Since few measured Na^+ molarities were available no adjustments were made to the molarities of the three principal anions, OH^-, NO_3^-, and NO_2^- to balance against measured Na+ concentrations. The charge balance calculations assumed that each ionic species was present in its most prevalent valence state; most importantly, Al was modeled as $Al(OH)_4^-$.

In order to account for the effect of temperature on solution densities so that the data in Table III and Table IV could be evaluated at different temperatures, molar concentrations were converted to molalities (Table V and Table VI). The molalities are based on calculated solution densities (Equation 11a).[34] The solution densities were calculated from a calculated Na^+ molarity, $\lfloor Na^+ \rfloor_{calc}$, using Equation 11b derived by Walker and Coleman[34] for H-Canyon waste solutions at 25°C.

$$m = M\left(\frac{weight\ \ solution}{(weight\ \ solution - total\ \ weight\ \ solutes)}\right)\left(\frac{1}{density_{calc}}\right) \qquad [11a]$$

where m = molality
M = molarity

$$\text{weight solutes} = \frac{dissolved\ \ solids\ \ (g/L)}{1000L}$$

$$\text{dissolved solids} = \begin{array}{l} Al(OH)_4^- + Cl^- + CO_3^{-2} + C_2O_4^{-2} + F^- + NO_2^- + NO_3^- \\ + OH^- + PO_4^{-3} + SO_4^{-2} + Fe(OH)_4^- + K^+ + H_2SiO_4^{-2} + \\ UO_2(OH)_{\frac{7}{3}} + [Na^+_{calc}] \end{array}$$

$$density_{calc} \equiv \rho = 1.0133 + 0.040469\left[Na^+\right]_{calc} \qquad [11b]$$

where ρ is the calculated solution density in g/cm^3 and $\left[Na^+\right]_{calc}$ is the calculated molar Na^+ concentration from Equation 11c.

$$\begin{array}{l} Na^+_{calc} = NaAl(OH)_4 + NaCl + Na_2CO_3 + Na_2C_2O_4 + NaF + \\ NaNO_2 + NaNO_3 + NaOH + Na_3PO_4 + Na_2SO_4 + NaFe(OH)_4^- \\ - KOH + Na_2H_2SiO_4 + Na(UO_2)_3(OH)_7 \end{array} \qquad [11c]$$

The molal contributions from CO_3^{-2} and $C_2O_4^{-2}$ were summed as a total CO_3^{-2} contribution, e.g. one mole of $C_2O_4^{-2}$ was considered to be two moles of CO_3^{-2} since Geochemist's Workbench can only accommodate one carbon species at a time. The NO_2^- and NO_3^- were summed as NO_3^- since Geochemist's Workbench can only accommodate one nitrogen species at a time.

In addition to reporting molar concentrations, Table III and Table IV compare calculated and measured solution densities. Solution densities were calculated from Equation 11b. Generally, measured and calculated densities agreed within 2-3%. Several comparisons are as high as 9%. It was assumed that these density measurements were in error but the actual measured values are shown in Table III and Table IV for comparison.

4.3 Quality of Analytic Data

The SRTC and the F-area laboratory both analyzed samples taken between February 2001 and June 2002. The two laboratories never measured the same sample taken on the same day so no comparisons of the analytic bias between the two laboratories can be made for this set of data. However, in Parts I[3] and Part II[4] of this study it was shown that the 210X

dilution performed by the F-area laboratory always caused their Si analyses to be biased high by ~7X compared to those of SRTC.

SRTC has developed a method by which the entire sample (70 mL) is filtered so that the total amount of Si (both soluble and colloidal) can be more accurately determined. The filtrate, representing the soluble silica, is homogeneous and can be accurately measured by ICP. The colloidal silica on the filter is dissolved and measured separately. The two are added together for a final total silica analysis that is representative of the entire sample[32,33] rather than a few milliliters of solution in a pipette. This is the method used to determine the silica for all samples beginning with HTK in Table III and Table IV.

Recently, Coleman[35] has tested a spectrophotometric method from the 1920's that uses molybdic acid to analyze simultaneously for the monosilicic acid in solution, the polysilicic acids, and colloids. Coleman's analyses have verified Wilmarth's analytic results. Because of the high bias in the F-area laboratory Si analyses, only the Si analyses reported by Wilmarth were used for modeling in Part I[3] and Part II[4] of this study. The recent tank data discussed in Section 9.0 of this study is overlain on the model from Part I of this study. The recent data was not used in this study to generate a new model. The recent data was used only for confirmatory understanding of the recent SRS Evaporator operations.

It was noted in Part I[3] and Part II[4] of this study that the evaporator feed tanks are stratified and that there are issues with how representative the dip samples used in modeling are of the entire tank contents. In Part I and Part II of this study, it was shown that the dip samples were fairly representative of the tank chemistry by comparing the modeling results from Variable Depth Samples (VDS) to the results of dip samples taken from the same tanks on the same days. Although there was some variation in the position of the VDS samples and the dip samples taken on the same day, the variation was not significant to the modeling (Table III shows triplicate samples taken on the same date from various heights within Tanks 30 and 32; the corresponding log $Q(NAS)_{25°C}$ are shown not to vary significantly in Table XII). This will be discussed in more detail in Sections 6.2 and 9.0.

Table III. Available Tank 30 and 32 Analytic Data for Recent SRS Evaporator Operation

Date	Description/ Reference	Height (inchs)	Al (M)	Cl (M)	CO_3 (M)	C_2O_4 (M)	F (M)	NO_2 (M)	NO_3 (M)	OH (M)	PO_4 (M)	SO_4 (M)	Fe (M)	K (M)	Si (M)	U (M)	Na Calc (M)	Na Meas (M)	wt salt, g/L	Dens calc g/ml	Dens meas g/ml
Tank 30																					
12/29/01	200202524	dip	0.7	7.60E-03	1.60E-01	2.82E-03	8.70E-03	2.09	2.38	5.46	7.40E-03	1.77E-02	0.00E+00	5.70E-02	9.00E-04	1.53E-05	10.97		670.25	1.46	1.43
10/21/01	200186142	dip	0.1	1.44E-03	5.00E-03	8.00E-03	6.10E-03	0.51	0.70	1.22	2.70E-03	1.94E-02	0.00E+00	3.00E-03	1.50E-03	8.03E-07	2.60		160.18	1.12	1.12
08/16/01	200173820	dip	0.39	7.20E-03	5.00E-03	2.82E-03	9.05E-03	2.98	2.37	5.68	4.10E-03	3.81E-03	0.00E+00	1.22E-03	8.00E-04	9.50E-06	11.47		682.79	1.48	1.49
05/30/01	200154415	dip	0.39	1.44E-03	5.00E-03	2.82E-03	1.20E-02	1.43	2.02	2.71	5.50E-03	4.80E-02	0.00E+00	3.40E-02	2.50E-03	1.82E-05	6.66		434.59	1.28	1.34
1/02	HTK-480[32]	VDS	1.1	1.49E-02	5.00E-03	2.85E-03	2.65E-03	1.72	1.26	9.73	9.10E-03	1.59E-02	5.59E-04	6.10E-02	1.64E-03	3.11E-05	13.85	13.61	751.68	1.57	
1/02	HTK-481[32]	VDS	0.6	1.49E-02	5.00E-03	2.85E-03	2.65E-03	1.76	1.26	9.42	9.10E-03	1.59E-02	5.59E-04	6.10E-02	2.85E-03	3.11E-05	13.08	13.15	683.21	1.54	
1/02	HTK-482[32]	VDS	1.1	1.49E-02	5.00E-03	2.85E-03	2.65E-03	1.92	1.37	9.58	9.10E-03	1.59E-02	5.59E-04	6.10E-02	2.67E-03	3.11E-05	14.01	14.38	768.98	1.58	
6/02	HTK-508[33]	221.9	1.1	1.49E-02	5.00E-03	2.85E-03	2.65E-03	1.70	1.25	11.4	9.10E-03	1.59E-02	5.59E-04	6.10E-02	2.42E-03	3.11E-05	15.49	14.5	816.36	1.64	
6/02	HTK-509[33]	156	0.83	1.49E-02	5.00E-03	2.85E-03	2.65E-03	1.20	0.92	7.8	9.10E-03	1.59E-02	5.59E-04	6.10E-02	1.89E-03	3.11E-05	10.79	13.3	577.89	1.45	
6/02	HTK-511[33]	4	0.97	1.49E-02	5.00E-03	2.85E-03	2.65E-03	1.14	0.85	7.34	9.10E-03	1.59E-02	5.59E-04	6.10E-02	1.28E-03	3.11E-05	10.33		565.84	1.43	
Tank 32																					
12/29/01	200202525	dip	0.32	1.60E-03	5.00E-03	3.20E-03	3.00E-03	0.61	0.88	5.69	6.50E-03	6.22E-02	0.00E+00	1.43E-02	4.00E-04	1.87E-06	7.65		393.69	1.32	1.21
09/17/01	200181081	dip	0.32	1.02E-02	5.00E-03	2.90E-03	8.60E-03	2.12	2.90	5.69	1.00E-02	1.74E-02	0.00E+00	5.40E-02	1.00E-04	1.62E-05	11.07		664.63	1.46	1.41
09/01/01	200181080	dip	0.32	1.50E-03	5.00E-03	3.00E-03	2.80E-03	1.32	2.08	3.975	2.80E-03	2.70E-03	0.00E+00	4.90E-02	1.00E-04	7.31E-06	7.68		467.29	1.32	1.35
08/16/01	200173819	dip	0.21	1.40E-03	5.00E-03	2.80E-03	2.60E-03	0.71	1.17	2.26	2.60E-03	6.20E-03	0.00E+00	2.30E-02	1.00E-04	6.47E-05	4.37		266.54	1.19	1.41
05/15/01	200156480	dip	0.13	6.70E-03	5.00E-02	3.20E-03	6.10E-03	1.04	2.02	3.83	6.80E-03	2.62E-02	0.00E+00	3.90E-02	1.90E-03	1.56E-05	7.17		423.59	1.30	1.44
6/02	HTK-505[33]	196.5	1.1	1.49E-02	5.00E-03	2.85E-03	2.65E-03	1.70	1.20	6.3	9.10E-03	1.59E-02	5.59E-04	6.10E-02	1.42E-03	3.11E-05	10.33		607.98	1.43	
6/02	HTK-506[33]	89	0.93	1.49E-02	5.00E-03	2.85E-03	2.65E-03	2.10	1.60	7.4	9.10E-03	1.59E-02	5.59E-04	6.10E-02	1.67E-03	3.11E-05	12.07	12.4	693.55	1.50	
6/02	HTK-507[33]	77	1	1.49E-02	5.00E-03	2.85E-03	2.65E-03	2.50	1.90	8.7	9.10E-03	1.59E-02	5.59E-04	6.10E-02	1.64E-03	3.11E-05	14.14	13.1	806.90	1.59	

Table IV. Available Tank 26, 46, 43 and 38 Analytic Data for Recent SRS Evaporator Operation

Date	Description/ Reference	Height (inchs)	Al (M)	Cl (M)	C_2O_4 (M)	CO_3 (M)	F (M)	NO_2 (M)	NO_3 (M)	OH (M)	PO_4 (M)	SO_4 (M)	Fe (M)	K (M)	Si (M)	U (M)	Na Calc (M)	Na Meas (M)	wt salt, g/L	Densc alc g/ml	Dens meas g/ml
Tank 38																					
12/26/01	200200335	dip	0.06	5.90E-03	1.90E-01	3.10E-03	2.90E-03	1.48	2.32	5.46	1.13E-02	4.29E-02	0.00E+00	2.20E-02	3.30E-03	1.51E-04	9.81		554.13	1.41	1.34
09/27/01	200180201	dip	0.005	1.40E-03	1.90E-01	2.90E-03	2.70E-03	0.42	0.78	1.82	2.70E-03	1.13E-02	0.00E+00	6.50E-03	1.50E-03	6.01E-05	3.44		191.50	1.15	1.13
07/08/01	200165175	dip	0.01	2.90E-03	1.00E-02	5.90E-03	5.50E-03	0.34	0.36	1.71	5.50E-03	8.60E-03	0.00E+00	1.33E-02	1.40E-03	3.90E-05	2.48		128.42	1.11	1.06
05/16/01	200156413	dip	0.16	3.30E-03	5.00E-02	9.00E-03	2.50E-03	0.46	0.51	1.71	2.50E-03	2.18E-02	0.00E+00	1.22E-02	4.50E-03	2.20E-04	3.01		173.17	1.13	1.17
Tank 43																					
12/27/01	200200601	dip	0.1	1.60E-03	8.00E-02	3.20E-03	3.00E-03	0.83	1.33	2.82	3.00E-03	2.09E-02	0.00E+00	7.10E-03	3.40E-03	1.22E-04	5.30		308.35	1.23	1.22
11/01/01	200188563	dip	0.09	3.90E-03	8.00E-02	3.00E-03	2.80E-03	0.81	1.31	3.02	6.10E-03	1.99E-02	0.00E+00	1.40E-02	1.20E-03	1.61E-04	5.44		311.75	1.23	1.23
10/08/01	200183245	dip	0.19	4.30E-03	1.20E-01	3.20E-03	3.00E-03	0.84	1.38	2.83	6.50E-03	2.24E-02	0.00E+00	1.60E-02	2.50E-03	1.99E-04	5.55		329.73	1.24	1.22
09/27/01	200180202	dip	0.005	3.60E-03	1.00E-01	3.00E-03	2.70E-03	0.85	1.44	3.65	6.70E-03	2.27E-02	0.00E+00	6.64E-03	2.50E-03	1.84E-05	6.23		344.16	1.27	1.24
07/04/01	No ID	dip	0.14	6.80E-03	1.00E-02	6.40E-03	5.90E-03	0.93	1.33	2.65	6.20E-03	2.26E-02	0.00E+00	1.44E-02	4.00E-04	5.76E-05	5.14		306.74	1.22	1.23
05/16/01	20015614	dip	0.5	5.70E-03	5.00E-03	2.90E-03	2.70E-03	0.83	1.23	3.01	6.90E-03	2.24E-02	0.00E+00	1.05E-02	6.70E-03	8.40E-05	5.67		348.32	1.24	1.27
03/08/01	200142705	dip	0.08	7.40E-03	5.00E-03	3.00E-03	2.70E-03	0.84	1.20	2.56	2.70E-03	1.84E-02	0.00E+00	6.50E-03	3.60E-03	5.04E-05	4.76		277.46	1.21	1.20
Tank 46																					
11/01/01	200188683	dip	0.06	2.50E-02	1.30E-01	3.00E-03	7.70E-03	1.95	1.68	9.72	1.34E-02	6.70E-03	0.00E+00	8.60E-02	1.70E-03	4.11E-05	13.68		693.80	1.57	1.46
08/15/01	200171513	dip	0.1	2.90E-03	5.00E-02	6.90E-03	6.90E-03	0.53	1.09	2	5.40E-03	5.97E-02	0.00E+00	1.60E-02	4.00E-04	4.54E-05	3.96		237.35	1.17	1.15
05/23/01	200157905	dip	0.07	3.59E-02	5.00E-03	2.80E-03	7.80E-03	2.48	2.03	1.23	1.76E-02	7.00E-03	0.00E+00	1.07E-01	3.40E-03	2.96E-05	5.84		410.59	1.25	1.55
Tank 26																					
11/01/01	200188682	dip	0.37	2.10E-02	1.40E-01	3.00E-03	2.80E-03	1.59	1.94	8.12	1.16E-02	1.30E-02	0.00E+00	7.50E-02	1.10E-03	2.39E-05	12.32		664.85	1.51	1.42
08/15/01	200171514	dip	0.95	2.49E-02	5.00E-03	2.90E-03	6.20E-03	2.03	1.56	9	1.31E-02	1.08E-02	0.00E+00	8.30E-02	7.00E-04	4.75E-05	13.57		752.92	1.56	1.46
05/27/01	200158849	dip	0.31	2.35E-02	5.00E-03	3.30E-03	3.10E-03	1.88	2.00	8.12	1.20E-02	1.90E-02	0.00E+00	8.10E-02	3.00E-03	2.16E-06	12.35		669.83	1.51	1.47

Table V. Tank 30 and 32 Modeling Data for Recent SRS Evaporator Operation

Date	Description/ Reference	Height (inches)	Al (m)	Cl (m)	CO_3+ C_2O_4 (m)	F (m)	NO_2 (m)	NO_3 (m)	OH (m)	PO_4 (m)	SO_4 (m)	Fe (m)	K (m)	Si (m)	U (m)	Na Calc (m)	NO_2+ NO_3 (m)
Tank 30																	
12/29/01	200202524	dip	8.89E-01	9.66E-03	2.10E-01	1.11E-02	2.66E+00	3.02E+00	6.94E+00	9.40E-03	2.25E-02	0.00E+00	7.24E-02	1.14E-03	1.95E-05	1.39E+01	5.68E+00
10/21/01	200186142	dip	1.04E-01	1.50E-03	2.19E-02	6.36E-03	5.29E-01	7.27E-01	1.27E+00	2.82E-03	2.02E-02	0.00E+00	3.13E-03	1.56E-03	8.37E-07	2.72E+00	1.26E+00
08/16/01	200173820	dip	4.91E-01	9.06E-03	1.34E-02	1.14E-02	3.74E+00	2.98E+00	7.15E+00	5.16E-03	4.80E-03	0.00E+00	1.53E-03	1.01E-03	1.20E-05	1.44E+01	6.73E+00
05/30/01	200154415	dip	4.60E-01	1.69E-03	1.25E-02	1.41E-02	1.68E+00	2.38E+00	3.20E+00	6.48E-03	5.66E-02	0.00E+00	4.01E-02	2.95E-03	2.15E-05	7.85E+00	4.06E+00
1/02	HTK-480[32]	VDS	1.34E+00	1.81E-02	1.30E-02	3.22E-03	2.09E+00	1.53E+00	1.18E+01	1.11E-02	1.93E-02	6.80E-04	7.42E-02	1.99E-03	3.78E-05	1.68E+01	3.63E+00
1/02	HTK-481[32]	VDS	6.98E-01	1.73E-02	1.25E-02	3.08E-03	2.05E+00	1.47E+00	1.10E+01	1.06E-02	1.85E-02	6.50E-04	7.10E-02	3.31E-03	3.62E-05	1.52E+01	3.51E+00
1/02	HTK-482[32]	VDS	1.36E+00	1.84E-02	1.32E-02	3.27E-03	2.37E+00	1.69E+00	1.18E+01	1.12E-02	1.96E-02	6.89E-04	7.52E-02	3.29E-03	3.83E-05	1.73E+01	4.06E+00
6/02	HTK-508[33]	221.9	1.34E+00	1.81E-02	1.30E-02	3.22E-03	2.06E+00	1.52E+00	1.38E+01	1.10E-02	1.93E-02	6.78E-04	7.41E-02	2.94E-03	3.77E-05	1.88E+01	3.58E+00
6/02	HTK-509[33]	156	9.52E-01	1.71E-02	1.23E-02	3.04E-03	1.38E+00	1.06E+00	8.95E+00	1.04E-02	1.82E-02	6.41E-04	7.00E-02	2.16E-03	3.57E-05	1.24E+01	2.43E+00
6/02	HTK-511[33]	4	1.12E+00	1.72E-02	1.24E-02	3.06E-03	1.32E+00	9.82E-01	8.48E+00	1.05E-02	1.84E-02	6.45E-04	7.05E-02	1.48E-03	3.59E-05	1.19E+01	2.30E+00
Tank 32																	
12/29/01	200202525	dip	3.44E-01	1.72E-03	1.23E-02	3.23E-03	6.58E-01	9.47E-01	6.12E+00	6.99E-03	6.69E-02	0.00E+00	1.54E-02	4.30E-04	2.01E-06	8.23E+00	1.60E+00
09/17/01	200181081	dip	4.02E-01	1.28E-02	1.36E-02	1.08E-02	2.66E+00	3.64E+00	7.14E+00	1.26E-02	2.18E-02	0.00E+00	6.78E-02	1.26E-04	2.03E-05	1.39E+01	6.30E+00
09/01/01	200181080	dip	3.73E-01	1.75E-03	1.28E-02	3.27E-03	1.54E+00	2.42E+00	4.64E+00	3.27E-03	3.15E-03	0.00E+00	5.72E-02	1.17E-04	8.53E-06	8.96E+00	3.97E+00
08/16/01	200173819	dip	2.27E-01	1.52E-03	1.15E-02	2.82E-03	7.72E-01	1.27E+00	2.45E+00	2.82E-03	6.71E-03	0.00E+00	2.49E-02	1.08E-04	7.01E-05	4.73E+00	2.04E+00
05/15/01	200156480	dip	1.48E-01	7.61E-03	6.41E-02	6.93E-03	1.18E+00	2.29E+00	4.35E+00	7.73E-03	2.98E-02	0.00E+00	4.43E-02	2.16E-03	1.77E-05	8.15E+00	3.47E+00
6/02	HTK-505[33]	196.5	1.34E+00	1.81E-02	1.30E-02	3.22E-03	2.06E+00	1.46E+00	7.65E+00	1.10E-02	1.93E-02	6.78E-04	7.41E-02	1.73E-03	3.78E-05	1.25E+01	3.52E+00
6/02	HTK-506[33]	89	1.15E+00	1.84E-02	1.32E-02	3.28E-03	2.60E+00	1.98E+00	9.16E+00	1.13E-02	1.97E-02	6.91E-04	7.55E-02	2.07E-03	3.85E-05	1.49E+01	4.58E+00
6/02	HTK-507[33]	77	1.28E+00	1.91E-02	1.37E-02	3.40E-03	3.21E+00	2.44E+00	1.12E+01	1.17E-02	2.04E-02	7.18E-04	7.84E-02	2.10E-03	3.99E-05	1.82E+01	5.65E+00

m = molal (mole/Kg H_2O)

Table VI. Tank 26, 46, 43 and 38 Modeling Data for Recent SRS Evaporator Operation

Date	Description/ Reference	Height (inchs)	Al (m)	Cl (m)	CO_3+ C_2O_4 (m)	F (m)	NO_2 (m)	NO_3 (m)	OH (m)	PO_4 (m)	SO_4 (m)	Fe (m)	K (m)	Si (m)	U (m)	Na Calc (m)	NO_2+ NO_3 (m)
Tank 38																	
12/26/01	200200335	dip	7.01E-02	6.89E-03	2.29E-01	3.39E-03	1.72E+00	2.71E+00	6.38E+00	1.32E-02	5.01E-02	0.00E+00	2.57E-02	3.85E-03	1.76E-04	1.15E+01	4.43E+00
09/27/01	200180201	dip	5.20E-03	1.46E-03	2.04E-01	2.81E-03	4.36E-01	8.09E-01	1.89E+00	2.81E-03	1.18E-02	0.00E+00	6.76E-03	1.56E-03	6.25E-05	3.58E+00	1.25E+00
07/08/01	200165175	dip	1.01E-02	2.94E-03	2.21E-02	5.58E-03	3.47E-01	3.64E-01	1.74E+00	5.58E-03	8.73E-03	0.00E+00	1.35E-02	1.42E-03	3.96E-05	2.52E+00	7.11E-01
05/16/01	200156413	dip	1.66E-01	3.43E-03	7.07E-02	2.60E-03	4.77E-01	5.26E-01	1.78E+00	2.60E-03	2.27E-02	0.00E+00	1.27E-02	4.68E-03	2.29E-04	3.13E+00	1.00E+00
Tank 43																	
12/27/01	200200601	dip	1.09E-01	1.74E-03	9.40E-02	3.26E-03	9.03E-01	1.45E+00	3.07E+00	3.26E-03	2.27E-02	0.00E+00	7.72E-03	3.70E-03	1.33E-04	5.77E+00	2.35E+00
11/01/01	200188563	dip	9.76E-02	4.23E-03	9.33E-02	3.04E-03	8.78E-01	1.42E+00	3.28E+00	6.62E-03	2.16E-02	0.00E+00	1.52E-02	1.30E-03	1.75E-04	5.91E+00	2.29E+00
10/08/01	200183245	dip	2.09E-01	4.73E-03	1.39E-01	3.30E-03	9.27E-01	1.52E+00	3.12E+00	7.16E-03	2.47E-02	0.00E+00	1.76E-02	2.75E-03	2.19E-04	6.11E+00	2.45E+00
09/27/01	200180202	dip	5.43E-03	3.91E-03	1.15E-01	2.93E-03	9.25E-01	1.57E+00	3.96E+00	7.27E-03	2.46E-02	0.00E+00	7.21E-03	2.71E-03	2.00E-05	6.76E+00	2.49E+00
07/04/01	No ID	dip	1.53E-01	7.43E-03	2.49E-02	6.45E-03	1.02E+00	1.45E+00	2.90E+00	6.78E-03	2.47E-02	0.00E+00	1.57E-02	4.37E-04	6.30E-05	5.62E+00	2.47E+00
05/16/01	20015614	dip	5.59E-01	6.37E-03	1.21E-02	3.02E-03	9.30E-01	1.38E+00	3.37E+00	7.72E-03	2.50E-02	0.00E+00	1.17E-02	7.49E-03	9.39E-05	6.34E+00	2.31E+00
03/08/01	200142705	dip	8.62E-02	7.97E-03	1.18E-02	2.91E-03	9.06E-01	1.30E+00	2.76E+00	2.91E-03	1.98E-02	0.00E+00	7.00E-03	3.88E-03	5.43E-05	5.13E+00	2.20E+00
Tank 46																	
11/01/01	200188683	dip	6.87E-02	2.86E-02	1.56E-01	8.82E-03	2.23E+00	1.92E+00	1.11E+01	1.53E-02	7.67E-03	0.00E+00	9.85E-02	1.95E-03	4.71E-05	1.57E+01	4.16E+00
08/15/01	200171513	dip	1.07E-01	3.10E-03	6.81E-02	7.37E-03	5.63E-01	1.17E+00	2.14E+00	5.77E-03	6.38E-02	0.00E+00	1.71E-02	4.27E-04	4.85E-05	4.23E+00	1.73E+00
05/23/01	200157905	dip	8.34E-02	4.28E-02	1.26E-02	9.30E-03	2.96E+00	2.42E+00	1.47E+00	2.10E-02	8.34E-03	0.00E+00	1.28E-01	4.05E-03	3.53E-05	6.96E+00	5.38E+00
Tank 26																	
11/01/01	200188682	dip	4.37E-01	2.48E-02	1.72E-01	3.31E-03	1.87E+00	2.29E+00	9.59E+00	1.37E-02	1.53E-02	0.00E+00	8.85E-02	1.30E-03	2.82E-05	1.45E+01	4.17E+00
08/15/01	200171514	dip	1.17E+00	3.08E-02	1.33E-02	7.66E-03	2.51E+00	1.93E+00	1.11E+01	1.62E-02	1.33E-02	0.00E+00	1.03E-01	8.65E-04	5.87E-05	1.68E+01	4.44E+00
05/27/01	200158849	dip	3.68E-01	2.79E-02	1.38E-02	3.68E-03	2.23E+00	2.37E+00	9.63E+00	1.42E-02	2.25E-02	0.00E+00	9.61E-02	3.56E-03	2.56E-06	1.46E+01	4.60E+00

m = molal (mole/Kg H_2O)

5.0 MODELING APPROACH

The molar tank compositions given in Table III and Table IV were converted into molal units which are the units of preference in the GWB software. The conversion formula takes the form[5]

$$\left[i^{+/-}\right]_m = \frac{\left[i^{+/-}\right]_M}{\rho - \sum \rho_{solutes}} \qquad [12]$$

where $\left[i^{+/-}\right]_M$ and $\left[i^{+/-}\right]_m$ are the molar and molal concentrations of ionic species i, respectively, ρ is the solution density in kg/L, and $\Sigma\rho_{solutes}$ is the sum of the partial densities of the dissolved solids. The solution density is calculated using Equation 11b. For each ionic species, the partial dissolved solids density is the product of its molarity and its ionic weight in g/mole. Ionic weights for the most prevalent species in basic solutions are used. These are $Al(OH)_4^-$, Cl^-, CO_3^{2-}, F^-, NO_2^-, NO_3^-, OH^-, PO_4^{3-}, SO_4^{2-}, $Fe(OH)_4^-$, K^+, $H_2SiO_4^{2-}$, $(UO_2)_3(OH)_7^-$, and Na^+. Table V and Table VI reflects the input data in molalities used for modeling.

There is limited solubility data for amorphous SiO_2 and $Al(OH)_3$ in very basic high ionic strength solutions such as those in the SRS 3H Evaporator. This is discussed in more detail in Part I.[3] Comparison with available SiO_2 solubility data in the literature showed that the solubility data used in GWB appeared to adequately represent amorphous SiO_2 equilibria in basic pH. GWB has the mononuclear silicate species H_4SiO_4 called $SiO_2(aq)$, $H_3SiO_4^-$ and $H_2SiO_4^{2-}$ of which the $H_2SiO_4^{2-}$ species is the most prevalent at pH values >13.[36] GWB also contains the two most abundant[37,36] polynuclear silicate species, the tetrameric $H_4(H_2SiO_4)_4^{4-}$ and $H_6(H_2SiO_4)_4^{2-}$ of which the tetrameric $H_4(H_2SiO_4)_4^{4-}$ is the most prevalent species at pH values >13.[36] Polynuclear Si(IV) species are only significant at pH>10 and a total dissolved Si concentrations larger than 10^{-3}M.[38] In addition, the significance of the polynuclear Si(IV) species tends to decrease with increasing temperature.[39] Since the SRS Evaporator Si concentrations are in the 10^{-4}M concentration range (Table III and Table IV) and the polynuclear Si(IV) species are of minimal importance at the elevated evaporator operating temperatures, the absence of the remaining polynuclear Si(IV) species in the GWB database is not considered to significantly impact the modeling.

Examination of the gibbsite solubility data in GWB with that in the literature indicated that Russell's[40] solubility data at a sodium molality of 8.5 would be more appropriate for modeling at the high ionic strength of the SRS Evaporators. The Russel solubility data for gibbsite (alpha aluminum trihydrate) and diaspore (alpha aluminum monohydrate) was added to GWB database and designated as "gibbsite-M" and "diaspore-M" to distinguish these modified aluminum hydroxides from the gibbsite and diaspore solubility already in GWB. The Russel gibbsite-M and diaspore-M were used for modeling the SRS 3H Evaporator solutions. The data for the solubility of $NaAlO_2$ and AlO_2^{-2} of Reynolds and Herting[41] were also added to GWB for completeness. Detailed descriptions of the manner in which the data were added to the GWB database appear in Part I.[3]

The data of Ejaz[20] for the solubility of the NAS gel and Zeolite-A was added to the GWB database as was the data of Gasteiger[23] for an amorphous precipitate containing Zeolite-A and nitrited sodalite, hereafter referred to as "mixed zeolite." The manner in which the aluminosilicate data was added to the GWB is discussed in greater detail in Part I.[3]

6.0 BOUNDING TEMPERATURES

The nominal evaporator process model was generated using a pooled temperature data set where some of the log $(Q/K)_{NAS}$ values had been calculated at 120°C and some had been calculated at 140°C. The log $(Q/K)_{NAS}$ saturation values had been calculated at 120°C for the SRS 2H and 2F Evaporators since these evaporators ran at ~120°C[f] during the time period modeled in Part I[3] of this study. The log $(Q/K)_{NAS}$ saturation values had been calculated at 140°C for the SRS 3H Evaporator since it ran between 135-140°C (data from Kent Gilbreath March 2001) during the time period modeled in Part I[3] of this study. The pooled data set was used for the following reasons:

- The pooled data spanned the actual operating temperatures of the evaporations that had been performed

- Figure B-13 in Part I[3] demonstrated that the solubility of the NAS_{gel} as taken from the literature is a linear function of 1/T(K) for the data examined. The log ([Al]*[Si]) at 120°C and at 140°C was calculated from the equation given in Figure B-13 indicating that there is little predicted change in the NAS_{gel} solubility at elevated temperature.

Currently, the 3H Evaporator is running at temperatures as high as ~180°C. Therefore, the applicability of the model over the range of operating conditions for all SRS evaporators, e.g., from 120°C to 180°C, was investigated to further evaluate the dependency of the log $(Q/K)_{NAS}$ saturation values in Figure 4 to temperature.

In order to evaluate the solution equilibria at elevated temperatures, the solution temperature was incrementally increased, using the polythermal reaction option in GWB. These calculations simulated evaporation by a stepwise removal of 40 wt % of the water from the solution. This amount of evaporation changes the solution density from about 1.4 g/cm^3 to about 1.6 g/cm^3, the latter number being the operational target density for the SRS Evaporators.

---

f Between 1996 and 1999 when the 2H evaporator was shut down, it ran at a nominal temperature of 120-125°C but ranged from a low of 99°C (12/06/97 morning report) to a high of 139°C (5/16/98 morning report).

6.1 Upper and Lower Temperature Bounds

The upper and lower temperature bounds were evaluated by fitting OLS models to the entire tank data set from Part I[3] (101 data points representing all the evaporator systems) shown in Figure 4 at 120°C, 140°C, 165, and 180°C. A comparison was then made of the upper and lower temperature bounds to the nominal evaporator process model developed with the pooled 120°C/140°C data set (Equation 10). The relation of the upper temperature bound to the lower temperature bound was also evaluated. Usage of the model at temperatures above 180°C is complicated by an increasingly large field of crystalline $NaAlO_2$ which intersects the field of NAS_{gel} on the stability diagrams so that Equation 10 no longer applies. In other words, the pertinent equilibrium above 180°C is an equilibrium between $NaAlO_2$ and NAS_{gel} and not AlOOH and NAS_{gel} as defined by Equation 10.

Log $(Q/K)_{NAS}$ values were calculated at 120°C for the 101 tank compositions, which represents the lower bounding temperature at 40 wt % evaporation (Equation 13). Similarly, the log $(Q/K)_{NAS}$ values were computed for all tank compositions at 180°C and 40 wt % evaporation to provide an upper bound for evaporator operations (Equation 14). Calculations at 140°C and 165°C and 40 wt % evaporation are provided as intermediate cases (Equations 15 and 16).

$$\text{Log } Q/K_{(NAS\ @120°C)} = 36.85 + 0.98 \log Q(NAS)_{25°C};\ R^2=0.92 \qquad [13]$$

$$\text{Log } Q/K_{(NAS\ @180°C)} = 37.57 + 0.97 \log Q(NAS)_{25°C};\ R^2=0.91 \qquad [14]$$

$$\text{Log } Q/K_{(NAS\ @165°C)} = 38.04 + 0.98 \log Q(NAS)_{25°C};\ R^2= 0.91 \qquad [15]$$

$$\text{Log } Q/K_{(NAS\ @140°C)} = 37.77 + 0.98 \log Q(NAS)_{25°C};\ R^2= 0.92 \qquad [16]$$

Comparison of Equations 10 and 13 indicated that the response of Equation 10 is dominated by the 78 $\log(Q/K)_{NAS}$ values calculated at 120°C rather than the 23 $\log(Q/K)_{NAS}$ values calculated at 140°C, e.g. the slopes differ by 0.013 and the intercepts by 0.4066. Comparison of Equations 13 and 14 indicates that the slopes of the low temperature (120°C) saturation correlation and the high temperature (180°C) saturation correlation differ by 0.0101. The main difference in the prediction of saturation at the lower temperature (120°C) and upper temperature (180°C) bound is expressed in the intercept term which has a difference of 0.7145 larger in Equation 14. Note that the use of the pooled temperature data set in Equation 10 yields a correlation with slightly more bias (a lower R^2 of 0.90) than the saturation correlations at a single temperature (Equations 13-16 with R^2 values of 0.91 and 0.92).

The 140°C, 165°C, and 180°C data fall within the conservative 95% bias bands (analogous to the error bands) shown in Figure 5 (black dashed lines). Figure 5 also shows that the regression fit for the 165°C (red OLS fit) and 180°C (green OLS fit) data is almost coincident with the regression fit for the pooled 120°C/140°C data (black OLS fit).

6.2 Operational Process Control Limit Temperature Effects

In Part I[3] of this study the nominal process control algorithm for Equation 10 has been tied to operating experience by using the most silica rich sample analyzed at SRTC that was run in the SRS 2F evaporator at 140°C without scaling (FTF-046 from Tank 46). This sample was from a drop tank and the material was recycled to the feed tank and experienced an evaporation of 36% confirming the prediction from the model that this sample could undergo an additional 40% evaporation and remain unsaturated with respect to NAS_{gel}. Sample FTF-046 intersects the abscissa as indicated by the vertical dashed line in Figure 5 below at log $Q(NAS)_{25°C}$ = -43.26. All values up to and including FTF-046 remain undersaturated (negative Q/K) with respect to NAS_{gel} at 180°C.

Table VII shows that the saturation values calculated at 120°C (Equation 13) and 180°C (Equation 14) are bounded within the 95% bias bands of Equation 10. As long as the errorless value for FTF-046 at 180°C, log $Q/K_{(NAS)}$ = -4.508, e.g. is more negative (less saturated) than log $Q/K_{(NAS)}$ = –0.576, the upper 95% bound of Equation 10, the FTF-046 sample solution is predicted to be undersaturated with respect to the NAS_{gel}. This is indeed the case as observed in Table VII.

Three additional samples analyzed in January, 2001 (see Table III samples HTK-480, HTK-481, and HTK-482) from the SRS 3H evaporator confirm the operating limit of log $Q(NAS)_{25°C}$ = -43.3 set using the analysis of sample FTF-046 (the exact number is -43.26). These samples from the SRS 3H evaporator system drop tank (Tank 30) were taken on the same day at different depths. The individual log $Q(NAS)_{25°C}$ values are –44.43, -44.14, and –41.42 respectively demonstrating the variation with depth in the tank. The average log $Q(NAS)_{25°C}$ values for these samples is -43.33, the same value (to the 1st decimal place) as sample FTF-046 from Tank 46 in the SRS 2F evaporator system. The 3H samples were also recycled to the drop tank and experienced a 15%evaporation confirming the prediction from the model that this sample could undergo an additional 40% evaporation and remain unsaturated with respect to NAS_{gel}.

Table VII shows that the saturation values calculated at 120°C (Equation 13) and 180°C (Equation 14) for the Tank 30 samples are lower than the upper 95% model bias given by Equation 10. As long as the errorless value for the pooled Tank 30 samples at 200°C, log $Q/K_{(NAS)}$ = -4.576, e.g. is more negative (less saturated) than log $Q/K_{(NAS)}$ = –0.628, the upper 95% bound of Equation 10, the solution is predicted to be undersaturated with respect to the NAS_{gel}. This is indeed the case as observed in Table VII.

Table VII. Calculated Log $(Q/K)_{NAS}$ for Operating Limit Samples from Tank 46 and Tank 30 at Varying Temperature

Temperature	**Equation Used**	**Log $(Q/K)_{NAS}$ for Sample FTF-046 from Tank 46**	**Log $(Q/K)_{NAS}$ for Pooled Samples HTK-480, 481 and 482 from Tank 30**
120/140°C pooled data	Upper 95% Error Equation 10	-0.576	-0.628
180°C	Equation 14	-4.508	-4.576
165°C	Equation 15	-4.232	-4.297
120/140°C pooled data	Equation 10	-5.501	-5.668
120°C	Equation 13	-5.662	-5.729
120/140°C pooled data	Lower 95% Error Equation 10	-10.426	-10.504

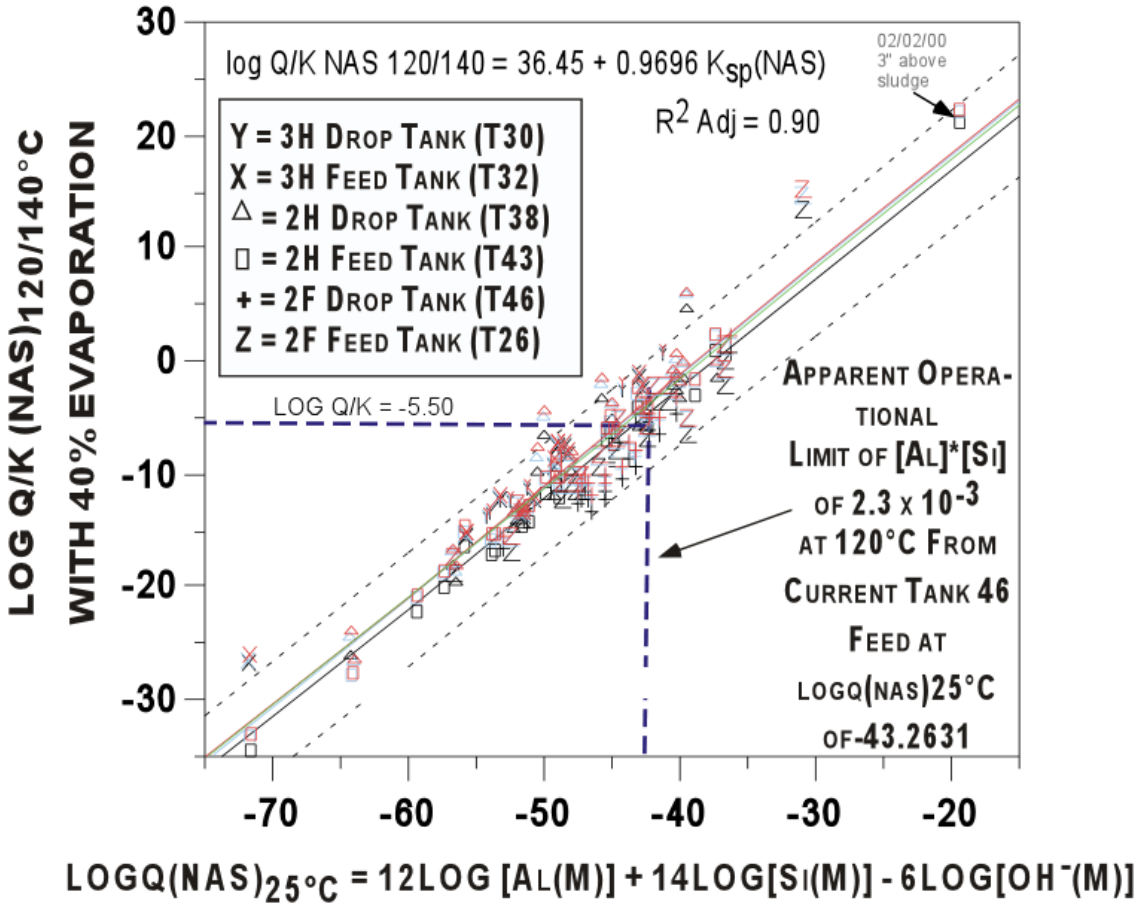

Figure 5. Temperature variation of the nominal process control model. The pooled data set at 120°C/140°C assuming a 40 wt % evaporation are shown in black with the corresponding upper and lower 95% error bands shown as black dashed lines. The 140°C data for 40 wt % evaporation are shown in light blue. The 165°C data at 40 wt % evaporation and the corresponding line of best fit are shown in red. The 180°C data at 40 wt % evaporation and the corresponding line of best fit are shown in green.

In order to quantify the temperature difference for a given tank solution one can subtract Equation 10 derived for the pooled 120/140°C data from Equation 14 derived at 180°C which gives

$$\Delta \text{Log } Q/K_{(NAS)} = (37.57\text{-}36.45) + (0.9726\text{-}0.9696) \log Q(NAS)_{25°C} \quad [17]$$

The solution of Equation 17 can then be solved for each of the 101 data samples and plotted as a function of log Q $(NAS)_{25°C}$ (Figure 6) which gives

$$\Delta \text{Log } Q/K_{(NAS)} = 1.12 + 0.003 \log Q\ (NAS)_{25°C} \quad [18]$$

Figure 6 shows that the temperature difference can be a minimum of 0.91 at log Q $(NAS)_{25°C}$ values of –70 or a maximum of 1.06 at $K_{sp(NAS)}$ of –20. Solving Equation 18 for sample FTF-046 at a $K_{sp(NAS)}$ = -43.3 gives a $\Delta \log Q/K_{(NAS)}$ of 0.99. This indicates that the higher temperature solutions are still undersaturated but they are less undersaturated (by log $(Q/K)_{NAS}$ = 0.91 to 1.06) than the lower temperature solutions, e.g., they have a more positive log $Q/K_{(NAS)}$.

In conclusion, the temperature effects on the log $(Q/K)_{NAS}$ saturation index are negligible in the temperature range over which the SRS evaporators operate, e.g. 120-180°C. Since the elevated temperature log $(Q/K)_{NAS}$ values fall within the 95% bias of the nominal evaporator process model, the errors associated with using the model developed for the pooled 120°C/140°C data for solutions being processed at 165°C is sufficiently accounted for.

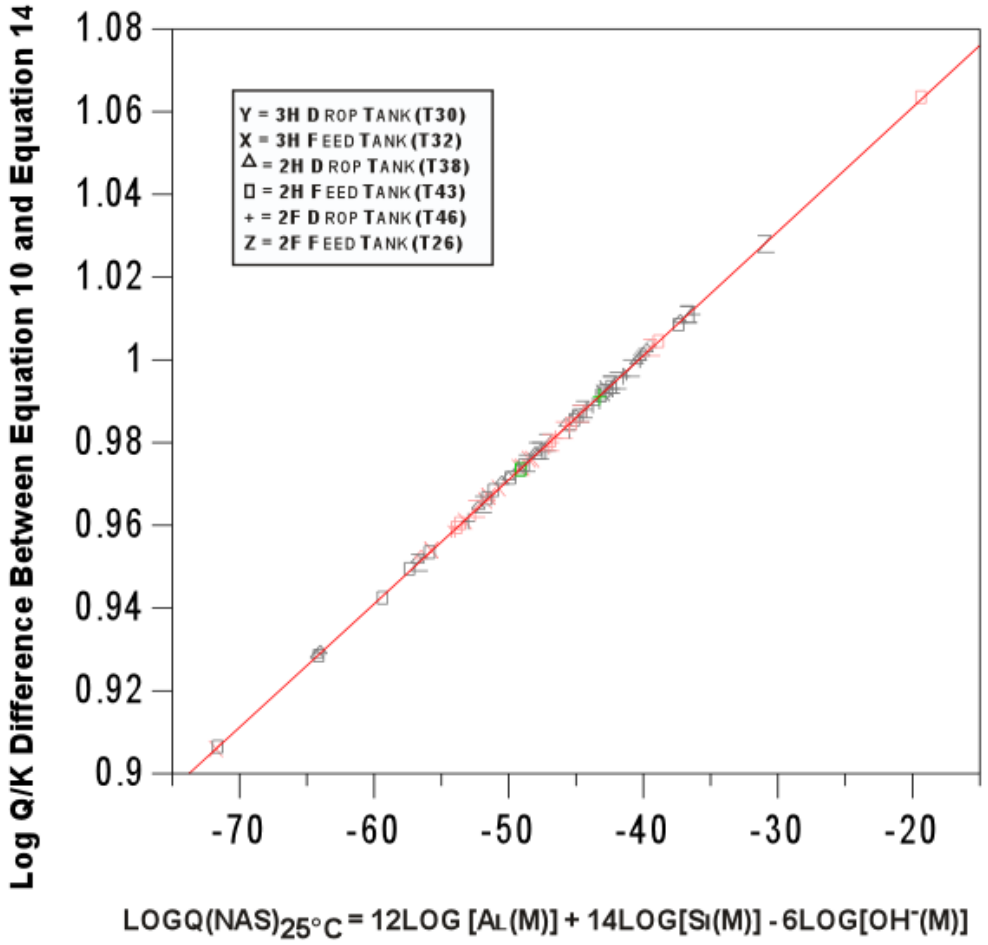

Figure 6. Difference in log Q/K calculation between Equation 10 (pooled 120°/140°C) and Equation 14 (180°C).

7.0 BOUNDING EVAPORATION PERCENTAGES

The nominal evaporator process model was generated assuming a nominal evaporation of 40 wt %. During routine operation the evaporators do not always achieve 40 wt %. This is especially true when the evaporator solutions approach their operational target density of 1.6 g/cm^3. Therefore, upper and lower bounds on evaporation were calculated spanning 10 wt % to 60 wt % evaporations. Since the temperature effects on the model were shown (see Section 6) to be of minimal impact (shifting the log $(Q/K)_{NAS}$ by only 0.91-1.06), the varying evaporation percentages will be calculated using the pooled 120°C/140°C data set. The calculation for the 101 data points from all the evaporator feed and drop tanks gives the following equations for various evaporation rates:

$$\text{Log } Q/K_{(\text{NAS @10 wt \% evaporation})} = 32.80 + 0.9587 \log Q\,(NAS)_{25°C};\ R^2=0.90 \qquad [19]$$

$$\text{Log } Q/K_{(\text{NAS @20 wt \% evaporation})} = 33.84 + 0.9618 \log Q\,(NAS)_{25°C};\ R^2=0.90 \qquad [20]$$

$$\text{Log } Q/K_{(\text{NAS @30 wt \% evaporation})} = 35.04 + 0.9653 \log Q\,(NAS)_{25°C};\ R^2=0.90 \qquad [21]$$

$$\text{Log } Q/K_{(\text{NAS @40 wt \% evaporation})} = 36.45 + 0.9696 \log Q\,(NAS)_{25°C};\ R^2=0.90 \qquad [10]$$

$$\text{Log } Q/K_{(\text{NAS @50 wt \% evaporation})} = 38.07 + 0.9734 \log Q\,(NAS)_{25°C};\ R^2=0.90 \qquad [22]$$

$$\text{Log } Q/K_{(\text{NAS @60 wt \% evaporation})} = 40.11 + 0.9786 \log Q\,(NAS)_{25°C};\ R^2=0.90 \qquad [23]$$

Equations 19-23 are shown visually in Figure 8 where they are overlain on Equation 10, the nominal evaporator model for 40 wt % evaporation. It is interesting to note that the 10-30 wt % and 50-60 wt % correlations fall within the 95% error of the model for the nominal 40 wt % evaporation model referred to in this study as the nominal evaporator model.

The log $(Q/K)_{NAS}$ values for sample FTF-046 at various evaporations lies within the 95% bias of the nominal evaporator model assuming that there is no model error. If the model error is considered, which it must be, then the upper 95% bias for each evaporation percentage will be the limiting value in determining what evaporation a given feed solution can experience without precipitating aluminosilicate scale.

Equations 10 and 19-23 can be solved for varying log $Q\,(NAS)_{25°C}$ values at the varying evaporation percentages (Table VIII). This allows operational flexibility in applying the model to evaporator operations when less than or more than a 40% nominal evaporation is being performed. The equations can be solved based on the upper 95% bounding log $(Q/K)_{NAS}$ in Table VII for the nominal evaporator model at 40 wt % evaporation, e.g. log $(Q/K)_{NAS}$ = - 0.576. The equations can also be solved based on the log $(Q/K)_{NAS}$ of Equation 10 assuming no model error, e.g. the value of –5.50. One can, therefore, solve

Equation 10 and Equations 19-23 assuming log $(Q/K)_{NAS}$ = -0.576 or –5.50 because they are equivalent in preventing saturation with respect to aluminosilicate scale, NAS_{gel}. The latter approach is chosen for convenience since the model value of –5.50 is shown in Part I[3] of this study and in Figure 4 of this report. The log Q $(NAS)_{25°C}$ values for the different evaporation percentages are given in Table VIII and the resulting OLS fit of the data shown in Figure 7.

Table VIII Percent Evaporation Vs. Ksp(NAS) Values for Process Control

Percent Evaporation	Log $(Q/K)_{NAS}$	log Q $(NAS)_{25°C}$
10	-5.50	-39.946
20	-5.50	-40.906
30	-5.50	-41.995
40	-5.50	-43.260
50	-5.50	-44.762
60	-5.50	-46.611

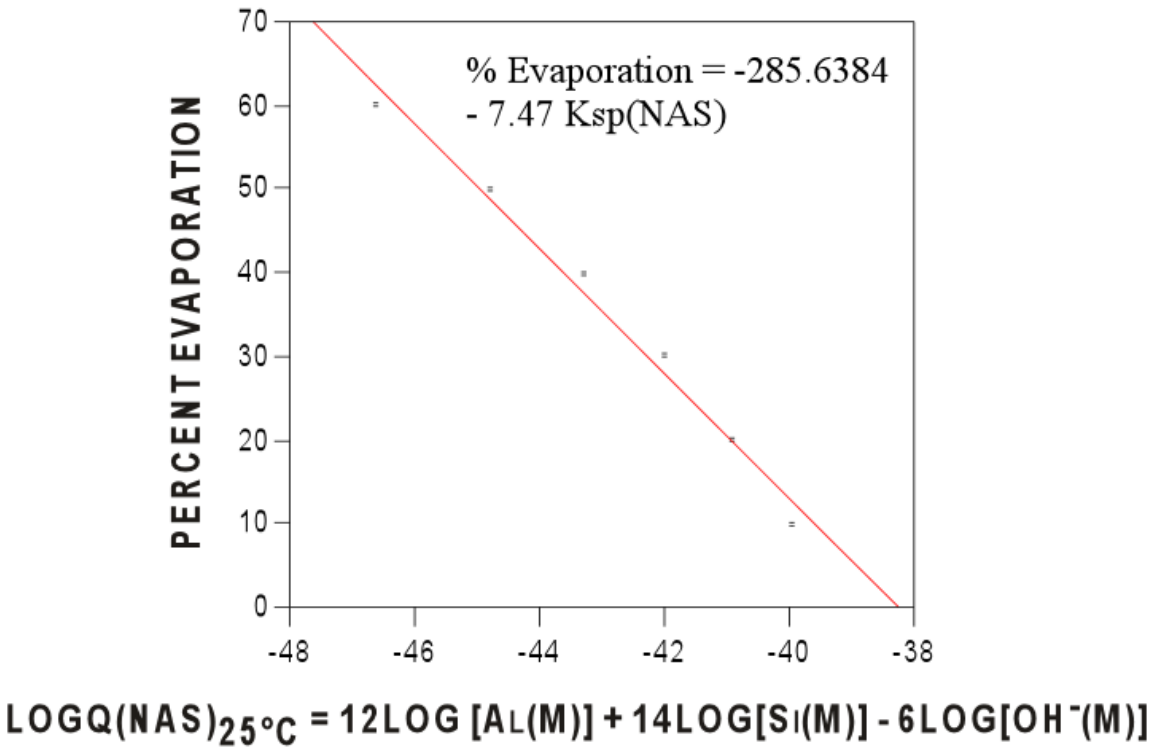

Figure 7. Relation of log Q $(NAS)_{25°C}$ to percent evaporation for process control.

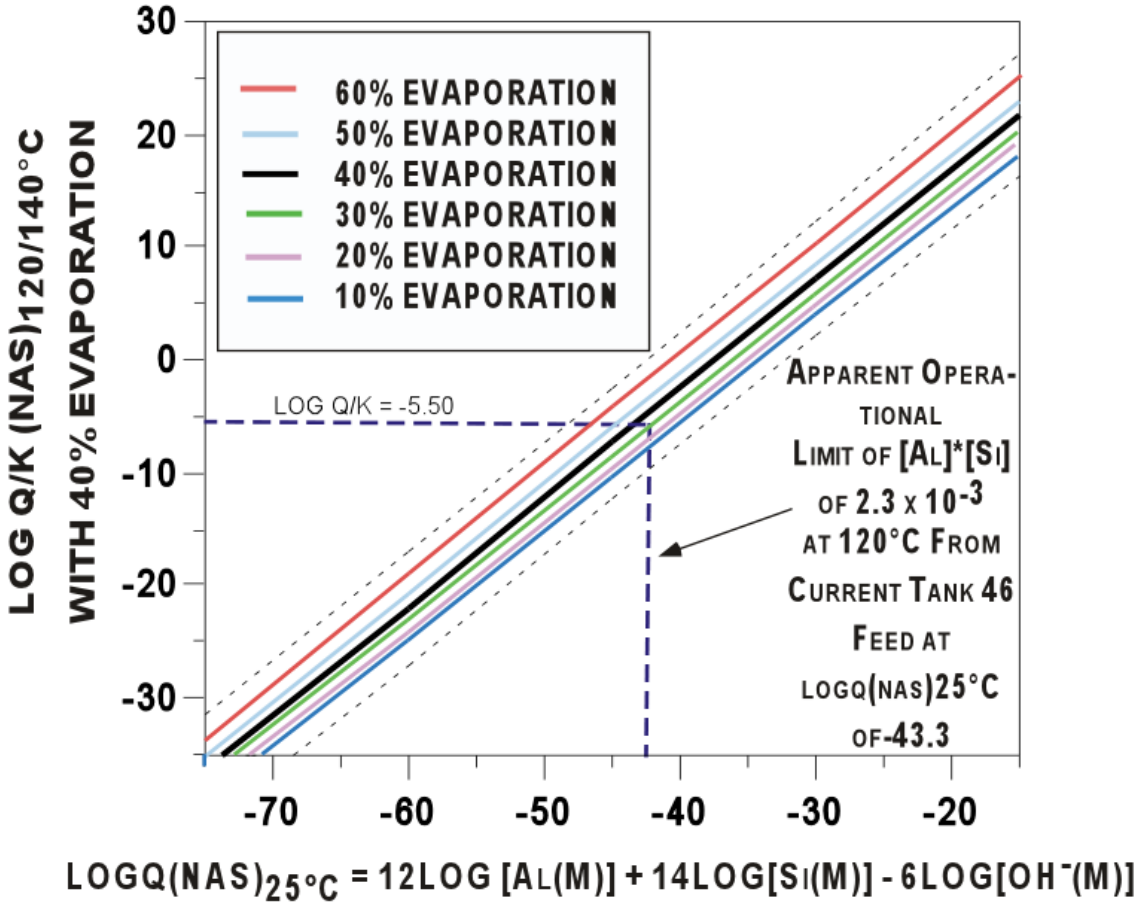

Figure 8. Evaporator model at various weight percent evaporations varying from 10% to 60%. Note that the 10 to 60 wt % evaporations fall within the 95% model bias bounds of the nominal 40 wt % evaporation model.

8.0 BOUNDING COMPOSITIONS[13]

Geochemist's Workbench (GWB) has been used to estimate the $\log(Q/K)_{NAS}$ for a number of components in the evaporator based upon 101 evaporator chemistries and comparative process histories (Part I[3] of this study). The ranges covered in the study to date are provided in Table IX. The NO_2 and NO_3 values are grouped because this is the way they will are treated in GWB. Na was omitted because the Na value was a calculated value from mass balance considerations (see Equation 11c). This left 12 composition parameters, plus temperature, plus evaporation as 14 of the allowable 16 parameters for the OLH analysis (see Section 2.3 for discussion).

Table IX. Ranges Modeled in Part I and Part II of This Study

	Minimum (M)	**Maximum (M)**
Al (M)	0.005	3.000
Cl (M)	0.0014	0.12
CO_3 (M)	0.005	0.62
C_2O_4 (M)	0.0012	0.15
F (M)	0.00000526	0.012
Fe (M)	0	0.358
NO_2 (M)	0.273	2.975
NO_3 (M)	0.300	3.423
$[NO_2]+[NO_3]$	0.654	5.343
OH (M)	0.5	15.2
K (M)	0.001215	0.18
PO_4 (M)	0.0025	0.0546
SO_4 (M)	0.0026	0.0821
Si (M)	0.00002136	0.1436588
U (M)	8.025E-07	0.0155
Na (M)	1.416	18.616

Reasonable maximum concentrations for $[NO_2]$, $[NO_3]$, and [OH] in the tank farm were determined[f] to be 4M, 7M, and 16M, respectively. Somewhat wider ranges for the upper concentration bounds for $[NO_2]$, $[NO_3]$, and [OH] of 6M, 7M, and 16M were used in modeling to examine the model flexibility. In addition, the temperature was varied between 40°C and 180°C and the evaporation percentage between 0 and 80%.

In Part I[3] of this study it was determined that the undersaturated log $(Q/K)_{NAS}$ values were found either when the [Si] or [Al] concentrations were very low. Furthermore, because

[f] D.T. Hobbs of SRTC

the predictions should be strong functions of the ln([]) values (and the concentrations, if measured, would likely be more lognormal than Gaussian in nature), the Orthogonal Latin Hypercube (OLH) designs were developed using ln([]) values. These are provided in Table X (where because the minimum [Fe] was 0.0, the minimum concentration for all those shown in the table—which is that for [U]—was substituted for the minimum [Fe]).

Table X. Tank Farm Bounding Regions Including Logarithmic Transformations Assumed in the OLH Statistical Analysis

	Min	**Min (log)***	**Max**	**Max (log)***
Al (M)	0.005	-2.3010	4	0.6021
Cl (M)	0.00020	-3.6990	0.12	-0.9208
CO_3 (M)	0.005	-2.3010	2.875	0.4586
C_2O_4 (M)	0.0005	-3.3010	0.15	-0.8239
$[CO_3]+[C_2O_4]$	0.0055	-2.2596	3.025	0.4807
F (M)	0.00000526	-5.2840	0.2415	-0.6171
Fe (M)	0	-6.3010	0.3581021	-0.4460
NO_2 (M)	0.0921	-1.0357	6.0	0.7782
NO_3 (M)	0.0173	-1.7620	7.0	0.8451
$[NO_2]+[NO_3]$	0.1094	-0.9610	13	1.1139
OH (M)	0.01	-2.000	16	1.2041
K (M)	0.001215	-2.9154	0.5	-0.3010
PO_4 (M)	0.0005	-3.3010	0.145	-0.8386
SO_4 (M)	0.0005	-3.3010	0.8875	-0.0518
Si (M)	0.00002136	-4.6716	0.1785714	-0.7482
U (M)	5.00E-07	-6.3010	0.0155	-1.8097
Na (M)	0.2015	-0.6957	23	1.3617

* the design was performed in natural log but values are given in this table as $\log_{10}$.

The optimized design resulting from the natural logarithmic-transformed ranges in Table X (see footnote) are provided in Table IX. The molar concentrations in these design matrices were then transformed into their corresponding molal concentrations; the total dissolved solids (TDS) values, specific gravities, and molal concentrations were estimated; and then the values were run through GWB. The GWB results for the optimized designs are provided in Table XII (and Figure 9), respectively. The results do an excellent job of covering the saturation points (i.e., $\log(Q/K)_{NAS} = 0$) for the NAS_{gel} phase as shown in Figure 9. Also the biases in the model predictions appear to be reasonably distributed for the optimized design; however, this may provide a false sense of security as all deviations shown are biases and not the random measurement errors normally associated with such plots.

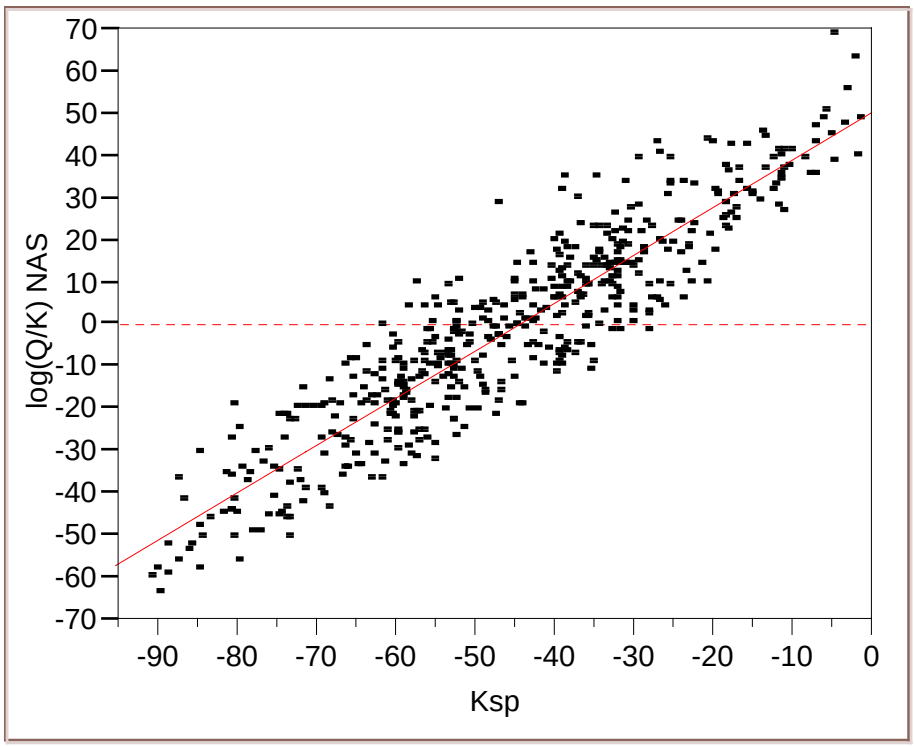

Linear Fit

log(Q/K) NAS = 50.283366 + 1.1324382 Ksp

Summary of Fit

RSquare	0.844761
RSquare Adj	0.844457
Root Mean Square Error	9.540176
Mean of Response	-1.51016
Observations (or Sum Wgts)	513

Figure 9. Bivariate Fit of log Q/K for NAS_{gel} versus log $Q(NAS)_{25°C}$ (K_{sp}) for the optimized Orthogonal Latin Hypercube model.

Table XI. OLH Logarithm-Based Design Matrix Corresponding to the Optimized T Matrix (concentrations are molar)

Al	Cl	CO_3	C_2O_4	F	Fe	NO_2	NO_3	OH	K	PO_4	SO_4	Si	U	T(ºC)	Evap
0.446	0.000	0.016	0.005	0.0004	0.0000	0.262	0.028	0.045	0.039	0.057	0.682	0.022	0.0062	142.5	0.455
1.804	0.015	0.056	0.001	0.0001	0.0001	0.270	0.028	0.228	0.004	0.002	0.011	0.000	0.0001	102.1	0.045
0.318	0.001	1.348	0.002	0.0003	0.0002	0.482	0.025	0.068	0.003	0.013	0.734	0.003	0.0008	112.7	0.444
1.188	0.011	0.357	0.006	0.0000	0.0000	0.149	0.019	0.034	0.105	0.002	0.004	0.000	0.0000	50.4	0.089
0.226	0.001	0.064	0.053	0.0000	0.0000	0.203	0.138	0.082	0.429	0.001	0.260	0.004	0.0001	143.1	0.552
0.742	0.008	0.005	0.017	0.0000	0.0000	0.141	0.024	0.012	0.007	0.014	0.003	0.000	0.0000	81.6	0.036
3.948	0.003	0.580	0.076	0.0000	0.0002	0.145	0.075	0.203	0.002	0.001	0.037	0.018	0.0008	134.3	0.745
0.272	0.119	0.187	0.023	0.0002	0.0000	0.563	0.099	0.013	0.043	0.029	0.002	0.000	0.0000	65.2	0.150
0.392	0.000	0.006	0.005	0.0032	0.0001	0.095	0.070	0.032	0.108	0.013	0.003	0.130	0.0001	168.2	0.700
2.849	0.013	0.009	0.003	0.2365	0.0000	0.170	0.036	0.065	0.003	0.002	0.200	0.001	0.0000	78.6	0.273
2.252	0.000	2.082	0.004	0.0162	0.0000	0.725	0.332	0.081	0.015	0.034	0.013	0.142	0.0001	138.2	0.608
3.510	0.069	0.316	0.001	0.0024	0.0000	0.616	0.236	0.222	0.091	0.001	0.825	0.000	0.0000	94.1	0.105
3.081	0.002	0.063	0.134	0.0344	0.0000	0.326	0.064	0.011	0.035	0.002	0.012	0.041	0.0001	142.0	0.714
0.335	0.093	0.036	0.092	0.0041	0.0001	0.417	0.049	0.256	0.001	0.047	0.107	0.000	0.0000	48.2	0.338
0.508	0.003	0.272	0.112	0.0672	0.0000	0.545	0.044	0.043	0.005	0.006	0.003	0.004	0.0003	169.3	0.556
0.279	0.017	2.243	0.021	0.0071	0.0003	0.573	0.344	0.055	0.151	0.137	0.276	0.000	0.0000	45.7	0.375
0.163	0.001	0.011	0.004	0.0001	0.0017	0.475	0.071	0.039	0.048	0.010	0.023	0.000	0.0014	136.3	0.717
0.927	0.006	0.052	0.002	0.0004	0.0056	0.427	0.133	0.176	0.004	0.002	0.003	0.003	0.0000	105.9	0.219
0.339	0.000	0.716	0.001	0.0007	0.0024	0.094	0.018	0.062	0.020	0.016	0.022	0.000	0.0002	131.1	0.531
1.712	0.011	0.137	0.001	0.0000	0.2115	0.459	0.295	0.313	0.112	0.001	0.001	0.038	0.0000	73.4	0.320
1.562	0.001	0.054	0.073	0.0000	0.2752	0.092	0.257	0.016	0.025	0.008	0.027	0.001	0.0002	132.7	0.686
1.301	0.049	0.020	0.018	0.0000	0.1124	0.160	0.205	0.389	0.002	0.041	0.003	0.013	0.0000	82.9	0.267
0.951	0.002	0.989	0.043	0.0006	0.1806	0.217	0.030	0.052	0.023	0.008	0.048	0.000	0.0011	123.4	0.791
0.326	0.030	1.176	0.010	0.0000	0.0033	0.354	0.039	0.372	0.129	0.103	0.002	0.009	0.0000	67.3	0.122
1.389	0.003	0.010	0.002	0.0043	0.0016	0.479	0.076	0.116	0.088	0.011	0.001	0.002	0.0108	167.1	0.761
0.201	0.044	0.006	0.005	0.0241	0.3488	0.101	0.263	0.084	0.009	0.003	0.029	0.023	0.0000	66.8	0.381
3.420	0.000	0.168	0.007	0.0398	0.0120	0.219	0.038	0.087	0.018	0.028	0.004	0.002	0.0119	166.9	0.516
1.976	0.103	1.052	0.002	0.0534	0.0011	0.124	0.027	0.279	0.086	0.003	0.249	0.103	0.0000	49.3	0.116
1.070	0.004	0.021	0.082	0.0618	0.0309	0.642	0.024	0.035	0.089	0.001	0.015	0.001	0.0028	135.2	0.548
0.184	0.034	0.069	0.131	0.0046	0.0022	0.098	0.155	0.083	0.003	0.011	0.099	0.019	0.0000	92.8	0.014
0.251	0.001	0.154	0.012	0.0231	0.0719	0.400	0.062	0.291	0.002	0.003	0.004	0.001	0.0002	126.7	0.763
0.880	0.008	0.821	0.061	0.0014	0.0043	0.298	0.021	0.019	0.032	0.055	0.074	0.033	0.0000	69.3	0.288
0.610	0.002	0.096	0.005	0.0004	0.0000	2.329	0.049	0.047	0.050	0.024	0.447	0.011	0.0000	167.7	0.667
0.381	0.020	0.005	0.001	0.0003	0.0000	1.064	0.036	0.166	0.004	0.004	0.002	0.001	0.0002	104.0	0.325
3.651	0.004	0.308	0.002	0.0000	0.0001	0.875	0.213	0.161	0.008	0.017	0.440	0.008	0.0001	139.8	0.658
0.179	0.110	0.481	0.001	0.0003	0.0000	2.632	0.061	0.106	0.052	0.002	0.001	0.000	0.0072	63.8	0.275
2.500	0.001	0.061	0.011	0.0000	0.0000	3.862	0.055	0.016	0.284	0.001	0.081	0.008	0.0000	116.8	0.588
1.002	0.077	0.006	0.139	0.0000	0.0000	5.440	0.117	0.020	0.002	0.049	0.008	0.000	0.0007	81.0	0.178
3.465	0.002	0.771	0.020	0.0000	0.0000	0.927	0.068	0.041	0.002	0.001	0.051	0.005	0.0000	139.5	0.659
0.286	0.105	1.839	0.030	0.0002	0.0002	3.099	0.020	0.020	0.158	0.100	0.002	0.000	0.0024	86.5	0.388
0.464	0.001	0.005	0.005	0.0035	0.0000	1.253	0.162	0.042	0.044	0.021	0.005	0.078	0.0000	111.4	0.639
1.016	0.015	0.012	0.004	0.1918	0.0000	2.446	0.226	0.197	0.004	0.003	0.026	0.000	0.0009	71.4	0.328
1.646	0.000	0.781	0.001	0.0262	0.0004	2.975	0.125	0.096	0.009	0.015	0.007	0.077	0.0000	110.5	0.577
4.000	0.051	0.371	0.004	0.1135	0.0002	3.335	0.144	0.121	0.079	0.002	0.149	0.000	0.0003	48.5	0.241
0.306	0.000	0.061	0.150	0.0016	0.0000	3.531	0.321	0.058	0.061	0.003	0.006	0.010	0.0000	114.6	0.736
3.897	0.010	0.052	0.070	0.2085	0.0001	1.284	0.021	0.132	0.005	0.010	0.090	0.001	0.0085	74.7	0.119
0.344	0.002	2.805	0.047	0.0055	0.0002	2.406	0.324	0.322	0.008	0.004	0.010	0.006	0.0000	125.6	0.748
0.290	0.011	0.249	0.024	0.0118	0.0002	0.813	0.035	0.100	0.029	0.038	0.206	0.000	0.0101	66.0	0.080
0.215	0.003	0.034	0.001	0.0001	0.0018	1.136	0.153	0.014	0.316	0.031	0.473	0.000	0.0000	147.7	0.670
0.232	0.007	0.050	0.001	0.0001	0.0025	1.653	0.031	0.018	0.002	0.001	0.004	0.003	0.0001	67.9	0.030
0.357	0.001	0.192	0.008	0.0004	0.3397	1.274	0.091	0.015	0.006	0.094	0.095	0.002	0.0000	118.5	0.447
0.529	0.012	0.178	0.007	0.0000	0.0020	5.097	0.080	0.074	0.351	0.001	0.009	0.091	0.0013	41.4	0.333
0.191	0.005	0.005	0.027	0.0000	0.3581	5.530	0.087	0.173	0.083	0.001	0.116	0.000	0.0000	121.2	0.691
0.147	0.007	0.013	0.019	0.0000	0.0598	4.191	0.065	0.091	0.012	0.030	0.001	0.012	0.0007	79.6	0.091
1.502	0.000	0.124	0.013	0.0000	0.0226	4.853	0.022	0.076	0.002	0.003	0.502	0.000	0.0000	144.5	0.420
3.796	0.047	0.160	0.012	0.0006	0.0046	1.405	0.021	0.019	0.095	0.016	0.001	0.035	0.0021	61.9	0.128
0.220	0.000	0.017	0.002	0.2221	0.0018	1.118	0.083	0.038	0.070	0.033	0.004	0.000	0.0000	175.1	0.564
1.925	0.007	0.010	0.002	0.0501	0.2680	5.951	0.180	0.111	0.004	0.003	0.032	0.015	0.0021	97.1	0.286
2.029	0.001	1.435	0.005	0.0012	0.0220	2.095	0.121	0.089	0.006	0.023	0.018	0.000	0.0000	176.4	0.653
1.127	0.063	0.183	0.001	0.0018	0.1388	0.997	0.031	0.070	0.084	0.001	0.509	0.005	0.0078	79.9	0.370
1.852	0.003	0.024	0.051	0.0094	0.0007	2.810	0.074	0.017	0.028	0.002	0.004	0.000	0.0000	157.0	0.494
0.283	0.057	0.026	0.084	0.0050	0.2978	1.233	0.071	0.346	0.002	0.012	0.096	0.105	0.0003	76.4	0.120
0.714	0.001	0.231	0.080	0.0025	0.0031	3.648	0.313	0.263	0.006	0.008	0.006	0.000	0.0000	120.7	0.689
0.752	0.023	1.382	0.013	0.0022	0.0081	1.524	0.272	0.072	0.035	0.095	0.231	0.123	0.0018	68.4	0.253

Al	Cl	CO_3	C_2O_4	F	Fe	NO_2	NO_3	OH	K	PO_4	SO_4	Si	U	T(ºC)	Evap
0.186	0.004	0.023	0.002	0.0003	0.0000	0.130	1.561	0.103	0.217	0.017	0.098	0.041	0.0028	100.4	0.586
0.159	0.006	0.022	0.005	0.0000	0.0000	0.128	1.489	0.028	0.008	0.001	0.007	0.000	0.0000	172.1	0.355
0.824	0.001	0.134	0.003	0.0001	0.0001	0.120	0.648	0.030	0.012	0.066	0.225	0.003	0.0025	102.3	0.416
0.792	0.026	0.156	0.001	0.0001	0.0000	0.098	3.505	0.168	0.202	0.003	0.016	0.001	0.0000	164.4	0.059
2.110	0.002	0.026	0.038	0.0001	0.0000	0.390	2.245	0.304	0.166	0.003	0.051	0.052	0.0010	83.5	0.589
0.458	0.065	0.060	0.039	0.0001	0.0000	0.115	3.805	0.039	0.020	0.019	0.002	0.000	0.0000	173.7	0.238
0.294	0.001	0.366	0.010	0.0000	0.0000	0.255	3.630	0.140	0.007	0.001	0.314	0.002	0.0025	49.6	0.539
0.695	0.010	1.565	0.011	0.0000	0.0000	0.311	0.518	0.088	0.058	0.011	0.005	0.000	0.0001	153.8	0.144
3.246	0.000	0.028	0.004	0.0145	0.0001	0.243	6.679	0.033	0.029	0.067	0.002	0.012	0.0019	57.5	0.733
3.001	0.098	0.020	0.001	0.0036	0.0002	0.154	2.905	0.332	0.003	0.001	0.672	0.001	0.0000	132.1	0.220
0.915	0.001	2.188	0.002	0.0074	0.0000	0.720	0.360	0.023	0.003	0.010	0.014	0.034	0.0009	73.6	0.561
0.660	0.029	2.357	0.002	0.0864	0.0001	0.568	0.456	0.027	0.253	0.001	0.039	0.001	0.0000	161.7	0.309
0.723	0.001	0.050	0.032	0.0179	0.0004	0.228	1.137	0.215	0.035	0.001	0.001	0.006	0.0068	55.0	0.583
0.626	0.023	0.009	0.043	0.0191	0.0000	0.189	0.800	0.260	0.015	0.117	0.380	0.000	0.0000	120.9	0.047
2.082	0.002	0.493	0.117	0.0014	0.0004	0.175	0.543	0.013	0.003	0.006	0.017	0.051	0.0080	82.7	0.739
0.353	0.064	0.566	0.126	0.0018	0.0000	0.737	0.506	0.033	0.400	0.014	0.268	0.000	0.0000	114.4	0.033
1.827	0.005	0.110	0.004	0.0000	0.0027	0.245	0.663	0.021	0.339	0.092	0.197	0.000	0.0029	54.5	0.550
0.153	0.057	0.006	0.006	0.0000	0.0960	0.381	0.772	0.016	0.002	0.001	0.011	0.005	0.0000	141.7	0.377
3.289	0.004	0.129	0.003	0.0005	0.0085	0.094	6.838	0.030	0.002	0.101	0.110	0.000	0.0002	87.0	0.520
0.155	0.099	1.365	0.004	0.0001	0.0114	0.663	0.695	0.018	0.205	0.001	0.005	0.008	0.0000	123.9	0.191
0.377	0.002	0.054	0.009	0.0000	0.0095	0.601	7.000	0.092	0.093	0.002	0.488	0.000	0.0038	60.0	0.530
0.440	0.013	0.076	0.127	0.0002	0.0183	0.515	3.154	0.079	0.007	0.014	0.002	0.024	0.0000	133.2	0.245
0.229	0.002	0.353	0.009	0.0001	0.2006	0.134	2.044	0.206	0.004	0.002	0.548	0.000	0.0001	41.6	0.477
0.330	0.008	0.304	0.077	0.0000	0.2350	0.162	1.011	0.044	0.042	0.026	0.001	0.002	0.0000	158.7	0.156
3.332	0.001	0.017	0.001	0.0044	0.0105	0.257	0.655	0.356	0.174	0.032	0.002	0.000	0.0007	46.8	0.727
0.868	0.101	0.038	0.001	0.0024	0.0018	0.611	6.153	0.037	0.022	0.002	0.042	0.004	0.0000	113.3	0.153
0.476	0.001	0.673	0.005	0.0070	0.0045	0.158	2.020	0.052	0.006	0.054	0.002	0.000	0.0023	89.8	0.725
1.098	0.016	2.416	0.002	0.0054	0.0986	0.125	4.590	0.071	0.131	0.008	0.068	0.012	0.0001	159.8	0.053
0.977	0.003	0.015	0.050	0.0013	0.0137	0.116	0.430	0.126	0.172	0.001	0.004	0.000	0.0003	84.0	0.544
0.245	0.031	0.011	0.024	0.1763	0.0148	0.423	6.448	0.037	0.010	0.014	0.168	0.047	0.0000	177.5	0.302
1.780	0.001	0.202	0.041	0.0013	0.0005	0.224	0.848	0.200	0.003	0.001	0.002	0.000	0.0037	46.6	0.495
1.251	0.055	0.753	0.128	0.0686	0.0007	0.106	1.294	0.034	0.043	0.021	0.024	0.073	0.0000	129.7	0.167
3.204	0.001	0.007	0.002	0.0001	0.0000	2.903	1.797	0.142	0.377	0.024	0.616	0.070	0.0000	63.2	0.730
0.964	0.097	0.051	0.007	0.0002	0.0000	3.618	0.583	0.014	0.011	0.001	0.018	0.000	0.0086	123.1	0.366
0.348	0.000	0.743	0.001	0.0000	0.0000	1.047	0.440	0.011	0.008	0.111	0.062	0.009	0.0001	64.9	0.570
2.775	0.012	2.328	0.001	0.0008	0.0000	2.486	2.142	0.102	0.450	0.004	0.001	0.001	0.0049	131.9	0.136
2.468	0.000	0.024	0.110	0.0007	0.0001	2.676	3.717	0.029	0.059	0.001	0.084	0.049	0.0000	77.2	0.439
1.690	0.076	0.089	0.019	0.0004	0.0000	1.587	6.081	0.138	0.003	0.010	0.001	0.000	0.0097	148.8	0.234
0.193	0.001	1.267	0.045	0.0000	0.0000	2.310	0.478	0.336	0.002	0.004	0.625	0.161	0.0000	64.6	0.569
0.772	0.007	1.816	0.124	0.0000	0.0000	5.352	2.708	0.014	0.028	0.064	0.007	0.000	0.0022	112.2	0.266
1.625	0.000	0.087	0.002	0.0172	0.0000	1.263	0.737	0.031	0.466	0.065	0.001	0.115	0.0000	68.2	0.408
2.194	0.051	0.069	0.003	0.0019	0.0000	1.005	1.927	0.011	0.003	0.003	0.115	0.002	0.0005	122.6	0.180
0.254	0.004	1.624	0.001	0.0605	0.0004	1.512	2.554	0.118	0.003	0.136	0.006	0.007	0.0000	79.1	0.403
0.199	0.009	1.221	0.007	0.1112	0.0002	1.371	3.009	0.029	0.067	0.001	0.044	0.000	0.0040	137.9	0.048
0.170	0.000	0.022	0.012	0.1343	0.0000	0.787	3.267	0.192	0.066	0.001	0.001	0.010	0.0000	51.2	0.427
3.846	0.006	0.043	0.014	0.0048	0.0000	5.309	0.763	0.119	0.014	0.031	0.073	0.000	0.0002	159.2	0.198
0.413	0.001	2.770	0.090	0.0246	0.0000	0.781	1.883	0.075	0.002	0.003	0.001	0.117	0.0000	49.0	0.489
0.835	0.014	0.143	0.070	0.1691	0.0004	3.678	0.396	0.021	0.096	0.015	0.284	0.001	0.0001	166.1	0.148
0.143	0.001	0.020	0.002	0.0000	0.0152	1.316	0.640	0.318	0.080	0.079	0.348	0.001	0.0000	62.7	0.616
1.426	0.005	0.015	0.001	0.0000	0.0037	3.990	1.098	0.095	0.020	0.005	0.006	0.107	0.0009	174.8	0.159
1.268	0.001	1.079	0.008	0.0000	0.3309	1.884	0.754	0.225	0.002	0.026	0.147	0.001	0.0000	101.8	0.448
0.939	0.040	0.121	0.006	0.0000	0.0006	2.061	5.537	0.022	0.039	0.007	0.001	0.065	0.0002	121.8	0.008
0.218	0.005	0.022	0.044	0.0002	0.0008	1.946	6.226	0.026	0.118	0.001	0.397	0.000	0.0000	59.1	0.464
0.149	0.007	0.011	0.056	0.0000	0.0014	2.387	4.179	0.059	0.003	0.021	0.012	0.119	0.0005	164.1	0.227
1.757	0.001	0.126	0.062	0.0001	0.1067	5.014	5.161	0.124	0.003	0.002	0.091	0.000	0.0000	106.4	0.597
0.846	0.055	0.181	0.009	0.0001	0.0582	5.266	0.868	0.025	0.064	0.069	0.017	0.033	0.0032	157.6	0.125
0.572	0.001	0.045	0.001	0.0199	0.0130	2.011	0.625	0.040	0.331	0.025	0.013	0.000	0.0000	81.3	0.772
0.782	0.019	0.007	0.001	0.0645	0.0008	1.174	6.918	0.017	0.004	0.001	0.581	0.008	0.0001	130.0	0.327
2.812	0.002	0.609	0.001	0.0012	0.0630	1.549	1.543	0.014	0.008	0.098	0.014	0.000	0.0000	65.7	0.780
0.397	0.086	0.452	0.001	0.0023	0.1352	4.023	0.531	0.099	0.382	0.001	0.386	0.055	0.0035	115.2	0.228
3.603	0.000	0.008	0.021	0.0236	0.1713	2.182	2.353	0.023	0.034	0.006	0.005	0.000	0.0000	93.6	0.669
2.634	0.109	0.008	0.111	0.0382	0.0026	2.236	0.720	0.267	0.002	0.105	0.634	0.004	0.0129	158.9	0.208
2.373	0.000	1.933	0.037	0.0461	0.0203	0.800	3.424	0.015	0.016	0.006	0.001	0.000	0.0000	59.4	0.461
2.312	0.073	2.603	0.029	0.0012	0.2289	0.882	0.976	0.242	0.356	0.077	0.218	0.003	0.0004	135.7	0.163
0.223	0.000	0.010	0.001	0.0008	0.0001	0.345	0.059	8.735	0.312	0.133	0.101	0.002	0.0110	115.7	0.263
2.739	0.008	0.085	0.001	0.0001	0.0000	0.164	0.220	8.991	0.002	0.001	0.003	0.000	0.0000	107.5	0.705
0.204	0.000	2.006	0.001	0.0005	0.0000	0.173	0.082	10.089	0.001	0.093	0.598	0.038	0.0004	146.9	0.303
1.900	0.007	0.185	0.003	0.0000	0.0000	0.456	0.046	14.258	0.343	0.001	0.007	0.000	0.0000	73.9	0.655
0.502	0.000	0.016	0.079	0.0000	0.0000	0.637	0.096	1.249	0.364	0.003	0.790	0.003	0.0073	166.6	0.344
2.962	0.016	0.008	0.012	0.0001	0.0001	0.198	0.020	10.843	0.010	0.036	0.001	0.002	0.0000	85.4	0.598

Al	Cl	CO_3	C_2O_4	F	Fe	NO_2	NO_3	OH	K	PO_4	SO_4	Si	U	T(ºC)	Evap
2.533	0.001	2.161	0.109	0.0002	0.0003	0.410	0.201	2.642	0.007	0.001	0.495	0.059	0.0001	125.3	0.002
1.142	0.077	0.400	0.013	0.0000	0.0000	0.316	0.021	1.869	0.115	0.020	0.001	0.000	0.0000	76.6	0.478
1.734	0.002	0.011	0.007	0.0323	0.0000	0.180	0.044	2.880	0.238	0.012	0.021	0.013	0.0038	175.6	0.278
0.407	0.054	0.023	0.003	0.1159	0.0000	0.669	0.079	6.455	0.005	0.008	0.280	0.000	0.0000	46.0	0.759
0.803	0.000	0.328	0.006	0.1491	0.0000	0.148	0.095	0.424	0.017	0.072	0.002	0.111	0.0002	149.1	0.069
1.668	0.026	1.299	0.001	0.0086	0.0000	0.163	0.215	0.644	0.026	0.002	0.175	0.000	0.0001	77.7	0.784
1.951	0.003	0.098	0.071	0.0731	0.0001	0.523	0.018	3.232	0.178	0.008	0.013	0.155	0.0001	144.2	0.031
0.238	0.060	0.035	0.038	0.0020	0.0000	0.582	0.242	4.502	0.004	0.060	0.022	0.000	0.0000	78.8	0.503
0.522	0.004	0.197	0.021	0.1315	0.0000	0.108	0.057	5.125	0.024	0.001	0.001	0.088	0.0005	166.3	0.247
0.174	0.017	1.453	0.074	0.0023	0.0000	0.181	0.069	0.406	0.198	0.042	0.156	0.000	0.0000	90.9	0.481
2.002	0.001	0.064	0.001	0.0002	0.0006	0.140	0.053	2.839	0.065	0.010	0.324	0.000	0.0001	163.6	0.383
0.643	0.062	0.042	0.001	0.0000	0.0059	0.121	0.178	1.304	0.005	0.001	0.001	0.026	0.0000	108.4	0.625
0.423	0.003	0.506	0.003	0.0000	0.0012	0.171	0.077	15.323	0.021	0.021	0.041	0.001	0.0026	175.9	0.295
0.275	0.014	1.489	0.001	0.0002	0.0841	0.129	0.285	0.489	0.483	0.002	0.014	0.109	0.0000	108.1	0.698
1.542	0.002	0.013	0.015	0.0000	0.0614	0.323	0.025	0.582	0.042	0.001	0.026	0.000	0.0002	130.5	0.113
0.429	0.048	0.005	0.022	0.0002	0.0140	0.296	0.340	0.765	0.018	0.087	0.001	0.056	0.0001	86.2	0.666
3.699	0.001	0.344	0.032	0.0009	0.0036	0.511	0.067	8.246	0.003	0.005	0.070	0.001	0.0043	120.1	0.172
1.445	0.111	1.162	0.083	0.0000	0.0664	0.213	0.328	5.920	0.291	0.011	0.003	0.019	0.0000	92.2	0.500
2.886	0.004	0.013	0.004	0.0471	0.0286	0.696	0.127	2.604	0.033	0.096	0.001	0.000	0.0008	176.2	0.127
0.165	0.088	0.048	0.001	0.2130	0.1425	0.192	0.098	0.565	0.005	0.001	0.180	0.079	0.0000	72.0	0.442
0.372	0.001	0.139	0.001	0.0067	0.1954	0.233	0.100	6.181	0.002	0.011	0.008	0.001	0.0090	135.4	0.019
1.522	0.012	2.108	0.003	0.0523	0.0054	0.279	0.260	9.388	0.230	0.002	0.589	0.003	0.0000	67.1	0.716
0.489	0.000	0.049	0.066	0.0033	0.0798	0.387	0.048	10.688	0.055	0.001	0.001	0.002	0.0132	150.5	0.158
3.557	0.016	0.007	0.020	0.0066	0.0009	0.193	0.097	1.081	0.002	0.043	0.338	0.169	0.0000	98.5	0.431
2.924	0.002	2.571	0.010	0.0128	0.1669	0.503	0.269	3.327	0.001	0.004	0.015	0.000	0.0069	163.0	0.331
0.362	0.089	0.390	0.114	0.0795	0.0011	0.184	0.029	12.524	0.139	0.106	0.141	0.022	0.0000	64.3	0.619
1.319	0.003	0.044	0.008	0.0000	0.0000	1.337	0.061	4.438	0.241	0.044	0.723	0.062	0.0001	175.4	0.225
0.265	0.041	0.015	0.001	0.0000	0.0000	4.933	0.170	6.548	0.003	0.005	0.003	0.002	0.0001	69.8	0.519
1.219	0.002	0.218	0.002	0.0000	0.0000	5.575	0.166	0.733	0.004	0.073	0.082	0.137	0.0000	128.9	0.011
0.402	0.038	1.001	0.002	0.0000	0.0001	1.613	0.118	3.375	0.040	0.001	0.002	0.002	0.0013	47.7	0.428
0.678	0.001	0.109	0.021	0.0001	0.0003	3.281	0.026	3.842	0.074	0.001	0.183	0.007	0.0000	169.9	0.056
0.903	0.022	0.015	0.054	0.0001	0.0000	1.359	0.030	1.528	0.004	0.040	0.011	0.000	0.0005	58.0	0.634
1.235	0.004	0.699	0.015	0.0004	0.0001	0.820	0.055	2.964	0.001	0.003	0.359	0.004	0.0000	116.6	0.017
0.157	0.039	0.532	0.058	0.0000	0.0000	4.893	0.030	13.077	0.126	0.048	0.002	0.001	0.0010	74.5	0.484
1.042	0.003	0.034	0.001	0.0013	0.0000	3.176	0.056	1.021	0.038	0.020	0.001	0.139	0.0000	161.1	0.258
0.258	0.033	0.029	0.001	0.0366	0.0003	5.713	0.196	0.682	0.011	0.003	0.023	0.000	0.0099	52.6	0.636
0.618	0.001	0.212	0.001	0.0221	0.0000	1.487	0.109	1.401	0.010	0.013	0.001	0.010	0.0000	122.3	0.106
0.536	0.020	0.801	0.001	0.0140	0.0000	3.308	0.132	1.179	0.069	0.004	0.023	0.000	0.0010	102.9	0.800
2.342	0.001	0.009	0.027	0.0060	0.0001	1.127	0.072	0.442	0.419	0.001	0.007	0.027	0.0000	113.8	0.308
1.483	0.072	0.008	0.030	0.0358	0.0002	1.475	0.141	12.890	0.023	0.009	0.075	0.001	0.0009	40.8	0.797
2.600	0.000	1.119	0.014	0.0031	0.0000	1.915	0.292	0.436	0.002	0.001	0.012	0.060	0.0000	132.4	0.294
2.055	0.079	1.728	0.048	0.0406	0.0000	3.894	0.113	6.740	0.026	0.009	0.054	0.000	0.0004	72.8	0.486
1.353	0.000	0.070	0.001	0.0002	0.0935	0.847	0.022	1.097	0.278	0.034	0.702	0.001	0.0000	110.3	0.350
3.121	0.043	0.083	0.007	0.0000	0.1502	1.681	0.027	7.784	0.011	0.002	0.001	0.002	0.0001	61.6	0.459
0.209	0.003	2.271	0.001	0.0000	0.0484	1.030	0.025	2.068	0.006	0.083	0.170	0.000	0.0000	155.9	0.289
0.248	0.007	1.026	0.001	0.0003	0.1217	3.831	0.088	2.423	0.094	0.004	0.004	0.020	0.0001	70.4	0.558
1.604	0.000	0.014	0.014	0.0008	0.0062	3.474	0.176	2.190	0.132	0.001	0.131	0.000	0.0000	119.0	0.364
1.876	0.050	0.102	0.012	0.0000	0.0083	2.200	0.104	3.140	0.006	0.114	0.004	0.010	0.0005	108.9	0.405
0.168	0.001	1.400	0.121	0.0002	0.0014	1.439	0.090	11.653	0.001	0.002	0.427	0.001	0.0000	162.8	0.117
1.371	0.006	1.206	0.060	0.0001	0.0238	3.560	0.029	12.705	0.386	0.031	0.008	0.017	0.0003	72.5	0.794
0.557	0.002	0.095	0.003	0.0433	0.0005	2.742	0.051	2.320	0.048	0.084	0.015	0.000	0.0000	139.3	0.347
0.367	0.018	0.016	0.001	0.0015	0.0335	4.510	0.123	0.896	0.006	0.003	0.024	0.121	0.0015	74.2	0.713
1.172	0.004	0.297	0.001	0.0716	0.0178	4.974	0.103	1.463	0.002	0.016	0.003	0.000	0.0000	172.6	0.081
0.181	0.037	0.441	0.004	0.0557	0.0100	1.640	0.084	7.897	0.071	0.002	0.145	0.016	0.0021	88.4	0.648
0.310	0.001	0.037	0.011	0.0028	0.0035	3.769	0.027	2.680	0.121	0.007	0.001	0.000	0.0000	177.8	0.092
1.464	0.010	0.012	0.053	0.0021	0.0326	0.934	0.309	2.798	0.005	0.009	0.078	0.015	0.0002	48.8	0.483
1.583	0.002	1.106	0.020	0.1621	0.0015	4.736	0.248	0.455	0.019	0.002	0.009	0.000	0.0000	169.1	0.206
0.483	0.049	0.252	0.028	0.0424	0.0382	0.989	0.086	0.541	0.027	0.037	0.125	0.007	0.0026	51.5	0.600
0.669	0.003	0.008	0.001	0.0000	0.0000	0.215	1.048	2.530	0.106	0.075	0.035	0.003	0.0008	85.9	0.367
0.207	0.022	0.106	0.003	0.0000	0.0001	0.541	3.045	2.388	0.005	0.005	0.001	0.001	0.0000	163.3	0.414
0.161	0.000	0.172	0.003	0.0000	0.0001	0.273	2.838	0.858	0.002	0.034	0.415	0.007	0.0135	93.0	0.189
2.436	0.006	0.525	0.002	0.0001	0.0000	0.183	0.703	6.837	0.046	0.002	0.002	0.000	0.0001	154.6	0.606
0.686	0.001	0.016	0.098	0.0003	0.0000	0.303	0.435	3.954	0.271	0.006	0.375	0.003	0.0075	100.2	0.077
0.550	0.022	0.040	0.010	0.0001	0.0000	0.102	2.325	7.563	0.004	0.078	0.010	0.002	0.0000	144.7	0.541
0.452	0.001	0.436	0.012	0.0001	0.0000	0.507	0.819	7.140	0.017	0.001	0.129	0.048	0.0124	40.3	0.313
1.203	0.015	0.538	0.033	0.0000	0.0000	0.107	1.192	0.653	0.259	0.050	0.003	0.000	0.0000	123.7	0.591
2.282	0.001	0.058	0.001	0.0351	0.0000	0.177	2.676	15.104	0.207	0.011	0.013	0.004	0.0006	88.7	0.025
0.635	0.070	0.033	0.001	0.0073	0.0001	0.266	0.405	5.430	0.001	0.008	0.037	0.000	0.0000	172.9	0.766
0.543	0.002	0.500	0.001	0.0100	0.0000	0.301	3.546	0.418	0.019	0.063	0.007	0.071	0.0039	52.0	0.177
0.302	0.018	1.686	0.002	0.0142	0.0000	0.532	3.081	0.557	0.026	0.001	0.092	0.000	0.0000	177.3	0.584

Al	Cl	CO_3	C_2O_4	F	Fe	NO_2	NO_3	OH	K	PO_4	SO_4	Si	U	T(ºC)	Evap
0.652	0.000	0.006	0.017	0.1089	0.0000	0.096	0.576	1.714	0.057	0.006	0.015	0.063	0.0003	45.5	0.205
2.704	0.021	0.008	0.027	0.0014	0.0001	0.577	0.495	1.113	0.008	0.013	0.022	0.001	0.0000	128.0	0.578
2.404	0.000	1.981	0.031	0.0021	0.0003	0.212	5.602	0.692	0.017	0.004	0.001	0.017	0.0003	83.2	0.078
3.041	0.074	0.512	0.093	0.0137	0.0000	0.241	2.645	0.634	0.039	0.026	0.837	0.000	0.0000	124.2	0.509
0.495	0.004	0.023	0.002	0.0000	0.2060	0.200	3.850	0.884	0.055	0.016	0.080	0.000	0.0002	107.0	0.094
0.172	0.016	0.046	0.005	0.0003	0.1282	0.467	4.754	1.066	0.013	0.001	0.002	0.007	0.0000	149.4	0.409
0.386	0.001	0.144	0.003	0.0003	0.1625	0.260	2.872	15.545	0.012	0.018	0.329	0.000	0.0004	91.7	0.023
0.813	0.013	0.395	0.003	0.0002	0.0092	0.647	4.328	0.936	0.488	0.005	0.000	0.003	0.0000	162.2	0.411
0.418	0.001	0.017	0.039	0.0000	0.0019	0.119	1.151	16.000	0.225	0.003	0.050	0.000	0.0001	59.7	0.283
0.515	0.014	0.065	0.020	0.0000	0.0064	0.731	1.309	6.006	0.001	0.045	0.001	0.028	0.0001	156.5	0.536
0.268	0.001	0.410	0.010	0.0000	0.0087	0.235	0.597	3.524	0.008	0.001	0.057	0.000	0.0034	70.1	0.342
1.084	0.009	0.336	0.025	0.0000	0.1154	0.714	2.092	1.484	0.145	0.145	0.009	0.005	0.0000	127.5	0.502
2.166	0.001	0.008	0.002	0.0297	0.0318	0.369	0.382	0.871	0.439	0.097	0.004	0.000	0.0002	62.1	0.022
1.113	0.067	0.009	0.004	0.0031	0.0044	0.308	2.437	13.655	0.013	0.002	0.064	0.028	0.0000	117.4	0.617
2.137	0.000	0.852	0.004	0.0090	0.0065	0.313	1.839	3.473	0.002	0.128	0.001	0.000	0.0054	43.3	0.255
2.566	0.066	1.604	0.003	0.0064	0.0102	0.606	1.421	9.524	0.144	0.005	0.027	0.179	0.0000	165.2	0.645
0.470	0.002	0.019	0.103	0.0187	0.1317	0.187	0.889	0.518	0.460	0.002	0.001	0.001	0.0047	67.6	0.169
0.322	0.015	0.056	0.088	0.0057	0.0006	0.306	2.408	14.465	0.020	0.020	0.189	0.172	0.0000	115.5	0.466
0.314	0.001	0.262	0.050	0.0015	0.0009	0.621	0.611	1.196	0.007	0.001	0.001	0.001	0.0011	98.0	0.097
0.989	0.010	0.376	0.089	0.0084	0.0097	0.133	2.584	2.009	0.060	0.010	0.046	0.005	0.0000	148.3	0.661
2.223	0.004	0.015	0.003	0.0000	0.0000	2.507	0.809	3.007	0.041	0.047	0.272	0.002	0.0000	79.4	0.027
0.188	0.068	0.031	0.003	0.0003	0.0002	1.223	5.283	0.754	0.005	0.007	0.014	0.000	0.0045	130.8	0.630
0.587	0.001	0.158	0.003	0.0001	0.0000	1.243	6.299	0.534	0.004	0.014	0.745	0.006	0.0000	41.9	0.292
1.285	0.019	1.645	0.007	0.0008	0.0000	1.574	1.060	3.733	0.031	0.002	0.001	0.000	0.0024	114.9	0.756
0.196	0.001	0.041	0.057	0.0000	0.0000	4.547	2.940	7.348	0.434	0.001	0.203	0.050	0.0000	49.8	0.058
0.564	0.007	0.031	0.029	0.0011	0.0000	4.056	0.829	13.459	0.002	0.011	0.016	0.000	0.0011	151.0	0.697
0.579	0.002	0.447	0.011	0.0001	0.0001	2.697	0.401	0.590	0.003	0.001	0.040	0.026	0.0000	43.0	0.363
0.435	0.019	0.164	0.091	0.0010	0.0000	4.089	5.222	4.980	0.034	0.080	0.003	0.001	0.0002	124.8	0.603
0.151	0.001	0.007	0.001	0.0068	0.0000	2.654	2.805	1.006	0.137	0.065	0.018	0.043	0.0000	85.1	0.108
0.891	0.005	0.117	0.005	0.0108	0.0000	1.109	6.524	3.279	0.012	0.001	0.173	0.001	0.0092	151.3	0.728
0.145	0.000	0.690	0.002	0.0104	0.0000	1.667	0.943	4.634	0.003	0.043	0.008	0.145	0.0000	58.6	0.330
2.669	0.005	0.128	0.007	0.0019	0.0001	1.463	2.974	5.669	0.182	0.004	0.343	0.000	0.0127	180.0	0.441
0.177	0.001	0.016	0.106	0.0390	0.0000	2.218	0.633	6.271	0.054	0.008	0.001	0.030	0.0000	93.9	0.378
0.762	0.006	0.059	0.009	0.0111	0.0002	1.393	0.932	1.050	0.003	0.042	0.253	0.001	0.0003	179.5	0.795
0.298	0.001	0.594	0.042	0.0018	0.0000	0.840	1.356	3.186	0.022	0.004	0.002	0.004	0.0000	91.4	0.272
1.157	0.010	0.148	0.009	0.0940	0.0000	1.627	3.760	0.469	0.134	0.071	0.054	0.000	0.0003	125.0	0.613
0.857	0.001	0.005	0.001	0.0000	0.0294	5.055	0.420	0.846	0.078	0.116	0.066	0.000	0.0001	101.3	0.398
1.056	0.027	0.082	0.002	0.0005	0.0019	4.365	1.124	1.642	0.013	0.004	0.001	0.061	0.0016	120.4	0.677
0.212	0.000	0.811	0.003	0.0001	0.0126	4.698	0.556	1.035	0.002	0.025	0.467	0.001	0.0000	90.6	0.138
3.747	0.007	0.665	0.005	0.0000	0.0007	1.931	3.673	11.994	0.054	0.005	0.001	0.035	0.0042	137.6	0.627
0.242	0.001	0.013	0.142	0.0001	0.1583	1.193	3.191	13.853	0.298	0.004	0.663	0.001	0.0000	103.7	0.348
0.602	0.008	0.025	0.012	0.0000	0.0004	1.722	1.655	8.487	0.001	0.109	0.008	0.018	0.0027	110.8	0.406
0.733	0.001	0.475	0.048	0.0004	0.0173	1.899	0.900	11.000	0.010	0.001	0.088	0.000	0.0000	60.5	0.098
1.408	0.024	0.199	0.040	0.0000	0.0005	4.225	3.305	1.231	0.368	0.130	0.010	0.005	0.0003	178.9	0.614
3.162	0.003	0.031	0.002	0.0451	0.0041	2.833	2.271	0.822	0.494	0.013	0.006	0.000	0.0000	100.7	0.233
0.261	0.096	0.006	0.006	0.0158	0.0073	1.536	4.644	15.771	0.014	0.002	0.364	0.113	0.0002	164.7	0.605
3.376	0.001	0.215	0.002	0.0116	0.0069	1.736	5.345	2.494	0.016	0.143	0.009	0.000	0.0000	54.2	0.042
0.595	0.102	2.299	0.001	0.0027	0.0008	1.995	1.085	0.672	0.110	0.005	0.228	0.150	0.0052	153.5	0.523
1.336	0.001	0.018	0.029	0.2175	0.0362	4.401	3.588	4.189	0.051	0.003	0.012	0.000	0.0000	56.1	0.013
0.705	0.042	0.074	0.130	0.0022	0.0075	0.807	0.483	0.977	0.004	0.074	0.135	0.006	0.0001	124.5	0.750
0.235	0.001	0.552	0.015	0.0285	0.0008	0.942	4.982	6.643	0.009	0.004	0.001	0.000	0.0000	76.1	0.063
1.029	0.008	1.014	0.123	0.0203	0.1095	1.962	0.525	1.422	0.244	0.052	0.044	0.005	0.0015	145.0	0.734
0.141	0.005	0.120	0.009	0.0011	0.0004	0.743	0.348	0.400	0.025	0.009	0.021	0.002	0.0001	110.0	0.400
0.045	0.056	0.907	0.015	0.0034	0.0169	2.112	4.278	3.575	0.016	0.001	0.001	0.000	0.0000	77.5	0.345
0.011	0.002	0.259	0.148	0.0088	0.0013	2.044	4.379	0.702	0.147	0.033	0.042	0.030	0.0001	117.9	0.755
0.063	0.038	0.011	0.036	0.0045	0.0007	1.145	4.810	2.354	0.186	0.006	0.001	0.001	0.0000	107.3	0.356
0.017	0.002	0.040	0.013	0.1588	0.0251	3.708	6.373	4.769	0.006	0.046	0.105	0.163	0.0027	169.6	0.711
0.088	0.024	0.223	0.001	0.1958	0.0864	2.720	0.879	1.952	0.001	0.119	0.002	0.001	0.0001	76.9	0.248
0.027	0.003	2.840	0.004	0.0960	0.2611	3.926	5.101	13.267	0.090	0.005	0.127	0.014	0.0007	138.4	0.764
0.005	0.009	0.025	0.001	0.1400	0.0009	3.800	1.617	0.787	0.405	0.126	0.012	0.000	0.0000	85.7	0.055
0.074	0.000	0.077	0.003	0.0058	0.0424	0.981	1.220	12.345	0.014	0.003	0.194	0.044	0.0005	154.8	0.650
0.051	0.087	2.539	0.015	0.0004	0.0023	5.807	1.734	5.052	0.006	0.005	0.158	0.000	0.0001	51.8	0.100
0.007	0.002	1.665	0.026	0.0000	0.0198	3.254	3.344	2.458	0.195	0.029	0.002	0.004	0.0015	141.4	0.527
0.009	0.106	0.007	0.018	0.0001	0.0372	0.762	0.365	1.980	0.040	0.002	0.033	0.000	0.0001	81.8	0.192
0.006	0.000	0.046	0.120	0.0005	0.0538	0.897	0.512	0.722	0.007	0.060	0.001	0.014	0.0083	125.9	0.695
0.006	0.011	0.229	0.001	0.0000	0.0647	1.694	1.905	14.888	0.017	0.039	0.038	0.000	0.0001	78.0	0.086
0.060	0.000	0.405	0.001	0.0003	0.0025	1.327	2.495	0.625	0.471	0.002	0.004	0.017	0.0012	171.8	0.463
0.039	0.009	0.053	0.001	0.0000	0.0188	1.014	2.772	3.680	0.125	0.012	0.133	0.001	0.0000	50.7	0.244
0.072	0.001	0.006	0.004	0.0002	0.0006	0.965	0.352	2.922	0.004	0.001	0.002	0.029	0.0023	174.3	0.425
0.123	0.030	1.283	0.018	0.0212	0.0001	1.164	1.714	4.070	0.013	0.007	0.020	0.081	0.0000	83.8	0.083

Al	Cl	CO_3	C_2O_4	F	Fe	NO_2	NO_3	OH	K	PO_4	SO_4	Si	U	T(ºC)	Evap
0.022	0.004	0.275	0.044	0.0028	0.0000	1.295	0.910	0.909	0.164	0.036	0.165	0.001	0.0020	114.1	0.581
0.059	0.053	0.020	0.058	0.0017	0.0001	5.903	6.758	2.567	0.030	0.005	0.020	0.013	0.0000	88.9	0.269
0.012	0.002	0.105	0.067	0.0291	0.0000	1.203	0.410	0.511	0.005	0.051	0.564	0.000	0.0140	146.6	0.480
0.013	0.041	0.265	0.001	0.0778	0.0000	6.000	0.472	10.236	0.024	0.009	0.016	0.003	0.0000	87.3	0.114
0.015	0.000	0.734	0.004	0.1878	0.0000	3.445	0.590	0.412	0.347	0.002	0.139	0.000	0.0008	137.1	0.533
0.021	0.011	0.015	0.002	0.0020	0.0000	2.548	4.082	3.051	0.026	0.009	0.009	0.013	0.0000	96.6	0.009
0.061	0.001	0.012	0.008	0.0442	0.0001	1.562	3.117	0.430	0.005	0.001	0.221	0.000	0.0031	152.7	0.678
0.014	0.007	1.471	0.041	0.0003	0.0001	1.155	1.598	1.381	0.007	0.006	0.460	0.002	0.0000	52.9	0.039
0.099	0.001	2.477	0.014	0.0001	0.0000	5.485	0.461	1.896	0.068	0.028	0.015	0.000	0.0002	153.2	0.419
0.006	0.061	0.086	0.011	0.0000	0.0000	2.527	3.229	1.843	0.033	0.003	0.104	0.002	0.0000	53.1	0.284
0.010	0.000	0.014	0.049	0.0000	0.0002	4.473	4.536	0.573	0.007	0.022	0.002	0.000	0.0008	170.7	0.684
0.019	0.006	0.681	0.001	0.0000	0.0000	0.861	5.041	4.567	0.007	0.088	0.030	0.003	0.0000	84.8	0.252
0.109	0.001	0.207	0.001	0.0003	0.0001	5.667	0.781	1.924	0.180	0.007	0.004	0.000	0.0011	127.2	0.786
0.080	0.028	0.094	0.006	0.0001	0.0000	1.382	1.950	0.549	0.295	0.028	0.102	0.005	0.0000	93.3	0.038
0.023	0.003	0.018	0.001	0.0009	0.0000	1.854	5.735	8.366	0.019	0.001	0.006	0.000	0.0019	150.7	0.513
0.033	0.013	0.150	0.016	0.0036	0.0123	0.237	2.466	3.424	0.012	0.003	0.001	0.000	0.0010	52.3	0.133
0.052	0.001	2.636	0.133	0.0047	0.0111	0.519	3.384	0.963	0.142	0.017	0.212	0.003	0.0000	116.0	0.475
0.005	0.006	0.047	0.046	0.2316	0.0017	0.631	0.569	0.992	0.073	0.004	0.001	0.001	0.0001	80.2	0.142
0.112	0.000	0.030	0.100	0.0039	0.0757	0.210	1.973	1.506	0.012	0.044	0.540	0.021	0.0000	156.2	0.525
0.008	0.032	0.234	0.007	0.2415	0.0278	0.143	2.193	9.803	0.002	0.086	0.005	0.000	0.0010	103.2	0.213
0.020	0.000	2.508	0.001	0.0580	0.0911	0.102	1.035	8.012	0.335	0.001	0.053	0.011	0.0000	139.0	0.622
0.006	0.010	0.019	0.004	0.0267	0.0820	0.596	1.776	3.898	0.288	0.085	0.009	0.001	0.0005	80.5	0.141
0.070	0.000	0.008	0.002	0.0076	0.0010	0.178	5.940	8.128	0.004	0.001	0.186	0.031	0.0000	133.5	0.413
0.043	0.032	2.875	0.016	0.0004	0.3223	0.441	0.746	3.787	0.014	0.003	0.086	0.000	0.0065	108.6	0.161
0.020	0.002	1.236	0.018	0.0000	0.0497	0.226	0.537	0.810	0.154	0.025	0.017	0.032	0.0000	148.6	0.472
0.012	0.120	0.018	0.147	0.0000	0.0005	0.186	0.965	1.666	0.065	0.005	0.065	0.000	0.0007	109.5	0.223
0.005	0.000	0.039	0.017	0.0000	0.0008	0.166	0.838	1.323	0.008	0.048	0.003	0.098	0.0000	171.5	0.559
0.065	0.117	0.237	0.000	0.0008	0.0060	0.157	0.378	2.758	0.010	0.025	0.071	0.000	0.0009	105.4	0.064
0.005	0.002	0.279	0.001	0.0000	0.0027	0.430	5.871	1.213	0.119	0.007	0.005	0.006	0.0000	145.3	0.681
0.058	0.010	0.005	0.002	0.0002	0.0012	0.230	0.373	0.497	0.076	0.020	0.043	0.001	0.0071	94.4	0.052
0.069	0.002	0.058	0.003	0.0001	0.0010	0.680	3.464	1.595	0.021	0.002	0.002	0.027	0.0000	154.0	0.720
0.093	0.008	0.420	0.143	0.0165	0.0001	0.486	0.791	11.822	0.002	0.002	0.001	0.016	0.0006	72.3	0.130
0.086	0.003	0.289	0.065	0.0152	0.0001	0.334	3.895	9.121	0.391	0.104	0.113	0.001	0.0001	152.1	0.770
0.056	0.017	0.075	0.009	0.0034	0.0000	0.434	1.324	10.384	0.098	0.001	0.005	0.002	0.0004	101.5	0.353
0.038	0.002	0.081	0.011	0.0701	0.0001	0.108	1.507	2.159	0.002	0.115	0.049	0.000	0.0000	178.6	0.467
0.105	0.005	2.736	0.003	0.0316	0.0000	0.100	1.388	0.923	0.007	0.090	0.004	0.017	0.0005	98.8	0.109
0.136	0.004	1.133	0.004	0.0812	0.0000	0.132	1.861	1.765	0.049	0.002	0.573	0.000	0.0000	140.4	0.709
0.013	0.114	0.116	0.006	0.0746	0.0000	0.114	5.408	2.098	0.302	0.027	0.001	0.009	0.0002	75.5	0.380
0.005	0.001	0.090	0.006	0.0023	0.0000	0.393	5.803	8.610	0.006	0.004	0.653	0.000	0.0000	158.1	0.672
0.091	0.060	0.863	0.036	0.0000	0.0001	0.494	1.455	4.250	0.009	0.002	0.120	0.084	0.0060	44.9	0.236
0.010	0.003	1.508	0.034	0.0000	0.0000	0.093	0.671	1.442	0.170	0.027	0.014	0.000	0.0000	122.9	0.514
0.010	0.036	0.010	0.016	0.0011	0.0000	0.264	1.000	1.790	0.102	0.003	0.024	0.012	0.0059	43.6	0.147
0.018	0.000	0.079	0.078	0.0007	0.0000	0.554	3.941	2.287	0.007	0.052	0.001	0.001	0.0000	140.1	0.430
0.011	0.009	0.587	0.001	0.0001	0.0003	0.197	1.636	9.254	0.022	0.032	0.123	0.015	0.0006	63.0	0.306
0.071	0.000	0.559	0.001	0.0003	0.0000	0.448	1.694	0.462	0.320	0.006	0.005	0.000	0.0000	143.6	0.680
0.028	0.024	0.062	0.001	0.0005	0.0001	0.151	0.387	0.607	0.100	0.010	0.077	0.090	0.0003	99.3	0.111
0.027	0.001	0.010	0.006	0.0006	0.0000	0.363	0.445	2.222	0.018	0.001	0.002	0.000	0.0000	151.6	0.547
0.108	0.005	0.617	0.034	0.0049	0.0344	4.259	0.078	1.550	0.003	0.004	0.005	0.000	0.0000	119.6	0.214
0.126	0.004	0.640	0.016	0.0847	0.0700	4.330	0.081	5.752	0.074	0.062	0.061	0.128	0.0002	47.9	0.445
0.024	0.025	0.107	0.024	0.0123	0.0013	4.622	0.187	5.275	0.050	0.001	0.002	0.001	0.0000	117.7	0.384
0.025	0.001	0.092	0.087	0.0155	0.0208	5.621	0.035	0.950	0.003	0.024	0.028	0.004	0.0004	55.6	0.741
0.009	0.015	0.545	0.002	0.0134	0.0264	1.416	0.054	0.526	0.004	0.027	0.009	0.000	0.0000	136.5	0.211
0.044	0.000	0.240	0.002	0.0226	0.0049	4.814	0.032	4.129	0.031	0.004	0.288	0.064	0.0015	46.3	0.563
0.068	0.022	0.039	0.008	0.1523	0.0164	2.164	0.033	1.145	0.085	0.051	0.001	0.002	0.0000	170.4	0.261
0.029	0.002	0.009	0.007	0.1727	0.2477	1.779	0.234	1.816	0.010	0.007	0.083	0.042	0.0001	66.3	0.656
0.006	0.091	0.519	0.019	0.0001	0.0023	2.273	0.018	4.909	0.021	0.001	0.264	0.000	0.0000	162.5	0.067
0.007	0.000	0.707	0.086	0.0003	0.0011	3.589	0.042	0.482	0.191	0.076	0.001	0.007	0.0002	87.9	0.580
0.022	0.021	0.007	0.031	0.0002	0.0042	0.768	0.336	6.937	0.220	0.007	0.033	0.000	0.0000	146.4	0.239
0.030	0.001	0.006	0.035	0.0000	0.0030	0.973	0.266	5.835	0.002	0.058	0.011	0.003	0.0007	58.3	0.491
0.028	0.020	0.286	0.002	0.0001	0.0005	2.426	0.106	0.743	0.017	0.058	0.319	0.001	0.0000	165.0	0.217
0.032	0.001	1.546	0.002	0.0001	0.2413	2.927	0.151	0.616	0.041	0.001	0.001	0.046	0.0033	99.1	0.753
0.010	0.012	0.029	0.001	0.0009	0.0005	3.150	0.223	12.168	0.188	0.012	0.025	0.000	0.0000	137.3	0.061
0.057	0.000	0.025	0.001	0.0007	0.0738	0.749	0.239	4.838	0.002	0.005	0.002	0.010	0.0055	105.6	0.767
0.011	0.005	0.131	0.018	0.0374	0.0001	2.254	0.183	7.673	0.002	0.001	0.002	0.040	0.0000	165.5	0.250
0.131	0.000	2.387	0.013	0.0658	0.0000	1.451	0.157	9.945	0.275	0.062	0.041	0.001	0.0106	78.3	0.423
0.006	0.005	0.111	0.023	0.0027	0.0000	5.855	0.018	5.352	0.309	0.001	0.004	0.036	0.0000	133.0	0.280
0.129	0.000	0.011	0.020	0.0251	0.0000	0.833	0.174	8.862	0.003	0.082	0.094	0.000	0.0002	96.1	0.609
0.053	0.015	0.269	0.008	0.0303	0.0000	0.919	0.017	1.739	0.007	0.046	0.001	0.016	0.0000	160.0	0.270
0.045	0.002	0.190	0.001	0.0079	0.0000	1.073	0.038	2.038	0.082	0.005	0.292	0.000	0.0048	86.8	0.555
0.087	0.011	0.041	0.008	0.0208	0.0000	4.123	0.059	0.776	0.149	0.030	0.001	0.037	0.0001	178.4	0.323

Al	Cl	CO_3	C_2O_4	F	Fe	NO_2	NO_3	OH	K	PO_4	SO_4	Si	U	T(ºC)	Evap
0.061	0.003	0.047	0.001	0.1801	0.0000	3.417	0.120	3.627	0.014	0.003	0.421	0.002	0.0030	61.3	0.644
0.006	0.028	0.841	0.056	0.0003	0.0000	2.147	0.185	0.449	0.004	0.002	0.256	0.029	0.0000	173.2	0.073
0.023	0.000	0.380	0.075	0.0005	0.0001	0.904	0.020	4.374	0.027	0.041	0.010	0.001	0.0004	106.7	0.647
0.042	0.035	0.021	0.014	0.0002	0.0000	3.502	0.060	3.095	0.101	0.001	0.235	0.014	0.0000	130.2	0.075
0.018	0.002	0.006	0.045	0.0002	0.0000	4.437	0.026	2.254	0.005	0.009	0.007	0.000	0.0001	60.2	0.747
0.020	0.008	0.953	0.002	0.0010	0.0000	4.775	0.282	1.267	0.004	0.057	0.122	0.087	0.0000	136.0	0.256
0.082	0.001	1.332	0.003	0.0000	0.0000	1.305	0.019	4.312	0.063	0.005	0.003	0.000	0.0033	42.5	0.498
0.011	0.039	0.071	0.002	0.0010	0.0003	2.466	0.143	0.799	0.184	0.053	0.238	0.100	0.0000	173.4	0.305
0.016	0.000	0.019	0.001	0.0000	0.0002	5.223	0.094	4.701	0.014	0.004	0.019	0.000	0.0006	90.3	0.633
0.006	0.031	2.031	0.037	0.0195	0.1185	0.190	0.067	1.129	0.002	0.003	0.001	0.000	0.0002	156.8	0.070
0.021	0.000	0.282	0.011	0.0063	0.1249	0.153	0.208	11.322	0.057	0.131	0.025	0.015	0.0000	96.9	0.434
0.057	0.085	0.019	0.072	0.2268	0.1542	0.528	0.275	14.054	0.075	0.001	0.007	0.000	0.0002	155.1	0.230
0.007	0.002	0.006	0.099	0.0015	0.2901	0.222	0.057	1.572	0.001	0.019	0.301	0.005	0.0000	88.1	0.664
0.008	0.053	0.602	0.001	0.0019	0.0034	0.207	0.033	5.508	0.010	0.110	0.005	0.000	0.0006	142.8	0.361
0.012	0.000	0.161	0.004	0.0029	0.1759	0.348	0.020	1.162	0.209	0.007	0.778	0.009	0.0000	71.2	0.566
0.103	0.025	0.011	0.002	0.0921	0.0133	0.239	0.254	0.476	0.373	0.019	0.001	0.000	0.0076	155.4	0.231
0.026	0.004	0.008	0.001	0.0568	0.0071	0.103	0.045	11.160	0.021	0.001	0.060	0.045	0.0000	107.8	0.534
0.012	0.068	0.166	0.039	0.0001	0.0156	0.437	0.164	5.200	0.001	0.001	0.409	0.000	0.0043	151.8	0.392
0.009	0.000	0.210	0.022	0.0007	0.0682	0.550	0.063	14.675	0.200	0.022	0.004	0.002	0.0000	97.4	0.620
0.079	0.007	0.009	0.145	0.0000	0.0005	0.366	0.047	1.361	0.212	0.001	0.072	0.001	0.0013	140.9	0.397
0.101	0.003	0.012	0.010	0.0000	0.0010	0.403	0.040	5.588	0.009	0.061	0.010	0.048	0.0000	82.1	0.752
0.118	0.116	0.648	0.006	0.0000	0.0193	0.702	0.037	0.834	0.009	0.081	0.305	0.000	0.0051	168.8	0.373
0.005	0.004	0.332	0.005	0.0003	0.0353	0.104	0.159	1.342	0.045	0.002	0.006	0.152	0.0000	60.8	0.602
0.048	0.027	0.005	0.001	0.0001	0.0447	0.708	0.064	2.128	0.268	0.022	0.813	0.000	0.0007	171.0	0.311
0.024	0.002	0.101	0.001	0.0000	0.0004	0.150	0.306	7.455	0.006	0.005	0.002	0.007	0.0001	53.9	0.652
0.140	0.045	0.725	0.040	0.1001	0.0000	0.420	0.189	0.504	0.008	0.001	0.001	0.004	0.0053	157.3	0.184
0.014	0.005	0.965	0.074	0.1044	0.0000	0.138	0.110	1.690	0.030	0.013	0.069	0.000	0.0000	45.2	0.641
0.016	0.030	0.013	0.009	0.1235	0.0000	0.293	0.161	0.712	0.262	0.003	0.003	0.003	0.0005	118.2	0.352
0.021	0.001	0.118	0.013	0.2042	0.0003	0.268	0.022	7.243	0.015	0.010	0.333	0.000	0.0000	98.2	0.792
0.092	0.005	0.656	0.002	0.0059	0.0002	0.284	0.019	6.093	0.005	0.071	0.001	0.011	0.0035	160.9	0.336
0.134	0.003	1.315	0.001	0.1371	0.0001	0.232	0.029	2.719	0.227	0.003	0.038	0.000	0.0000	55.9	0.573
0.011	0.027	0.114	0.001	0.0176	0.0000	0.110	0.023	1.285	0.236	0.037	0.005	0.096	0.0137	113.6	0.203
0.024	0.000	0.080	0.009	0.0106	0.0000	0.105	0.139	6.362	0.010	0.001	0.027	0.000	0.0000	62.4	0.675
0.035	0.025	0.320	0.094	0.0001	0.0000	0.275	0.194	4.012	0.002	0.003	0.035	0.058	0.0094	138.7	0.028
0.026	0.001	2.056	0.096	0.0000	0.0002	0.471	0.018	9.662	0.162	0.112	0.001	0.000	0.0001	90.0	0.473
0.007	0.013	0.024	0.105	0.0010	0.0000	0.357	0.079	11.486	0.077	0.001	0.032	0.020	0.0004	154.3	0.020
0.050	0.000	0.032	0.137	0.0006	0.0000	0.137	0.228	1.618	0.002	0.050	0.001	0.000	0.0000	104.8	0.572
0.006	0.080	1.707	0.004	0.0001	0.0000	0.253	0.051	7.037	0.018	0.013	0.087	0.068	0.0006	126.4	0.131
0.008	0.000	1.750	0.001	0.0000	0.0001	0.247	0.168	0.599	0.256	0.001	0.001	0.001	0.0000	61.1	0.592
0.008	0.071	0.007	0.002	0.0000	0.0000	0.691	0.035	10.535	0.037	0.012	0.532	0.011	0.0095	160.6	0.339
0.009	0.000	0.006	0.003	0.0011	0.0000	0.626	0.124	0.662	0.002	0.001	0.002	0.001	0.0000	84.3	0.638
0.090	0.084	1.417	0.051	0.0016	0.0028	1.600	2.068	0.018	0.002	0.001	0.004	0.002	0.0000	104.3	0.538
0.007	0.003	0.170	0.102	0.0092	0.1903	3.362	0.550	0.018	0.305	0.102	0.143	0.044	0.0017	112.5	0.095
0.098	0.059	0.007	0.116	0.0026	0.2825	3.202	1.472	0.016	0.455	0.001	0.001	0.000	0.0000	73.1	0.497
0.011	0.003	0.078	0.026	0.0762	0.0052	1.213	2.614	0.011	0.002	0.091	0.067	0.025	0.0088	146.1	0.145
0.040	0.090	0.873	0.001	0.0593	0.0510	0.868	1.264	0.128	0.002	0.028	0.001	0.001	0.0000	53.4	0.456
0.007	0.001	1.862	0.006	0.0183	0.0030	2.787	6.010	0.015	0.062	0.002	0.556	0.002	0.0041	134.6	0.202
0.008	0.036	0.007	0.001	0.0062	0.0006	1.348	0.604	0.061	0.087	0.108	0.001	0.000	0.0001	94.7	0.798
0.018	0.000	0.036	0.006	0.0631	0.1854	1.751	5.668	0.086	0.005	0.004	0.480	0.022	0.0012	143.4	0.322
0.012	0.013	1.252	0.010	0.0000	0.0459	3.074	2.740	0.056	0.003	0.006	0.021	0.000	0.0000	44.4	0.522
0.049	0.000	0.625	0.026	0.0000	0.3058	0.827	1.525	0.025	0.123	0.009	0.002	0.020	0.0061	174.0	0.041
0.025	0.052	0.044	0.014	0.0000	0.0040	3.738	1.279	0.378	0.036	0.001	0.245	0.000	0.0000	70.9	0.731
0.012	0.001	0.011	0.081	0.0001	0.0524	3.390	0.563	0.249	0.024	0.039	0.003	0.008	0.0001	142.3	0.016
0.010	0.008	0.146	0.001	0.0000	0.0016	1.056	6.601	0.050	0.003	0.009	0.034	0.000	0.0001	75.8	0.769
0.084	0.000	0.415	0.002	0.0006	0.0039	0.949	0.501	0.036	0.136	0.001	0.020	0.102	0.0146	141.2	0.297
0.038	0.006	0.073	0.004	0.0000	0.0090	5.139	2.117	0.031	0.025	0.055	0.353	0.000	0.0000	53.7	0.553
0.115	0.001	0.010	0.001	0.0005	0.0887	3.049	1.755	0.394	0.003	0.002	0.003	0.085	0.0014	129.1	0.319
0.010	0.021	0.226	0.063	0.0051	0.0003	3.958	2.298	0.056	0.009	0.007	0.001	0.132	0.0001	56.4	0.417
0.031	0.000	0.340	0.140	0.1460	0.0000	4.584	0.679	0.123	0.122	0.140	0.453	0.000	0.0031	111.6	0.175
0.047	0.009	0.028	0.022	0.2000	0.0001	3.228	1.579	0.010	0.029	0.003	0.011	0.007	0.0000	44.1	0.505
0.073	0.002	0.010	0.067	0.0083	0.0000	4.294	0.425	0.327	0.001	0.038	0.031	0.000	0.0016	111.9	0.102
0.013	0.014	1.092	0.005	0.0512	0.0000	1.708	4.867	0.275	0.015	0.068	0.017	0.093	0.0000	89.5	0.688
0.047	0.000	2.669	0.003	0.0053	0.0000	1.869	0.356	0.209	0.033	0.001	0.849	0.000	0.0001	133.8	0.134
0.005	0.045	0.042	0.002	0.0014	0.0001	1.082	1.818	0.019	0.222	0.014	0.006	0.003	0.0000	99.9	0.628
0.014	0.000	0.012	0.001	0.1430	0.0000	2.590	0.369	0.027	0.002	0.006	0.154	0.000	0.0014	127.8	0.300
0.007	0.006	1.148	0.019	0.0000	0.0000	0.794	0.954	0.061	0.019	0.001	0.692	0.053	0.0000	43.8	0.673
0.121	0.000	0.300	0.115	0.0000	0.0000	2.879	1.235	0.283	0.114	0.070	0.002	0.000	0.0012	148.0	0.358
0.054	0.048	0.103	0.136	0.0002	0.0000	2.367	1.206	0.026	0.324	0.007	0.058	0.004	0.0000	84.6	0.781
0.013	0.002	0.007	0.025	0.0000	0.0000	1.979	0.467	0.017	0.003	0.036	0.001	0.001	0.0004	152.9	0.084
0.041	0.107	0.293	0.001	0.0004	0.0000	1.428	2.524	0.015	0.011	0.120	0.517	0.003	0.0000	69.5	0.642

Al	Cl	CO_3	C_2O_4	F	Fe	NO_2	NO_3	OH	K	PO_4	SO_4	Si	U	T(ºC)	Evap
0.006	0.001	2.134	0.004	0.0002	0.0002	2.856	1.249	0.148	0.360	0.002	0.001	0.000	0.0081	121.5	0.369
0.007	0.012	0.006	0.008	0.0001	0.0000	1.100	0.450	0.048	0.409	0.018	0.030	0.008	0.0000	57.0	0.469
0.055	0.000	0.037	0.001	0.0000	0.0002	2.999	4.130	0.013	0.004	0.001	0.003	0.000	0.0066	155.7	0.181
0.015	0.009	0.324	0.009	0.0829	0.0050	0.413	1.996	0.036	0.003	0.002	0.001	0.000	0.0001	44.6	0.575
0.076	0.001	0.929	0.055	0.1209	0.0552	0.112	0.712	0.024	0.176	0.014	0.161	0.002	0.0001	150.2	0.281
0.016	0.013	0.066	0.042	0.0491	0.0471	0.099	0.728	0.218	0.140	0.001	0.005	0.000	0.0013	91.1	0.789
0.050	0.001	0.014	0.033	0.1022	0.0021	0.342	1.023	0.047	0.015	0.054	0.209	0.002	0.0000	172.3	0.372
0.030	0.029	0.132	0.004	0.0096	0.0007	0.168	4.699	0.042	0.008	0.124	0.002	0.001	0.0058	50.1	0.744
0.022	0.001	0.941	0.001	0.0120	0.0301	0.406	3.987	0.105	0.156	0.002	0.039	0.009	0.0000	162.0	0.166
0.016	0.005	0.021	0.005	0.0030	0.0029	0.674	2.219	0.054	0.424	0.024	0.001	0.001	0.0003	103.4	0.783
0.127	0.001	0.027	0.001	0.0279	0.0067	0.113	4.034	0.012	0.005	0.001	0.242	0.006	0.0000	145.5	0.316
0.019	0.009	0.425	0.085	0.0010	0.0413	0.174	2.167	0.157	0.016	0.004	0.369	0.000	0.0112	58.9	0.542
0.078	0.001	0.487	0.104	0.0000	0.0006	0.097	0.618	0.235	0.053	0.022	0.019	0.023	0.0000	167.4	0.164
0.032	0.018	0.068	0.064	0.0001	0.0778	0.372	1.111	0.114	0.060	0.006	0.713	0.000	0.0016	97.7	0.694
0.037	0.001	0.018	0.095	0.0001	0.0567	0.167	0.921	0.136	0.009	0.017	0.019	0.031	0.0000	117.1	0.000
0.009	0.046	1.527	0.003	0.0002	0.0013	0.490	1.675	0.362	0.001	0.075	0.063	0.000	0.0011	106.2	0.492
0.013	0.000	1.909	0.002	0.0000	0.0009	0.375	0.858	0.012	0.027	0.008	0.006	0.004	0.0000	179.2	0.003
0.008	0.063	0.013	0.005	0.0004	0.2171	0.289	0.415	0.367	0.247	0.123	0.036	0.000	0.0056	87.6	0.506
0.010	0.000	0.008	0.002	0.0000	0.0403	0.142	1.072	0.024	0.023	0.008	0.008	0.037	0.0000	147.2	0.314
0.015	0.095	0.204	0.060	0.0081	0.0000	0.652	5.472	0.146	0.002	0.002	0.001	0.003	0.0046	109.7	0.450
0.006	0.001	0.174	0.010	0.0545	0.0000	0.329	4.431	0.021	0.056	0.030	0.644	0.002	0.0001	158.4	0.341
0.096	0.008	0.006	0.079	0.0481	0.0000	0.536	4.924	0.077	0.107	0.001	0.003	0.021	0.0114	64.1	0.511
0.081	0.003	0.014	0.069	0.0040	0.0000	0.144	1.372	0.066	0.006	0.018	0.118	0.000	0.0001	149.6	0.242
0.012	0.058	1.039	0.005	0.0017	0.0000	0.159	0.687	0.073	0.005	0.121	0.003	0.075	0.0004	101.0	0.436
0.011	0.000	0.141	0.006	0.0337	0.0000	0.251	1.164	0.051	0.099	0.001	0.111	0.000	0.0000	111.1	0.395
0.119	0.043	0.010	0.001	0.0052	0.0001	0.384	1.340	0.014	0.414	0.041	0.001	0.005	0.0002	57.2	0.683
0.015	0.004	0.012	0.001	0.0102	0.0000	0.155	4.228	0.013	0.002	0.002	0.059	0.000	0.0000	147.5	0.006
0.036	0.012	0.152	0.025	0.0000	0.0003	0.202	2.380	0.069	0.013	0.001	0.029	0.135	0.0117	80.7	0.453
0.055	0.001	0.895	0.068	0.0009	0.0000	0.123	0.988	0.178	0.103	0.023	0.018	0.000	0.0000	145.8	0.088
0.017	0.006	0.048	0.064	0.0000	0.0000	0.111	1.178	0.109	0.281	0.005	0.151	0.024	0.0006	47.4	0.719
0.110	0.001	0.033	0.017	0.0000	0.0000	0.337	1.438	0.020	0.009	0.033	0.003	0.000	0.0000	131.6	0.152
0.065	0.046	0.385	0.007	0.0005	0.0001	0.147	4.483	0.060	0.005	0.011	0.434	0.018	0.0017	42.2	0.708
0.014	0.002	1.191	0.001	0.0006	0.0000	0.592	0.391	0.057	0.116	0.008	0.006	0.000	0.0000	171.3	0.317
0.013	0.016	0.013	0.004	0.0000	0.0001	0.117	0.489	0.351	0.032	0.038	0.048	0.074	0.0044	50.9	0.594
0.041	0.000	0.057	0.003	0.0000	0.0000	0.559	1.404	0.296	0.022	0.002	0.004	0.001	0.0000	168.5	0.200
0.030	0.007	1.794	0.054	0.1555	0.0214	2.569	0.116	0.063	0.006	0.001	0.013	0.001	0.0000	134.1	0.433
0.097	0.001	0.136	0.023	0.1066	0.0021	1.022	0.040	0.067	0.111	0.015	0.392	0.004	0.0004	56.7	0.386
0.124	0.075	0.084	0.028	0.1288	0.0022	2.028	0.043	0.186	0.250	0.002	0.001	0.001	0.0000	127.0	0.611
0.008	0.004	0.027	0.033	0.0131	0.0048	3.024	0.172	0.023	0.013	0.035	0.215	0.012	0.0001	65.4	0.194
0.029	0.018	0.918	0.001	0.0038	0.1463	1.824	0.279	0.040	0.002	0.012	0.001	0.001	0.0000	119.8	0.723
0.036	0.001	0.362	0.008	0.0098	0.1012	5.396	0.052	0.021	0.160	0.001	0.046	0.002	0.0018	75.3	0.259
0.044	0.038	0.033	0.006	0.0126	0.0271	1.091	0.148	0.022	0.037	0.082	0.003	0.000	0.0000	179.7	0.488
0.017	0.002	0.027	0.002	0.0980	0.1039	5.181	0.102	0.245	0.002	0.001	0.137	0.166	0.0003	96.3	0.209
0.009	0.021	0.246	0.119	0.0000	0.0257	3.124	0.045	0.011	0.003	0.007	0.034	0.001	0.0000	131.3	0.775
0.032	0.000	0.430	0.097	0.0002	0.0015	2.078	0.299	0.029	0.477	0.009	0.012	0.066	0.0019	47.1	0.034
0.037	0.010	0.029	0.107	0.0001	0.0057	1.838	0.034	0.383	0.032	0.001	0.059	0.000	0.0000	168.0	0.623
0.066	0.001	0.009	0.032	0.0001	0.0038	1.039	0.039	0.287	0.024	0.139	0.005	0.032	0.0155	42.7	0.216
0.031	0.082	2.215	0.005	0.0000	0.0144	5.760	0.210	0.093	0.011	0.012	0.029	0.000	0.0000	174.5	0.595
0.007	0.001	1.772	0.003	0.0009	0.0032	0.957	0.245	0.144	0.081	0.006	0.020	0.005	0.0149	92.0	0.222
0.008	0.092	0.007	0.002	0.0006	0.0006	2.611	0.022	0.231	0.036	0.019	0.297	0.000	0.0000	136.8	0.722
0.007	0.000	0.028	0.001	0.0001	0.0053	2.291	0.046	0.252	0.016	0.003	0.001	0.019	0.0003	95.8	0.291
0.040	0.006	0.633	0.049	0.0256	0.0000	2.764	0.031	0.181	0.011	0.004	0.006	0.014	0.0000	113.0	0.706
0.116	0.001	0.312	0.015	0.0040	0.0000	1.183	0.025	0.150	0.047	0.142	0.191	0.001	0.0002	70.6	0.391
0.052	0.026	0.100	0.026	0.0042	0.0000	2.129	0.042	0.010	0.049	0.004	0.001	0.158	0.0000	128.3	0.777
0.025	0.002	0.036	0.022	0.0078	0.0000	0.854	0.028	0.171	0.001	0.016	0.887	0.001	0.0007	57.8	0.389
0.048	0.017	0.831	0.002	0.1184	0.0001	4.659	0.105	0.010	0.003	0.023	0.009	0.095	0.0001	160.3	0.517
0.039	0.002	0.220	0.004	0.0883	0.0000	0.756	0.093	0.027	0.500	0.002	0.862	0.000	0.0001	63.5	0.264
0.075	0.034	0.035	0.007	0.0309	0.0000	2.348	0.203	0.045	0.072	0.068	0.008	0.147	0.0000	149.9	0.458
0.018	0.003	0.043	0.003	0.0902	0.0000	0.774	0.058	0.108	0.004	0.000	0.047	0.001	0.0143	92.5	0.298
0.009	0.035	1.885	0.046	0.0000	0.0000	1.499	0.317	0.184	0.001	0.001	0.108	0.010	0.0000	157.9	0.778
0.018	0.000	1.585	0.017	0.0004	0.0000	1.794	0.050	0.012	0.047	0.045	0.007	0.000	0.0050	102.6	0.183
0.009	0.078	0.017	0.017	0.0001	0.0000	1.765	0.066	0.046	0.327	0.001	0.801	0.054	0.0000	176.7	0.545
0.008	0.000	0.009	0.024	0.0002	0.0000	0.912	0.085	0.017	0.004	0.015	0.016	0.000	0.0022	54.8	0.155
0.043	0.011	0.762	0.001	0.0001	0.0000	2.951	0.136	0.309	0.001	0.029	0.524	0.006	0.0000	152.4	0.631
0.062	0.002	0.256	0.001	0.0002	0.0003	1.809	0.050	0.011	0.030	0.004	0.002	0.000	0.0003	104.5	0.334
0.064	0.032	0.055	0.001	0.0008	0.0002	0.890	0.198	0.134	0.092	0.134	0.756	0.006	0.0000	122.0	0.703
0.020	0.002	0.038	0.001	0.0002	0.0000	4.156	0.047	0.080	0.010	0.007	0.010	0.001	0.0012	71.7	0.139
0.009	0.006	0.977	0.023	0.0330	0.0232	0.220	0.150	0.053	0.015	0.002	0.002	0.002	0.0005	140.6	0.773
0.106	0.000	0.464	0.029	0.0037	0.0012	0.452	0.023	0.212	0.128	0.011	0.031	0.025	0.0000	89.2	0.170
0.034	0.040	0.091	0.028	0.0168	0.0108	0.445	0.019	0.300	0.152	0.005	0.001	0.001	0.0003	178.1	0.508

Al	Cl	CO_3	C_2O_4	F	Fe	NO_2	NO_3	OH	K	PO_4	SO_4	Si	U	T(ºC)	Evap
0.016	0.001	0.009	0.011	0.0016	0.0392	0.351	0.114	0.043	0.019	0.040	0.403	0.057	0.0000	105.1	0.044
0.102	0.018	0.349	0.001	0.1261	0.0077	0.122	0.041	0.022	0.001	0.059	0.002	0.000	0.0002	170.2	0.742
0.035	0.004	0.458	0.003	0.0012	0.2543	0.136	0.146	0.012	0.265	0.006	0.028	0.039	0.0000	69.0	0.103
0.035	0.014	0.032	0.007	0.0217	0.0015	0.205	0.302	0.271	0.193	0.127	0.011	0.000	0.0152	177.0	0.438
0.046	0.001	0.088	0.001	0.0013	0.2229	0.135	0.023	0.032	0.018	0.001	0.163	0.006	0.0000	95.2	0.197
0.132	0.029	1.957	0.052	0.0002	0.0436	0.208	0.043	0.159	0.004	0.001	0.025	0.000	0.0004	134.9	0.692
0.022	0.005	0.123	0.016	0.0001	0.0117	0.498	0.019	0.049	0.052	0.056	0.003	0.003	0.0000	68.7	0.072
0.138	0.081	0.021	0.036	0.0001	0.0079	0.331	0.128	0.035	0.214	0.002	0.056	0.000	0.0064	161.4	0.470
0.007	0.005	0.113	0.010	0.0007	0.0012	0.378	0.041	0.028	0.003	0.017	0.001	0.069	0.0000	40.0	0.359
0.113	0.025	0.884	0.001	0.0000	0.3139	0.249	0.191	0.026	0.011	0.010	0.310	0.000	0.0103	126.1	0.422
0.026	0.004	0.243	0.008	0.0001	0.0010	0.397	0.130	0.152	0.233	0.002	0.002	0.003	0.0000	40.5	0.005
0.067	0.037	0.024	0.002	0.0007	0.0244	0.658	0.089	0.050	0.028	0.018	0.178	0.001	0.0006	128.6	0.528
0.017	0.002	0.097	0.008	0.0000	0.0160	0.340	0.032	0.341	0.005	0.001	0.008	0.023	0.0000	95.0	0.188
0.023	0.034	2.702	0.062	0.0273	0.0000	0.109	0.288	0.189	0.008	0.001	0.007	0.009	0.0001	118.8	0.402
0.019	0.001	0.176	0.035	0.0026	0.0001	0.127	0.108	0.097	0.045	0.018	0.607	0.000	0.0000	99.6	0.123
0.094	0.113	0.018	0.030	0.0149	0.0000	0.118	0.218	0.155	0.395	0.003	0.001	0.006	0.0003	129.4	0.663
0.005	0.003	0.022	0.014	0.0415	0.0003	0.286	0.033	0.013	0.011	0.015	0.767	0.000	0.0000	82.4	0.173
0.083	0.020	1.065	0.001	0.0113	0.0000	0.463	0.038	0.012	0.002	0.020	0.001	0.004	0.0036	116.3	0.452
0.033	0.003	0.573	0.006	0.1839	0.0004	0.321	0.073	0.019	0.445	0.001	0.055	0.000	0.0000	109.2	0.394
0.027	0.044	0.030	0.002	0.0030	0.0000	0.291	0.135	0.015	0.062	0.089	0.005	0.175	0.0017	159.5	0.702
0.014	0.001	0.072	0.002	0.1656	0.0004	0.131	0.037	0.130	0.002	0.001	0.045	0.001	0.0000	41.1	0.186
0.006	0.009	0.470	0.047	0.0000	0.0000	0.195	0.053	0.195	0.001	0.006	0.076	0.008	0.0030	119.3	0.567
0.077	0.000	2.447	0.013	0.0001	0.0000	0.360	0.026	0.010	0.044	0.035	0.001	0.000	0.0001	55.3	0.195
0.006	0.019	0.067	0.034	0.0001	0.0000	0.318	0.023	0.064	0.038	0.001	0.052	0.082	0.0122	165.8	0.758
0.034	0.000	0.006	0.059	0.0005	0.0002	0.277	0.112	0.238	0.006	0.015	0.002	0.000	0.0000	66.5	0.277
0.015	0.023	0.791	0.003	0.0000	0.0000	0.126	0.034	0.038	0.012	0.023	0.036	0.125	0.0020	163.9	0.788
0.028	0.001	0.195	0.001	0.0006	0.0000	0.685	0.251	0.164	0.168	0.001	0.003	0.001	0.0001	95.5	0.050
0.085	0.033	0.026	0.005	0.0000	0.0002	0.587	0.024	0.024	0.069	0.017	0.875	0.011	0.0002	143.9	0.738
0.019	0.003	0.014	0.001	0.0001	0.0000	0.282	0.231	0.113	0.002	0.001	0.010	0.001	0.0000	75.0	0.066

Table XII. GWB Results Corresponding to the Optimized Design Matrix

	$\log_{10}$(Q/K)				$\log_{10}$(Q/K)				$\log_{10}$(Q/K)		
FileNo	NAS	Zeolite	K_{sp}	FileNo	NAS	Zeolite	K_{sp}	FileNo	NAS	Zeolite	K_{sp}
1	30.589	26.957	-19.241	172	-16.189	-6.984	-58.45	343	-38.783	-26.028	-71.128
2	-0.711	6.711	-47.52	173	32.232	33.73	-15.498	344	14.241	10.894	-32.178
3	15.483	18.026	-33.575	174	-21.337	-0.888	-47.042	345	-24.863	-9.104	-56.762
4	-4.662	11.13	-55.107	175	41.743	40.151	-9.982	346	4.563	0.667	-46.094
5	23.067	19.315	-34.759	176	-20.968	-4.202	-57.058	347	-35.487	-26.85	-66.36
6	20.061	26.467	-39.875	177	2.505	8.365	-38.846	348	-8.63	-6.446	-45.277
7	44.327	42.461	-13.108	178	-4.563	11.746	-36.38	349	-37.1	-20.377	-71.864
8	0.885	12.316	-52.273	179	-19.007	-16.01	-62.454	350	9.463	8.223	-35.752
9	39.38	32.252	-8.296	180	3.132	14.681	-33.347	351	-44.804	-23.724	-74.094
10	21.726	30.807	-30.396	181	-18.656	-10.583	-59.712	352	7.401	3.357	-36.822
11	48.681	45.425	-1.082	182	9.37	15.026	-27.981	353	-52.309	-38.363	-85.506
12	12.524	20.987	-39.256	183	-25.729	-22.013	-59.644	354	-41.459	-38.189	-86.473
13	63.575	57.605	-1.807	184	0.645	13.918	-29.824	355	-26.258	-17.12	-52.009
14	-6.197	8.862	-53.273	185	-30.587	-24.334	-68.912	356	-40.087	-35.067	-68.714
15	28.347	23.713	-29.103	186	22.363	30.652	-17.776	357	-25.368	-16.328	-59.347
16	-7.452	8.982	-53.318	187	-6.988	-4.853	-53.429	358	-55.687	-49.405	-87.097
17	-8.841	-7.815	-61.572	188	-11.273	-1.162	-39.561	359	-17.878	-6.499	-52.327
18	15.199	18.812	-31.439	189	-21.404	-18.579	-60.016	360	-34.565	-31.631	-74.632
19	0.595	2.171	-48.024	190	5.809	21.156	-26.4	361	-18.777	-12.445	-44.165
20	29.295	37.578	-13.977	191	-1.486	0.384	-55.58	362	-57.59	-51.38	-89.918
21	23.079	22.792	-27.45	192	6.281	19.96	-32.622	363	-43.37	-32.422	-68.125
22	18.873	26.435	-22.726	193	-7.094	3.443	-39.014	364	-21.789	-19.228	-59.926
23	8.086	10.873	-42.091	194	-12.853	-11.322	-52.495	365	-9.038	0.997	-34.858
24	8.734	19.55	-31.971	195	1.814	9.043	-39.431	366	-15.349	-14.358	-58.792
25	22.601	19.71	-31.136	196	-12.531	-8.342	-49.132	367	-9.167	1.708	-39.615
26	19.342	27.48	-24.722	197	-9.25	-0.68	-41.007	368	-43.654	-39.323	-80.553
27	30.482	28.039	-25.369	198	-14.102	-10.412	-46.642	369	-31.884	-15.097	-54.89
28	35.981	47.302	-6.922	199	-1.306	15.122	-27.778	370	4.228	2.743	-42.651
29	34.038	31.3	-30.667	200	-17.148	-10.512	-62.881	371	-53.24	-32.941	-85.88
30	40.681	41.209	-26.448	201	-7.087	4.918	-37.059	372	-19.271	-16.141	-55.666
31	-3.318	-1.253	-48.03	202	-34.031	-28.934	-66.157	373	-57.549	-44.356	-84.492
32	40.029	46.823	-11.021	203	25.254	36.913	-16.962	374	-12.734	-11.816	-44.675
33	33.454	28.841	-22.225	204	-8.511	-7.143	-59.706	375	-45.48	-25.724	-75.991
34	6.238	10.651	-39.883	205	10.163	24.13	-20.44	376	-5.99	-4.025	-38.208
35	37.67	36.187	-18.17	206	6.318	9.918	-38.709	377	-55.963	-37.06	-79.427
36	-9.15	4.467	-55.428	207	31.534	39.523	-19.099	378	-5.486	-5.04	-38.433
37	45.758	45.434	-13.53	208	9.78	14.234	-44.676	379	-41.871	-28.933	-71.635
38	34.998	41.297	-38.338	209	-9.379	-1.864	-53.281	380	-27.212	-25.697	-55.802
39	36.653	35.246	-17.878	210	6.959	6.41	-39.118	381	-40.842	-31.152	-75.024
40	-5.119	4.952	-50.945	211	-48.712	-32.828	-76.739	382	-15.472	-13.154	-48.526
41	35.615	35.026	-11.272	212	11.963	11.356	-36.904	383	-26.967	-12.809	-66.319
42	-4.309	8.786	-50.567	213	-50.303	-29.081	-73.296	384	-28.592	-26.988	-58.232
43	43.005	43.562	-6.92	214	3.41	3.66	-29.972	385	-28.236	-18.595	-63.327
44	4.015	21.386	-49.01	215	-45.399	-27.351	-74.348	386	10.403	14.337	-40.19
45	43.142	41.356	-26.824	216	9.866	12.377	-32.747	387	17.356	16.881	-34.088
46	26.608	36.426	-32.319	217	-5.071	10.211	-43.303	388	10.314	19.492	-57.248
47	17.148	18.263	-34.004	218	2.276	7.534	-27.991	389	15.287	11.355	-34.414
48	-10.332	2.962	-54.369	219	-21.903	-1.178	-57.379	390	-7.516	6.295	-52.909
49	5.549	4.562	-47.498	220	28.234	26.692	-11.436	391	-1.946	-1.502	-52.562
50	19.064	27.598	-31.893	221	-4.84	7.786	-46.48	392	-32.845	-23.948	-76.553
51	10.054	12.238	-33.492	222	5.986	10.014	-23.558	393	15.88	13.159	-37.912
52	34.685	46.142	-11.091	223	-14.051	-5.34	-51.732	394	-12.727	2.618	-65.132
53	-2.966	0.875	-54.971	224	9.319	9.821	-33.905	395	13.948	10.16	-29.951
54	18.946	25.901	-30.511	225	2.123	14.17	-35.457	396	-34.039	-19.135	-79.195
55	19.381	19.277	-38.648	226	-12.971	-8.744	-61.335	397	4.966	2.878	-48.884
56	47.569	56.421	-3.003	227	14.964	29.959	-31.885	398	-26.878	-14.046	-80.566
57	-5.953	-6.588	-60.109	228	-20.707	-11.681	-60.542	399	28.793	24.426	-18.126
58	36.866	40.931	-16.453	229	0.855	16.009	-31.886	400	-19.525	-3.389	-69.06
59	13.248	13.02	-38.997	230	-33.641	-27.261	-65.918	401	24.221	22.614	-23.836
60	24.374	31.951	-24.154	231	17.088	30.756	-23.743	402	21.713	30.43	-28.81
61	30.117	27.48	-36.695	232	-11.932	-5.965	-53.32	403	-9.168	-4.335	-66.316
62	26.511	33.074	-17.517	233	12.117	19.415	-29.031	404	35.393	44.517	-34.552
63	-4.489	0.506	-59.483	234	-0.284	1.915	-44.52	405	-22.505	-15.493	-73.133
64	35.588	43.538	-7.356	235	4.621	17.26	-25.815	406	13.742	18.616	-33.724
65	23.901	26.09	-22.224	236	-17.494	-12.661	-59	407	-19.252	-15.373	-70.207
66	-4.949	-5.844	-63.595	237	-4.731	3.466	-35.128	408	0.318	3.634	-52.287

	$\log_{10}$(Q/K)				$\log_{10}$(Q/K)				$\log_{10}$(Q/K)		
FileNo	NAS	Zeolite	K_{sp}	FileNo	NAS	Zeolite	K_{sp}	FileNo	NAS	Zeolite	K_{sp}
67	20.141	23.845	-26.612	238	2.967	2.901	-41.62	409	-8.256	-7.055	-64.768
68	16.042	14.412	-39.114	239	-8.43	1.025	-42.546	410	11.397	22.476	-36.517
69	37.233	43.276	-10.99	240	0.051	4.572	-50.209	411	-12.895	-10.984	-68.174
70	6.379	5.501	-54.765	241	-3.668	4.534	-47.737	412	32.178	35.542	-38.811
71	10.313	23.901	-37.791	242	25.47	26.835	-18.024	413	5.234	1.921	-52.685
72	-1.914	-0.643	-52.154	243	-9.241	0.613	-52.755	414	1.146	11.652	-42.138
73	41.27	52.393	-11.612	244	21.248	23.193	-20.038	415	-36.569	-30.394	-87.085
74	17.958	20.08	-37.156	245	-24.933	-14.679	-56.044	416	-0.814	9.297	-47.208
75	34.475	41.904	-11.198	246	-1.237	4.841	-32.523	417	4.126	2.838	-56.247
76	14.66	13.414	-32.761	247	-45.618	-24.611	-73.147	418	-19.583	-3.922	-72.121
77	15.06	27.219	-29.182	248	19.259	18.198	-31.327	419	8.248	6.263	-41.074
78	-8.861	-3.899	-56.051	249	9.082	17.112	-39.785	420	-35.289	-25.351	-81.233
79	55.876	59.148	-2.98	250	5.988	5.765	-27.446	421	10.916	6.97	-44.872
80	14.557	16.767	-44.559	251	-12.481	6.881	-56.707	422	-11.697	3.273	-56.05
81	1.024	16.359	-43.042	252	37.031	33.234	-13.221	423	9.786	6.646	-42.576
82	16.759	14.053	-31.807	253	-27.415	-7.401	-65.464	424	-4.529	-0.326	-55.78
83	13.762	23.998	-40.276	254	11.143	13.049	-32.617	425	27.931	24.201	-30.223
84	18.516	18.412	-28.607	255	-27.494	-12.245	-60.915	426	-24.278	-9.334	-79.66
85	3.83	17.738	-49.673	256	13.576	13.87	-33.121	427	20.036	15.336	-32.569
86	44.088	40.138	-20.345	257	-3.323	0.843	-45.736	428	-2.466	3.014	-60.132
87	-13.72	3.724	-59.295	258	-34.83	-20.009	-72.231	429	23.169	21.421	-33.022
88	13.743	11.47	-34.711	259	7.041	8.001	-43.953	430	-29.724	-22.277	-75.975
89	-0.821	16.608	-45.379	260	-17.988	-10.646	-57.898	431	-0.171	-2.724	-44.43
90	33.467	34.743	-25.112	261	6.042	3.736	-36.366	432	-44.371	-32.942	-81.49
91	1.434	9.985	-46.196	262	-20.778	-7.918	-56.713	433	14.771	9.757	-34.415
92	32.187	29.547	-19.609	263	-10.849	-8.159	-51.597	434	4.907	7.513	-52.627
93	-1.179	8.511	-55.721	264	-36.826	-25.235	-78.365	435	0.51	-2.086	-55.092
94	42.88	36.777	-17.378	265	-8.961	-8.107	-39.199	436	39.487	46.118	-29.019
95	-6.976	10.47	-54.65	266	-45.987	-25.178	-83.177	437	4.246	2.485	-58.125
96	49.187	45.774	-5.967	267	-15.636	-14.222	-61.076	438	11.395	13.662	-31.761
97	45.399	54.732	-5	268	-59.453	-44.287	-90.39	439	-11.275	-8.024	-63.491
98	17.683	19.423	-39.464	269	-8.727	-8.107	-52.217	440	12.46	22.976	-31.829
99	17.983	27.991	-22.758	270	-63.263	-46.093	-89.665	441	-0.103	-1.651	-61.648
100	22.183	24.103	-32.125	271	9.789	6.884	-38.2	442	21.804	26.869	-22.56
101	69.009	72.399	-4.375	272	-30.979	-13.175	-62.369	443	-21.417	-19.092	-73.697
102	21.107	20.96	-39.146	273	-4.089	-5.21	-38.154	444	18.439	27.894	-38.043
103	27.428	36.224	-16.841	274	4.401	12.954	-29.901	445	2.919	3.209	-51.912
104	4.92	10.734	-47.307	275	-18.278	-13.369	-60.034	446	18.122	30.388	-31.456
105	40.398	48.063	-1.555	276	1.066	9.52	-43.449	447	-16.815	-17.299	-65.073
106	34.208	34.493	-23.348	277	-29.866	-27.533	-77.495	448	-0.631	10.585	-35.893
107	14.385	22.983	-31.546	278	-33.224	-21.345	-64.023	449	-9.719	-10.711	-58.851
108	-6.138	-3.659	-56.615	279	-19.01	-16.754	-68.747	450	-1.452	-0.806	-52.459
109	13.421	25.764	-32.68	280	-11.497	-4.076	-49.382	451	11.13	21.948	-38.978
110	10.608	12.203	-51.858	281	-8.454	-7.956	-59.502	452	-0.595	1.021	-52.041
111	41.651	51.355	-10.92	282	-21.506	-5.972	-60.336	453	14.412	22.074	-42.34
112	23.787	21.153	-36.582	283	-18.979	-15.974	-66.751	454	-2.391	-0.237	-50.466
113	-7.742	5.5	-48.821	284	-28.588	-12.655	-66.104	455	6.995	15.628	-44.831
114	50.7	44.688	-5.593	285	-29.914	-27.85	-84.55	456	-15.354	-15.879	-63.694
115	13.994	19.963	-35.806	286	-25.007	-13.565	-60.805	457	17.168	20.074	-28.592
116	47.332	45.588	-6.981	287	-22.639	-17.084	-65.025	458	4.372	3.154	-54.413
117	28.627	38.683	-46.797	288	-0.739	6.096	-43.443	459	39.485	46.955	-25.315
118	42.447	36.076	-15.481	289	-44.227	-38.602	-80.452	460	-21.38	-20.69	-74.51
119	9.248	16.241	-53.265	290	-39.029	-20.609	-69.247	461	5.984	18.765	-31.767
120	39.652	35.304	-12.046	291	-1.809	2.1	-51.589	462	-19.747	-18.298	-71.033
121	-3.7	6.984	-53.04	292	-37.83	-25.972	-73.302	463	-6.262	-0.074	-52.764
122	43.361	41.179	-19.838	293	6.769	5.23	-36.044	464	-22.373	-20.524	-72.373
123	10.74	24.179	-35.67	294	-49.27	-38.456	-77.943	465	-2.408	1.942	-46.797
124	34.059	34.058	-16.449	295	-17.351	-14.902	-53.135	466	13.678	14.77	-38.191
125	17.004	25.293	-42.947	296	-43.623	-30.306	-73.594	467	-10.218	1.807	-52.354
126	33.648	31.211	-25.154	297	-5.377	-3.051	-40.527	468	31.524	27.773	-14.733
127	21.116	34.21	-33.241	298	-41.282	-30.973	-80.2	469	-9.489	3.273	-54.569
128	24.39	25.218	-28.145	299	3.56	1.506	-40.905	470	28.584	23.338	-18.177
129	-24.201	-16.709	-51.283	300	-47.661	-38.478	-84.553	471	-10.509	1.853	-61.5
130	-25.717	-14.392	-57.384	301	-4.423	-7.749	-42.462	472	30.619	25.352	-17.125
131	0.184	1.183	-34.224	302	-33.466	-24.377	-64.649	473	-13.895	-7.228	-58.725
132	-31.167	-13.663	-57.059	303	-12.469	-12.393	-59.153	474	3.244	0.465	-48.17
133	4.304	3.644	-38.563	304	-20.596	-12.471	-57.468	475	-18.507	-11.664	-63.482
134	-9.488	3.362	-38.91	305	5.188	3.724	-37.103	476	23.181	16.63	-34.094
135	30.886	31.915	-14.919	306	-18.578	-5.08	-43.975	477	-18.664	-5.799	-80.036

	$\log_{10}$(Q/K)				$\log_{10}$(Q/K)				$\log_{10}$(Q/K)			
FileNo	NAS	Zeolite	K_{sp}	FileNo	NAS	Zeolite	K_{sp}	FileNo	NAS	Zeolite	K_{sp}
136	-19.89	-5.513	-53.56	307	-25.612	-21.922	-59.58	478	5.769	3.996	-44.993
137	10.192	9.685	-26.341	308	-31.024	-21.21	-57.981	479	-18.146	-11.371	-67.914
138	-36.23	-15.619	-61.521	309	-43.775	-39.636	-80.382	480	6.2	7.112	-39.74
139	32.331	28.581	-12.277	310	7.055	12.557	-36.502	481	-8.935	1.81	-57.568
140	0.38	12.371	-42.588	311	-17.965	-14.429	-60.962	482	-6.611	-7.519	-56.016
141	27.245	25.916	-10.907	312	-15.065	-3.902	-52.825	483	14.33	19.186	-30.137
142	-45.694	-29.183	-73.346	313	-52.035	-46.766	-88.469	484	-13.643	-14.986	-59.587
143	9.898	8.621	-22.413	314	-1.141	13.633	-31.364	485	14.524	15.047	-30.931
144	-21.778	-10.964	-67.636	315	-33.963	-28.383	-75.02	486	-14.495	-14.653	-59.586
145	-24.045	-19.186	-62.663	316	-22.908	-7.253	-52.475	487	17.44	24.331	-25.555
146	9.696	13.549	-25.157	317	-26.354	-23.149	-67.319	488	-25.718	-25.284	-67.729
147	-27.838	-23.526	-56.921	318	-28.541	-13.725	-54.778	489	8.845	12.297	-38.153
148	25.405	26.997	-18.339	319	-26.984	-23.446	-73.956	490	-11.996	-9.058	-62.442
149	-13.349	-8.302	-57.748	320	4.58	7.905	-31.989	491	-2.5	6.588	-46.952
150	14.693	21.206	-21.265	321	-50.229	-45.036	-84.117	492	-7.862	-8.89	-65.658
151	-3.002	3.735	-39.185	322	-26.797	-19.816	-69.249	493	9.128	19.402	-32.473
152	6.46	15.164	-26.704	323	3.423	17.768	-27.877	494	-11.52	-8.027	-56.345
153	-13.779	-10.062	-54.955	324	-30.578	-23.83	-64.86	495	-8.651	5.157	-49.853
154	12.769	21.178	-23.299	325	-10.83	3.215	-52.359	496	1.181	1.292	-48.927
155	-22.39	-17.299	-52.662	326	-35.872	-32.047	-80.482	497	-1.955	2.365	-41.263
156	-7.537	7.785	-38.787	327	-4.23	10.515	-36.708	498	6.569	7.74	-43.736
157	-19.913	-16.003	-49.335	328	-12.814	-12.736	-53.682	499	-21.605	-14.663	-73.448
158	39.081	42.824	-4.387	329	-6.205	5.195	-39.319	500	8.871	7.262	-38.718
159	2.588	4.85	-44.265	330	-44.492	-40.96	-79.861	501	-15.112	-7.109	-71.435
160	-10.797	3.893	-35.226	331	-8.444	-1.192	-54.317	502	9.583	10.983	-35.428
161	17.857	16.434	-19.351	332	-50.395	-44.395	-80.275	503	-10.414	-6.323	-58.949
162	-19.828	-4.811	-50.398	333	-33.227	-16.646	-58.711	504	23.045	16.683	-18.325
163	37.547	36.283	-10.24	334	-16.787	-16.488	-62.291	505	-19.491	-4.897	-60.145
164	-15.444	2.118	-46.601	335	9.611	13.73	-35.422	506	-2.726	-2.402	-51.687
165	2.286	2.525	-35.423	336	-58.74	-50.969	-88.493	507	-18.871	-3.133	-64.026
166	-14.402	1.994	-48.897	337	-18.139	-11.207	-46.914	508	15.479	8.709	-34.765
167	1.892	7.015	-35.692	338	-16.591	-16.698	-48.43	509	-35.005	-20.745	-78.252
168	-32.796	-16.892	-61.25	339	-29.697	-15.103	-59.666	510	19.51	13.714	-26.008
169	33.578	29.776	-11.813	340	-15.293	-13.584	-51.197	511	-14.38	-7.732	-58.856
170	-17.098	0.015	-58.903	341	-36.351	-24.357	-62.865	512	24.222	20.195	-30.558
171	7.592	10.152	-31.34	342	-4.749	-5.802	-41.8	513	-15.505	-5.95	-58.351

The OLH design indicates that the nominal evaporator control model fits within but does not cover the entire bounding composition range indicated in Table X in its present form. Comparison of the OLH composition space analysis at temperatures between 40°C and 180°C and between zero to 80% evaporation are overlayed in Figure 10 with the nominal SRS evaporator model developed for the 120-140°C operating temperature and 40% evaporation. The nominal model fits comfortably within the space defined by the OLH analysis, thereby validating the calculation method used for the nominal model and the conditions over which it was developed.

On Figure 10 it should be noted that at a Ksp (log $Q(NAS)_{25°C}$ of –43.3 that values of $\log(Q/K)_{NAS}$ can be as large as +40 indicating a great deal of supersaturation with respect to NAS_{gel}. This was evaluated and the design points in the superaturated range are primarily those at low OH^- concentrations, e.g. values <1M OH^-. This is a limitation of the model in that the solubility data used for the NAS_{gel} from the Bayer aluminum industry was solubility data at 8.5M OH^-. Therefore, the minimum OH^- modeled should be truncated at 1M OH^-. Further investigation of concentration constraints is needed once SRS evaporator specific solubility data for NAS_{gel} becomes available (see Part IV). Any additional minimum concentrations of major components will be addressed in Part V if the absence of a component such as Al causes a phase other than NAS_{gel} to precipitate and/or a different phase boundary to be intersected.

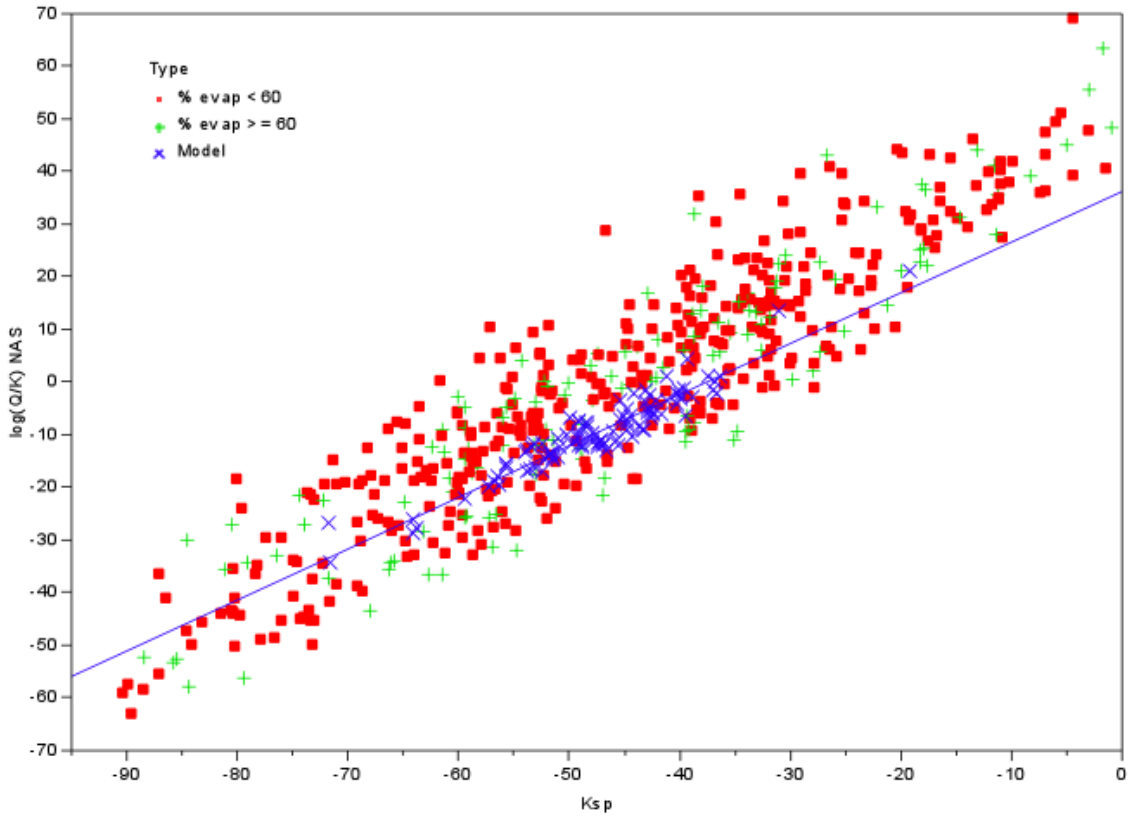

Figure 10. Comparison of the OLH composition space analysis at temperatures of 40°C-180°C, at evaporations spanning zero to 80% compared to the SRS evaporator nominal model at 120-140°C operating temperature and 40% evaporation.

9.0 RECENT TANK DATA

The recent tank data discussed in Section 9.0 of this study is overlain on the model from Part I[3] of this study. This data was not used to generate a new model, only for confirmatory understanding of the recent SRS Evaporator operations in light of the nominal evaporator model.

The recent tank data from February 2001 to June 2002 is shown on the nominal evaporator process control model in Figure 11. The data shown in deep purple is the recent data for all tanks. The deep purple Y's and X' are for Tanks 30 and 32, respectively. The solid purple squares are Tanks 43 and Tank 38. All of the data for the SRS 2H Evaporator feed tank (Tank 43) is labeled by date since the tank solutions analyzed were not fed to the 2H Evaporator until October, 2001 (after the evaporator was cleaned of aluminosilicate scale). The purple +'s and z's are Tanks 46 and 26, respectively. All of the data indicated in purple was analyzed by the F-Area laboratory. The orange colored Y's and X's for Tanks 30 and 32 are the February 2002 and June 2002 samples analyzed at SRTC.

Several interesting conclusions can be drawn from Figure 11 about recent processing history in the SRS 2H Evaporator system. It is obvious from the trends shown in

Figure 11 that the solutions decreased in supersaturation with time as long as the SRS 2H Evaporator was inoperable. The sample analyzed on 5/16/01 had a log Q $(NAS)_{25°C}$ of –36.9, much more positive than the –43.3 process control limit set by sample FTF-046 from Tank 46. This corresponded to a calculated log $(Q/K)_{NAS}$ of +0.7. By 7/04/01 the log Q $(NAS)_{25°C}$ of the Tank 43 solutions had dropped to -60.4 and the log $(Q/K)_{NAS}$ was –22.1. Moreover, by 9/27/01 the log Q $(NAS)_{25°C}$ was –67.4 and log $(Q/K)_{NAS}$ was –28.9. This indicates that it only took two months for the saturated May 2001 solutions to react leaving the tank supernate undersaturated with respect to NAS_{gel} precipitation.

The decrease in supersaturation in Tank 43 continued as long as the tank was quiescent (through September 2001). Once the SRS 2H Evaporator began operation again the solutions, as given by the dates on Figure 11, have become more saturated with respect to NAS_{gel}. It should be noted that none of the Tank 43 solutions have reached the log Q $(NAS)_{25°C}$ limit of –43.3.

The data shown on Figure 11 with respect to the SRS 3H Evaporator system are also interesting. It shows an increase in the degree of supersaturation of the Tank 32 solutions with time, e.g. compare the purple X's and Y's analyzed by F-Area to the most recent solutions indicated by the orange X's and Y's analyzed by SRTC. While no feed tank solutions have violated the log Q $(NAS)_{25°C}$ limit of being more positive than –43.3, several of the drop tank analyses have been more positive than –43.3 (Table XIII). When Equation 10 is used to calculate the log $(Q/K)_{NAS}$ for the samples with more positive log Q $(NAS)_{25°C}$ values than –43.3 (samples HTK-482 and HTK-508, it is clear that these samples were more supersaturated than log $(Q/K)_{NAS}$ of –5.50 but at no time did the log $(Q/K)_{NAS}$ values become positive indicating supersaturation (Table XIII).

Table XIII. Recent Tank Data in the SRS 3H Evaporator System

Tank	Sample	log Q $(NAS)_{25°C}$	Calculated log $(Q/K)_{NAS}$
Tank 30 (Drop)	HTK-505	-44.15	-6.36
Tank 30 (Drop)	HTK-506	-44.46	-6.66
Tank 30 (Drop)	HTK-507	-44.64	-6.83
Tank 32 (Feed)	HTK-480	-44.43	-6.63
Tank 32 (Feed)	HTK-481	-44.14	-6.35
Tank 32 (Feed)	HTK-482	-41.42	-3.71
Tank 32 (Feed)	HTK-508	-42.46	-4.73
Tank 32 (Feed)	HTK-509	-44.46	-6.66
Tank 32 (Feed)	HTK-511	-45.84	-8.00

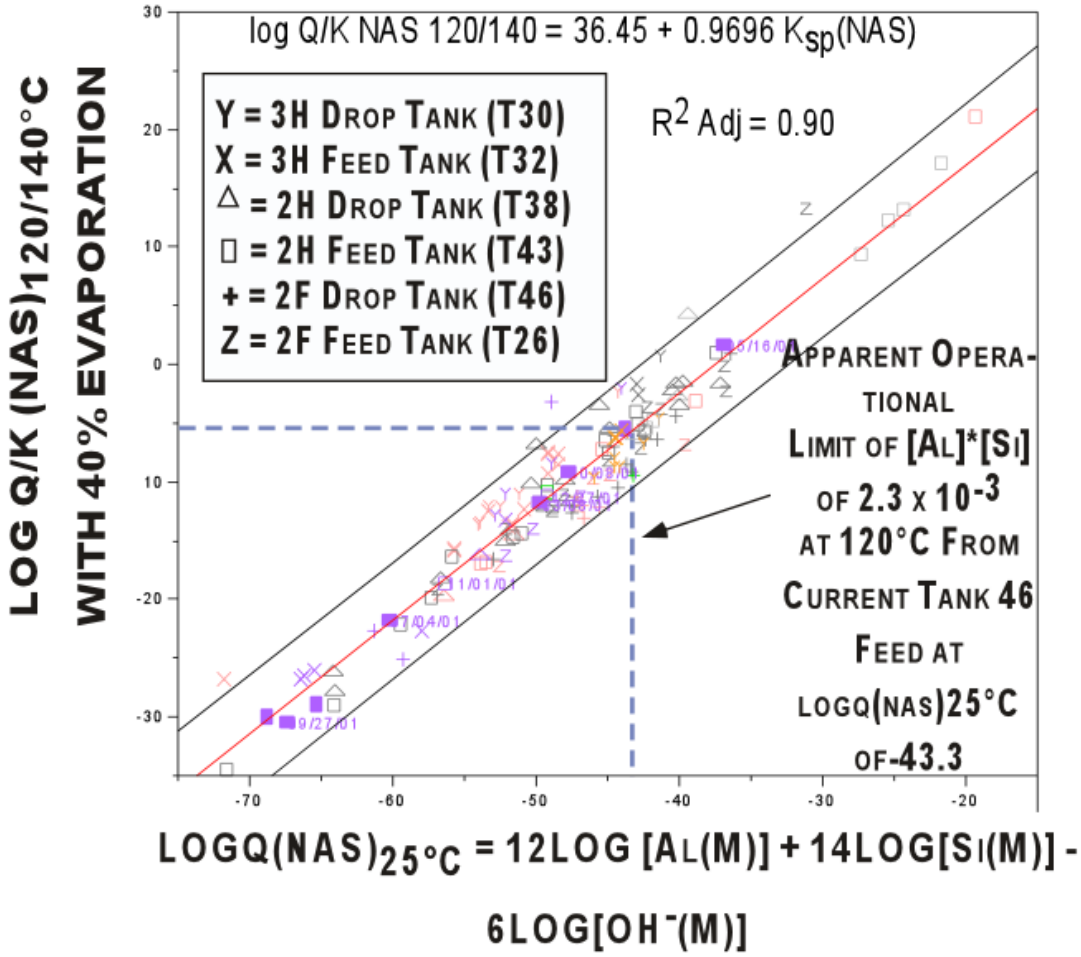

Figure 11. Recent Tank Data (February 2001-June 2002).

10.0 CONCLUSIONS

The SRS evaporator model presented in Part I of this study [3] is for the following nominal evaporator operating conditions:

- 40 wt % evaporation
- 120°C to 140°C

The data and calculations presented in this follow on study are summarized below:

- temperature effects on the log $(Q/K)_{NAS}$ saturation index are negligible in the temperature range over which the SRS evaporators operate, e.g. 120-180°C

- the elevated temperature log $(Q/K)_{NAS}$ values fall within the 95% bias of the nominal evaporator process model, the errors associated with using the model developed for the pooled 120°C/140°C data (Equation 10) for solutions being processed at 180°C is sufficiently accounted for

- the model does not apply above 180°C because of an intersecting stability field for $NaAlO_2$ which creates an equilibrium boundary between this phase and NAS_{gel} instead of between AlOOH and NAS_{gel}

- the upper bounding log $(Q/K)_{NAS}$ for the nominal evaporator model at 40 wt% evaporation is just about at saturation, e.g. log $(Q/K)_{NAS}$ is approximately zero (-0.576) for solutions with a log Q $(NAS)_{25°C}$ of –43.3

- lower percentages of evaporation (10 wt %, 20 wt %, and 30 wt %) have negative upper 95% bounding log $(Q/K)_{NAS}$ values for solutions with a K_{sp} of –43.3

- larger percentages of evaporation (50 wt % and 60 wt %) have positive upper 95% bounding log $(Q/K)_{NAS}$ values for solutions with a K_{sp} of –43.3

- the amount of evaporation can be correlated to log $(Q/K)_{NAS}$ of –5.50 and still be conservative with respect to preventing aluminosilicate scale since the upper 95% error bounds for log Q $(NAS)_{25°C}$ = -43.3 is log $(Q/K)_{NAS}$ of –0.567

- process control based on varying amounts of evaporation is recommended based on log $(Q/K)_{NAS}$ of –5.50 which gives a correlation between the saturation in the evaporator pot and the percent evaporation of

$$\% \text{ evaporation} = -285.64 - 7.47 \log Q\,(NAS)_{25°C}$$

- an orthogonal latin hypercube (OLH) statistical design validates that the evaporator control model covers maximum composition ranges indicated below plus the temperature range 40°C to 180°C and evaporation ranges between 0 and 80%

- recent tank data indicates that it only took about 2 months for the solutions in Tank 43 of the SRS 2H Evaporator system to react so that the supernates became undersaturated with respect to NAS_{gel} (assuming that the tank remains quiescent)

- after the SRS 2H Evaporator system became operational again, the solutions became more supersaturated with respect to NAS_{gel} but have not violated the log Q $(NAS)_{25°C}$ criteria of being more positive than –43.3.

- the SRS 3H Evaporator system has become more saturated with respect to NAS_{gel} than in prior operating history and is operating close to the log Q $(NAS)_{25°C}$ criteria of being more positive than –43.3 since many of the feed tank samples have log Q $(NAS)_{25°C}$ values of –44 while several drop tank samples have log Q $(NAS)_{25°C}$ values of –41 and –42

- recent tank data from the SRS 3H Evaporator system has verified the operational limit of –43.3 proposed in Part I of this study[3]

- the orthogonal latin hypercube (OLH) design demonstrated that the model predicts high degrees of supersaturation with respect to NAS_{gel} for solutions that have OH- concentrations <1M; this is a consequence of the fact that NAS_{gel} solubility used in GWB was for 8.5M OH^- solutions

- a minimum limit of 1M OH^- should be imposed for usage of the GWB model for SRS evaporators

- the concentration ranges of applicability of the SRS evaporator model need to be re-evaluated when the SRS evaporator specific solubility data for NAS_{gel} becomes available (see Part IV

- any additional minimum concentrations of major components will be addressed in (Part V) if the absence of a component such as Al causes a phase other than NAS_{gel} to precipitate and/or a different phase boundary to be intersected.

11.0 ACKNOWLEDGEMENTS

Kent Gilbreath from the SRS H-Area Tank farm is thanked for providing the data about sludge levels, feed pump levels, and operating temperatures of the SRS 3H from the Tank Farm morning reports. Ken Jones of the F-Area laboratory is acknowledged for discussions about the F-Area Si analytic methodology and dilution factors.

Many thanks are due to David Hobbs and Bill Wilmarth of SRTC for their frequent and always helpful counsel. Kevin G. Brown, formerly of SRTC, is also thanked for his encouragement and help in setting up computer interfaces between the GWB, Excel, and JMP softwares to eliminate human error when transferring database calculations between the different software packages.

This work was performed under contract No. DE-AC09-96SR18500 with the Department of Energy and co-funded by the Tank Focus Area under Technical Task Plan # SR-1-9-WT-31.

12.0 REFERENCES

1 W. R. Wilmarth, C. J. Coleman, A. R. Jurgensen, W. M. Smith, J. C. Hart, W. T. Boyce, D. Missimer, C. M. Conley, **"Characterization and Dissolution Studies of Samples from the 242-16H Evaporator,"** WSRC-TR-2000-00038, Rev. 0 (January 31, 2000).

2 W. R. Wilmarth, C. J. Coleman, J. C. Hart, and W. T. Boyce, **"Characterization of Samples from the 242-16H Evaporator Wall,"** WSRC-TR-2000-00089 (March 20, 2000).

3 C.M. Jantzen, J.E. Laurinat, and K.G. Brown **"Thermodynamic Modeling of the SRS Evaporators: Part I. The 2H and 2F Systems (U),"** WSRC-TR-2000-00293, Rev. 1 (April 4, 2002).

4 C.M. Jantzen, J.E. Laurinat, and K.G. Brown **"Thermodynamic Modeling of the SRS Evaporators: Part II. The 3H System (U),"** WSRC-TR-2001-00155, Rev. 1 (April 8, 2002).

5 C.M. Jantzen and J.M. Pareizs, **"Thermodynamic Modeling of the SRS Evaporators: Part IV. Incorporation of SRS Evaporator Specific Aluminosilicate Solubility Data,"** WSRC-TR-2002-00330 (August 1, 2002).

6 J.M. Pareizs and C.M. Jantzen, **"Thermodynamic Modeling of the SRS Evaporators: Part V. Validation,"** WSRC-TR-2002-00331 (September 1, 2002).

7 W. R. Wilmarth, S. D. Fink, D. T. Hobbs, M. S. Hay, **"Characterization and Dissolution Studies of Samples from the 242-16H Evaporator Gravity Drain Line,"** WSRC-TR-97-0326, Rev.0 (October 16, 1997).

8 C.S. Boley, M.C. Thompson, W.R. Wilmarth, and K.G. Brown, **"Technical Basis for the 242-16H Evaporator Cleaning Process,"** WSRC-TR-2000-00211, Rev. 1 (November, 2000).

9 Iman, R. L. and J. C. Helton**, "An Investigation of Uncertainty and Sensitivity Analysis Techniques for Computer Models,"** Risk Analysis, 8, 71-90, 1988.

10 Sacks, J., S. B. Schiller, and W. J. Welch, **"Designs for Computer Experiments,"** Technometrics, 31, 41-47,1989.

11 Sacks, J., W. J. Welch, T. J. Mitchell, and H. P. Wynn**, "Design and Analysis of Computer Experiments,"** Statistical Science, 4, 409-435, 1989.

12 Ye, K. Q., **"Orthogonal Column Latin Hypercubes and Their Application in Computer Experiments,"** Journal of the American Statistical Association, 93, 1430-1439, 1998.

13 K.G. Brown, "**Designed SRS Evaporator Experiments Using Geochemist's Workbench,"** SRTC-GPD-2002-00058 (May 15, 2002).

14 R.M. Barrer, "**Hydrothermal Chemistry of Zeolites**," Academic Press,London (1982).

15 **The American Heritage Dictionary**, Second College Edition, Houghton Mifflin Co., Boston, MA, (1982).

16 G.M. Barrow, **"Physical Chemistry,"** 2nd edition, McGraw-Hill Book Company, New York, 843pp., (1966).

17 M.C. Barnes, J.A. Mensah, and A.R. Gerson, **"The Mechanism of the Sodalite-to-Cancrinite Phase Transformation in Synthetic Spent Bayer Liquor,"** Microporous and Mesoporous Materials, 31, 287-302 (1999).

18 A.R. Gerson and K. Zheng, **"Bayer Process Plant Scale: Transformation of Sodalite to Cancrinite,"** J. of Crystal Growth, 171, 209-218 (1997).

19 R. M. Barrer, J. W. Baynham, F. W. Bultitude, and W. M. Meier, **"Hydrothermal Chemistry of the Silicates. Part V23I, Low-Temperature Crystal Growth of Aluminosilicates, and of Some Gallium and Germanium Analogues,"** 195-208 (1959).

20 T. Ejaz A.G. Jones and P. Graham, **"Solubility of Zeolite-A and Its Amorphous Precursor Under Synthesis Conditions,"** J. Chem. Eng. Data, 44, 574-576 (1999).

21 J.C. Buh. And J. Lons, **"Synthesis and Crystal Structure of Nitrate Enclathrated Sodalite, Na8[AlSiO4]6(NO3)2,"** Journal of Alloys and Compounds, v.235, 41-47 (1996).

22 W. R. Wilmarth, D. D. Walker, S. D. Fink, **"Sodium Aluminosilicate Formation in Tank 43H Simulants,"** WSRC-TR-97-00389, Rev. 0 (November 15, 1997).

23 H. A. Gasteiger, W. J. Frederick, and R. C. Streisel, **"Solubility of Aluminosilicates in Alkaline Solutions and a Thermodynamic Equilibrium Model,"** Ind. Eng. Chem. Res., 31, 1183-1190 (1992).

24 B. Subotic, D. Skrtic, I. Smit, L. Sekovanic, **"Transformation of Zeolite-A into Hydroxysodalite,"** J. Crystal Growth, 50, 498-508 (1980).

25 S. Bosnar and B. Subotic, **"Mechanism and Kinetics of the Growth of Zeolite Microcrystals; Part I. Influence of the Alkalinity of the System on the Growth of Zeolite-A Microcrystals,"** Microporous and Misoporous Materials, 28, 483-493 (1999).

26 A.J. Mattus, C.H. Mattus, and R.D. Hunt, **"Kinetic Testing of Nitrate-Based Sodalite Formation Over the Temperature Range of 40 to 100°C,"** U.S. DOE Report ORNL/TM-2001, Oak Ridge National Laboratory, UT-Battelle, LLC, Oak Ridge, TN (April 13, 2001).

27 R.K. Iler, **"The Colloid Chemistry of Silica and Silicates,"** Cornell University Press, Ithaca, NY, 324pp. (1955).

28 A.K. Varshneya, **"Fundamentals of Inorganic Glasses,"** Academic Press, Inc., New York, 570pp. (1994).

29 S.M. Budd, **"The Mechanisms of Chemical Reaction Between Silicate Glass and Attacking Agents,"** Phys. Chem. Glasses, 2[4], 111-114 (1961).

30 S.V. Mattigod and B.P. McGrail, **"Estimating the Standard Free Energy of Formation of Zeolites Using the Polymer Model,"** Microporous and Mesoporous Materials, 27, 41-47 (1999).

31 D.E. White, W.W. Brannock, and K.J. Murata, **"Silica in Hot-Spring Waters,"** Geochim. Cosmochim. Acta, 10, 27-59 (1956).

32 W.R. Wilmarth **"Tank 30H Sample Analysis,"** SRT-LWP-2002-00053 (may 29, 2002).

33 W.R. Wilmarth **"Tank 30H and 32H Sample Analysis,"** SRTC-LWP-2002-00058 (June 19, 2002).

34 D.D. Walker and C.J. Coleman, **"Densities and Weight% Solids of Simulated Salt Solutions,"** WSRC-TR-91-176 (April 1991).

35 C. Coleman, personal communication

36 C.F. Baes, Jr. and R.E. Mesmer, **"The Hydrolysis of Cations,"** John Wiley & Sons, New York, 489pp. (1976).

37 S. Sjoberg, L.Ohman, N. Ingri, **"Equilibrium and Structural Studies of Silicon(IV) and Aluminum(III) in Aqueous Solution. 11. Polysilicate Formation in Alkaline Aqueous Solution. A Combined Potentiometric and 29Si NMR Study,"** Acta Chemica Scandinavica , A39, 93-107 (1985).

38 I. Grenthe, et. al., **"Chemical Thermodynamics of Uranium,"** North Holland, New York (1992).

39 R.H. Busey, R.E. Mesmer, **"Ionization Equilibria of Silicic Acid and Polysilicate Formation in Aqueous Sodium Chloride Solutions to 300°C,"** Inorg. Chem., 16, 2444-2450 (1977).

40 A.S. Russell, J.D. Edwards, and C.S. Taylor, **"Solubility and Density of Hydrated Aluminas in NaOH Solutions,"** J. of Metals, p.1123-1128 (October, 1955).

41 D.A. Reynolds and D.L. Herting, **"Solubilities of Sodium Nitrate, Sodium Nitrite, and Sodium Aluminate in Simulated Nuclear Waste,"** U.S. DOE Report, RHO-RE-SST-14P, Westinghouse Hanford Company, Richland, WA (September, 1984).